MxiE-dependent gene regulation in *Shigella flexneri*

Chelsea Patrice Hall
Chesapeake, VA

Master of Science in Biological and Physical Sciences, University of Virginia, 2019

Bachelor of Science in Biology, University of Richmond, 2013

A Dissertation presented to the Graduate Faculty of the University of Virginia in Candidacy for the Degree of
Doctor of Philosophy of Science in

Microbiology, Immunology, and Cancer Biology

University of Virginia
November 2022

Abstract

Shigella spp. are the causative agents of bacillary dysentery, in which the hallmark symptom is bloody diarrhea. According to a recent estimate, there are approximately 270 million and nearly 200,000 deaths per year due to *Shigella* infection and there is currently no effective vaccine available. *S. flexneri* is the most widespread and studied species. Necessary for its virulence, the large virulence plasmid of *S. flexneri* encodes a type 3 secretion system, virulence effector proteins, as well as virulence regulators. Expression of virulence genes follows a sophisticated regulatory cascade involving three transcriptional regulators: i) VirF, ii) VirB, and iii) MxiE. Prior to my thesis work, the factors involved in MxiE-dependent gene expression were still unclear. My thesis work has improved our understanding of MxiE- and H-NS-dependent gene regulation in *S. flexneri* (Chapter 2). We identified novel chromosomal MxiE-dependent genes (*yccE* and *yfdF*) that require an intact MxiE box sequence in their promoter regions for gene expression. In addition, based on the AT-rich nature of MxiE-dependent genes, I hypothesized that H-NS, a protein involved in nucleoid organization, is mediating their transcriptional repression. We used a dominant negative H-NS to show that representative MxiE-dependent virulence plasmid and chromosome genes are expressed when H-NS is sequestered. Additionally, we show that a known anti-silencer of H-NS, VirB, is not required for MxiE-

dependent gene expression when MxiE and its co-activator, IpgC, are overexpressed. Finally, we demonstrate that MxiE is no longer necessary for gene expression when H-NS is sequestered. These data led us to propose a model of MxiE-mediated counter-silencing of H-NS, which is a previously unreported role for MxiE. In summary, my work has provided insights into previously unknown layers of MxiE-dependent gene regulation, which contributes to the overall understanding of *S. flexneri* virulence.

Acknowledgements

I owe a huge debt of gratitude to Hervé Agaisse for all of the time he devoted to my mentoring and training throughout my doctoral research. He instilled in me a scientific curiosity and fearlessness in pursuing answers to experiments. I'd also like to thank both the present and former members of the Agaisse and Derré labs, for always being there, whether for help in finding reagents or troubleshooting experiments. A huge thanks to my wonderful thesis committee, Dr. Sarah Ewald, Dr. Isabelle Derré, Dr. Bill Petri, and Dr. Ulrike Lorenz for the constructive discussions and helpful feedback that encouraged me to strive to bring out the best in my research and my capabilities as a scientist.

A special shout out to my fellow graduate students and lab members, I'm forever grateful for your friendship and support. I appreciate all of the times you were there for me to celebrate the highs and to help me persevere through the lows of graduate school. Forever supporting me throughout every endeavor, are my family and husband. I am eternally thankful to have them in my life and for their constant love and words of encouragement. Importantly, I need to thank my crazy but sweet furbaby, Ollie. Coming home to his wigglebutt after tough days was a huge comfort and helped me survive graduate school.

Table of Contents

List of Figures and Tables

List of Abbreviations

ABM, actin-based motility
AFM, atomic force microscopy
ANOVA, analysis of variance
ARA, arabinose
CDS, coding sequence
CFP, cyan fluorescent protein
CFU, colony-forming unit
ChIP, chromatin immunoprecipitation
CR, Congo red dye
DBD, DNA-binding domain
DTT, dithiothreitol
EIEC, Enteroinvasive *E. coli*
EMSA, electromobility shift assay
Fis, factor inversion stimulation protein
FBS, fetal bovine serum
HGT, horizontal gene transfer
Hha, hemolysin expression-modulating protein
H-NS, histone-like nucleoid structuring protein
Hpi, hours post-infection
HTH, helix-turn-helix
HU, heat unstable protein
IHF, integration host factor protein
IPTG, isopropyl β-D-1 thiogalactopyranoside
IS, insertion sequence
KmR, Kanamycin resistance cassette
LB, lysogeny broth
Mb-YFP, membrane-YFP
NAP, nucleoid-associated protein
ORF, open reading frame
PBS, phosphate buffered saline
RNAP, RNA polymerase
Seq, sequencing
T3SS, type three secretion system
T3SSA, type three secretion system apparatus
VP, virulence plasmid
WB, western blot
WHO, World Health Organization
WT, wildtype

1. Introduction

Introduction to *Shigella*

Members of the family Enterobacteriaceae, *Shigella* spp. are gram-negative, facultative, non-motile, non-spore forming, rod-shaped bacteria that are human-specific intracellular pathogens and the causative agents of bacillary dysentery, also known as shigellosis (1). The hallmark symptom of bacillary dysentery is bloody diarrhea; however, other symptoms include abdominal pain and cramps, fever, and tenesmus (2). *Shigella* spp. infect the colonic epithelium and once intracellular, spread cell-to-cell, which results in destruction of the colonic epithelium and disease symptoms (3-5). As few as 10-100 organisms, of *Shigella* is sufficient to cause disease, as determined in human volunteer challenge studies (6). *Shigella* spp. is transmitted via the fecal-oral route, which could include contaminated food and water as well as improper hand hygiene (7). However, there is no known environmental reservoir for *Shigella* (7). According to a study in 2016, *Shigella* causes an estimated 270 million cases and 200,000 deaths globally each year, with most cases occurring in low and middle-income countries, including Africa and Asia (8). Children under the age of 5 years are most adversely affected by *Shigella* infection and often repeat infections, which can lead to stunting (8).

As indicated by the genus name, *Shigella* was first discovered by Kiyoshi Shiga in 1898 following isolation from feces obtained from patients during a dysentery epidemic in Japan (7). Subsequently, four species of *Shigella* were identified: *S. dysenteriae*, *S. flexneri*, *S. boydii*, and *S. sonnei*. All species cause disease, however, *S. sonnei* is the most prevalent in high-income countries and *S. flexneri* is more prevalent in low and middle-income countries (9). *S. dysenteriae* serotype 1 is the only strain to express Shiga toxin and therefore causes the most fatal epidemics, however, it has a low occurrence today (7). *S. boydii* has historically remained low in occurrence (9). Due to travel, including that by military personnel, *S. flexneri* is the most widespread species and therefore the most studied in laboratories (7).

There is no effective vaccine available for *Shigella* spp. Treatments for *Shigella* spp. infection include hydration therapy and antibiotics, with ciprofloxacin and azithromycin being the first and second-line therapies, respectively, as recommended by WHO in 2005 (10). However, the occurrence of antimicrobial resistance, and therefore the development of novel treatments for *Shigella* is of utmost importance (11).

Evolution from non-pathogenic *E. coli*

Seminal work conducted by Lennox, Luria, and Burrous indicated that *E. coli* and *Shigella* are closely related based on their ability to share genetic information (12, 13). Horizontal gene transfer (HGT) was also discovered by Luria and Burrous to be a means of bacterial evolution (13). Through DNA sequencing of housekeeping genes, it was determined that there were several evolutionary events that occurred resulting in *Shigella* divergence from *E. coli* as soon as 35,000 – 270,000 years ago (14, 15). It was confirmed that *Shigella* was phylogenetically similar to *E. coli* following the first whole genome sequencing of *S. flexneri* 2a strain 2457T in 2003 (16). Indeed, it has been the subject of debate whether or not *Shigella* spp. should have its own genus or be included with *E. coli* (14, 17). However, for ease of clarity for clinical purposes, *Shigella* has remained phylogenetically distinct (7).

While sharing a core genome, *Shigella* spp. diverged from *E. coli* following the horizontal acquisition of a large (~200kb) virulence plasmid (VP) (17, 18). Similar to *Shigella*, Enteroinvasive *E. coli* (EIEC) also gained its virulence through acquisition of a VP (19, 20). HGT is a common mechanism for the acquisition of DNA by bacteria to promote virulence, as also exemplified by the well-studied pathogenicity islands in *Salmonella enterica* serovar Typhimurium (21). In addition to fast-tracking bacterial virulence by inheriting large regions of genetic

sequence, *Shigella* spp. also adapted to occupy an intracellular niche by a reduction in gene function by either gene deletion or inactivation (22-24).

Virulence Plasmid

All *Shigella* spp. contain a circular chromosome (4.6 Mb) and a large VP (~200 kb) (18, 24). The nomenclature for the VP is different for each strain, but the collective term is pINV (25). Sequence analysis by Buchrieser *et al.* revealed that the VP is a mosaic of elements that were likely acquired from different origins due to the difference in the GC-content (26). Approximately one-third of the VP is composed of insertion (IS) elements and is proposed to be the reason for differences in restriction sites in the VP across strains and serotypes (26, 27).

Importantly, the VP contains blocks of genes that encode proteins necessary for virulence (26). The core 31-kb fragment necessary and sufficient for invasion of host cells, which is required for pathogenicity, is termed the entry region (3, 28-30). The entry region is composed of the *mxi-spa* locus, which encodes the components of the type 3 secretion system apparatus (T3SSA), as well as genes for translocators (IpaB, IpaC, and IpaD), chaperones (IpgA, IpgC, IpgE, and Spa15), transcriptional regulators (VirB and MxiE), and some virulence effector proteins (IpaA, IpgB1, IpgD, and IcsB) (26). The VP encodes approximately 25 virulence effector proteins that are scattered across the VP and

that are essential for pathogenesis (31). There are families of effectors (i.e, Osp and IpaH) that arose following duplication events (26). In addition, some chromosomal loci are also involved in virulence (32, 33). However, the chromosome mostly encodes genes for metabolism (32).

Maintenance of horizontally-acquired genes via H-NS

When bacteria horizontally-acquire genes, such as the VP by *Shigella*, it is energetically costly and detrimental to the fitness of the organism (34). Therefore, regulatory mechanisms are critical to ensure that these genes are expressed only when necessary. It has been proposed that the histone-like nucleoid structuring (H-NS) protein functions to provide a mechanism for maintaining genes acquired through HGT (34, 35).

Foreign genes introduced by HGT are AT-rich compared to the ancestral genome, which provides a means for differentiation (36). The VP in *Shigella* has an AT-content of up to 70% for many of the protein-encoding genes (26). As a nucleoid-associated protein (NAP), H-NS functions to condense and organize DNA by preferentially binding AT-rich regions (37, 38). Oligomerization of H-NS along these regions of DNA results in repression of gene transcription, which is termed xenogeneic silencing (39, 40).

H-NS is a 137 amino acid protein with an N-terminal oligomerization domain, comprised of two dimerization interfaces, connected with a flexible linker to a C-terminal DNA-binding domain (DBD) (37, 41, 42). H-NS is a small (15.4 kDa) protein that is capable of forming dimers as well as higher order oligomers, which is necessary for its function (43). H-NS is 100% identical in *E. coli*, and is responsible for silencing up to 5% of its genome (38). This makes research conducted on H-NS in *E. coli* translatable to *Shigella*.

The domain architecture of H-NS is conserved in other H-NS-like proteins, such as the paralogues found in *Shigella* (StpA and Sfh in *S. flexneri*) (44). Due to similarity with H-NS, StpA (56.2% identical) and Sfh (59.1% identical) have been found to be able to compensate for the loss of H-NS in some instances (44, 45). Likewise, StpA and Sfh have been shown to form heteromeric complexes with H-NS and with each other (44). H-NS and StpA are 100% conserved in *E. coli*, while Sfh is found only in *S. flexneri* strain serotype 2a 2457T (44). StpA is also conserved in *Salmonella* and has been proposed to have arisen as a result of an *hns* gene duplication prior to evolutionary divergence of *E. coli*, *Shigella*, and *Salmonella* (46). In *S. flexneri* strain 2a 2457T, H-NS protein levels are relatively similar throughout growth, however, StpA protein levels are the highest at exponential phase, whereas, Sfh is highest at stationary phase (44, 47).

Although a consensus binding sequence (tCGATAAATT) has been experimentally determined in *S. flexneri*, it is generally thought that H-NS preferentially binds AT-rich sequences (48). AT-rich regions tend to have more DNA curvature, for which, H-NS has a higher binding affinity (36, 48, 49). H-NS can cooperatively bind regions of high affinity, referred to as nucleation sites, and then oligomerize along the regions of low affinity DNA to form filaments (36, 50).

Mechanisms of transcriptional silencing via H-NS include: blocking transcription initiation by binding to the promoter region where the RNA polymerase (RNAP) would normally bind, prevention of transcriptional elongation by RNAP by oligomerizing downstream of the promoter elements, and by the formation of H-NS:DNA bridges which occludes the promoter and/or traps RNAP within the DNA loop (Figure 1.1) (50-54). Alternatively, there are mechanisms for counter-silencing H-NS to activate transcription. The mechanisms for alleviating H-NS-mediated repression in *S. flexneri* will be discussed below.

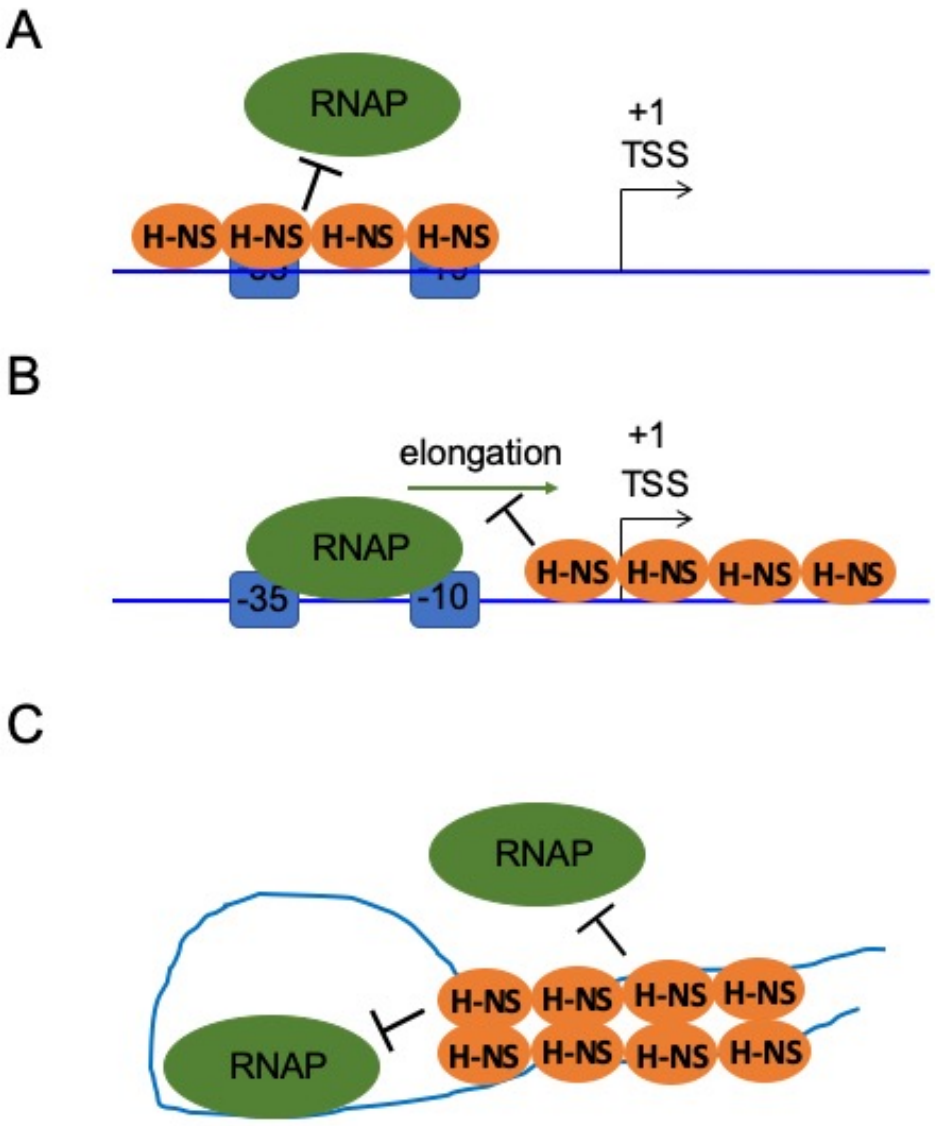

Figure 1.1. H-NS-mediated transcriptional silencing mechanisms. Schematic depicting the various ways that H-NS can silence transcription. (A) H-NS binds promoter elements (-10 and -35), relative to the +1 transcriptional start site (TSS), and prevents binding by RNAP, (B) H-NS oligomerizes downstream of promoter elements and prevents transcriptional elongation, and (C) H-NS oligomerization results in the formation of a DNA bridge, which could either occlude the promoter from RNAP or trap RNAP.

The Type 3 Secretion System

All *Shigella* spp. possess a type 3 secretion system (T3SS), which is necessary for virulence. The T3SSA is a needle-like structure (often referred to as an injectosome) that allows for the direct injection of virulence effector proteins into the host cell cytosol (55). At 30°C, the virulence plasmid, including the T3SS genes, is not expressed (Figure 1.2A). Assembly of the T3SSA occurs at 37°C, which is approximately the temperature inside the human body (Figure 1.2B) (56). The T3SSA consists of ~50 proteins that assemble to form the cytoplasmic sorting platform, the basal body that spans the inner and outer membranes of *Shigella*, as well as the hollow needle that protrudes outwards from the basal body, and the tip complex (57-60). Activation of the T3SS occurs when *Shigella* comes into contact with a host cell membrane (Figure 1.2C) (56). However, there are ways to activate the T3SS *in vitro* through the use of bile salts, Congo red dye, as well as mutations in the T3SS needle tip proteins (IpaB and IpaD) (56, 61-63).

Secreted by the T3SS, virulence effector proteins are necessary for host cell entry, cell-to-cell spread, and modulation of host cell signaling (64). Approximately 25 VP-encoded effectors are secreted by the T3SS at various times during infection (26). There are 7 IpaH family effectors encoded on the *S. flexneri* chromosome that are also secreted via the T3SS (65).

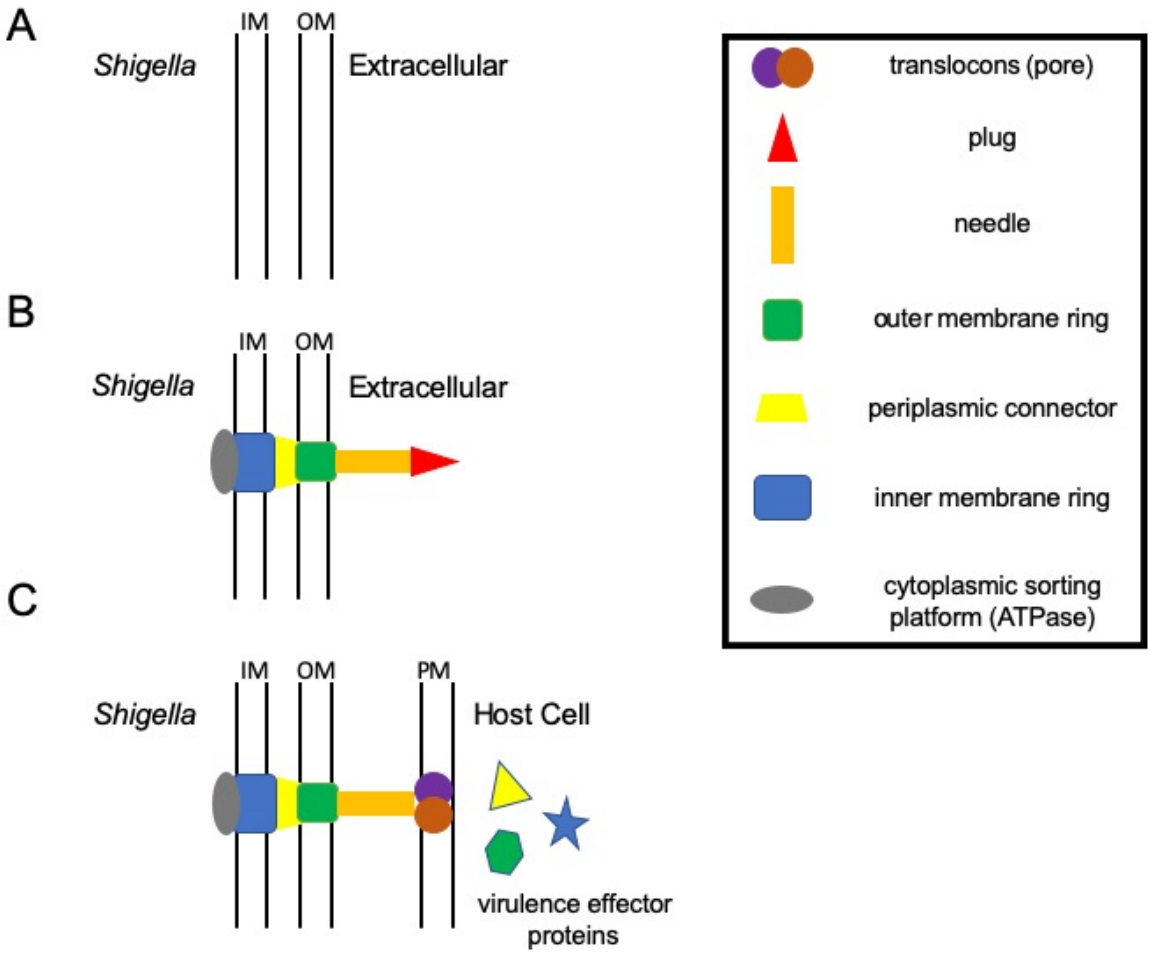

Figure 1.2. Assembly and activation of the T3SS needle.
Schematic depicting the assembly and activation states of the T3SS needle under different conditions. (A) At 30°C, the T3SS is not expressed, (B) at 37°C, the T3SS is expressed and assembled in the *Shigella* membrane, however, it is inactive due to a tip complex acting as a plug, and (C) upon contact with a host cell membrane, the T3SS needle becomes active by formation of a pore to translocate virulence effector proteins into the host cell cytosol.

Virulence gene regulation in *Shigella*

The dogma in the field is that there are two subsets of effector genes, those that are pre- and post-epithelial cell invasion, that are expressed depending on the activation state of the T3SS (66). At 30°C, the virulence plasmid, including the T3SS genes, are silenced by H-NS (Figure 1.3A). The early effectors are expressed and pre-stored in the bacterial cytosol at 37°C (Figure 1.3B) (67). Upon host cell contact, the pre-stored effectors are secreted by the T3SSA and then the post-invasion effectors are expressed (Figure 1.3C) (68). The proteins involved in the transcriptional regulatory cascade of the early and late effector genes will be discussed below.

First-tier transcriptional regulator: VirF

Referred to as the master regulator in *Shigella*, VirF is a transcriptional activator encoded on the large VP. VirF is a member of the AraC family of transcriptional regulators, which includes more than 800 proteins, which generally function to activate the transcription of genes involved in the regulation of carbon metabolism, stress response, and virulence (69). AraC members have a conserved region in consisting of 99 amino acids that is within the DNA-binding domain (DBD), which is comprised of two helix-turn-helix (HTH) motifs (69). Some AraC members, including VirF, have a companion

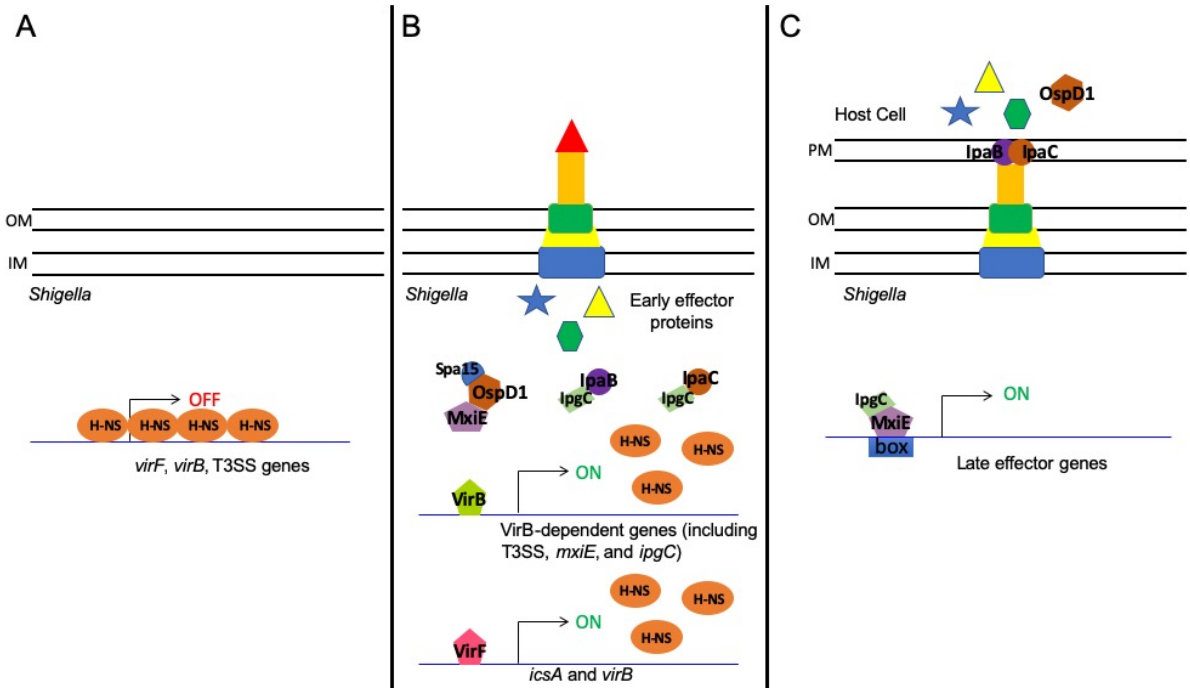

Figure 1.3. Three-tiered regulation of the virulence genes in *S. flexneri*. Schematic adapted from (McKenna and Wing, 2020) depicting the regulation occurring during different environmental cues. (A) At 30°C, virulence-associated genes, such as the T3SS, are repressed by H-NS. (B) At 37°C, VirF is expressed and subsequently activates *virB*, which de-represses and activates the early effector genes necessary for invasion and genes encoding the T3SS. The T3SS is assembled but inactive, because the translocons (IpaB and IpaC) are chaperoned by IpgC. MxiE, the next transcriptional activator, is bound by an anti-activator, OspD1, and its chaperone Spa15. (C) When in contact with a host cell membrane, the translocons form the pore at the tip of the T3SS needle and translocate the pre-stored VirB-dependent effectors, including OspD1. This frees MxiE and IpgC to interact and activate the late set of effector genes.

domain which is more variable and is thought to be the region responsible for oligomerization and cofactor binding (70).

Proteins in the AraC family are typically insoluble and therefore difficult to purify for biochemical analyses (69). For this reason, there have only been a few cases where VirF has been purified to attempt to investigate its mechanism of action, and often a MalE-VirF fusion is used to improve solubility (71-74). There are 3 classes of AraC family members: 1) regulators that respond to chemical signals, 2) regulators involved in the stress response, and 3) regulators that respond to a physical signal, which is often temperature (69, 75). VirF is a member of the third class and regulates gene expression in response to temperature, although this may be an indirect response, as discussed below (69).

At 30°C, VirF is repressed by H-NS, which binds to two specific sites in the *virF* promoter region and oligomerizes to form a DNA bridge, resulting in occlusion of the promoter from RNAP (Figure 1.1C) (76-78). However, upon a shift to 37°C, the DNA topology changes, such that, H-NS is no longer able to bind and prevent transcription, and *virF* is expressed (77). Temperature-mediated changes in DNA topology is one known mechanism in *Shigella* for the counter-silencing of H-NS (Figure 1.4A) (79).

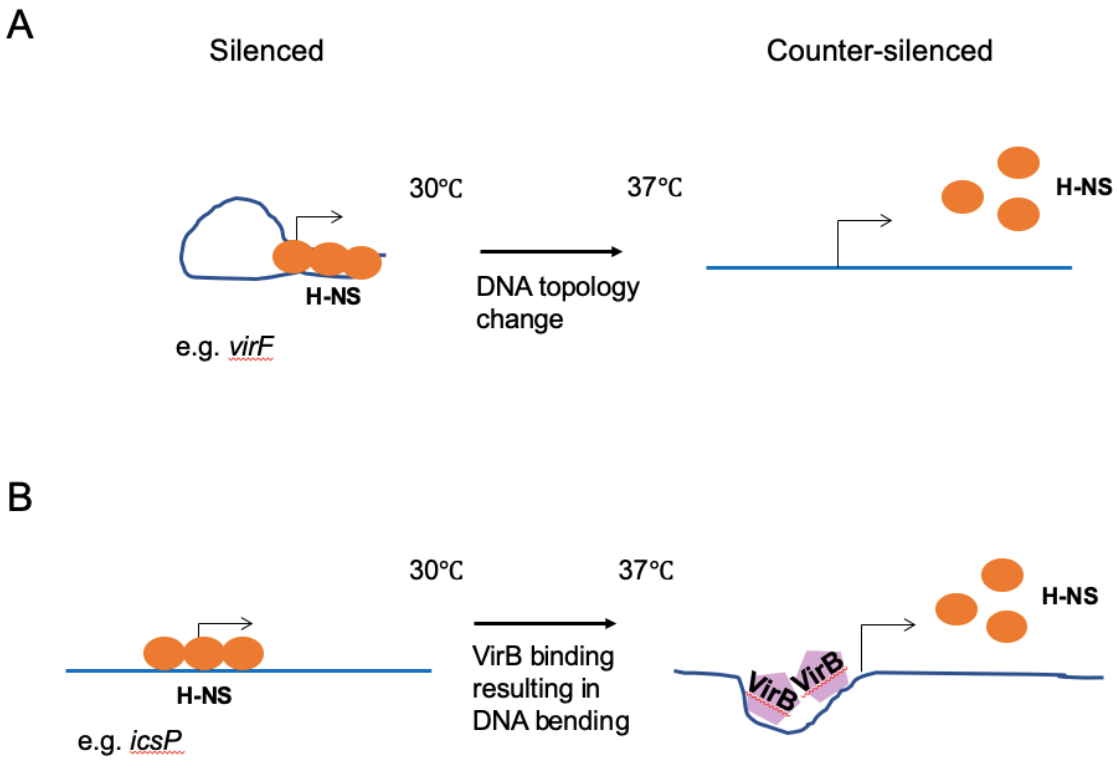

Figure 1.4. Mechanisms for counter-silencing H-NS in *S. flexneri*.
Schematic adapted from (Picker and Wing, 2016) depicting the mechanisms in *Shigella* for counter-silencing H-NS-mediated repression. The two known mechanisms are the (A) temperature-mediated mechanism, where a shift from 30°C to 37°C results in a change in the surrounding DNA topology, such that H-NS is unable to bind and the (B) VirB-mediated mechanism, where VirB binds and oligomerizes upstream of H-NS bound regions of DNA and induces local DNA bending, resulting in displacement of H-NS.

Upon expression of *virF* at 37°C, VirF activates expression of *icsA*, the protein responsible for actin-based motility, and *virB*, the next transcriptional regulator in the virulence gene regulatory cascade (Figure 1.3B) (73, 80, 81). VirF binding sites were mapped to upstream of the CDS of VirB, as were H-NS binding sites (73). It was hypothesized that VirF may disrupt H-NS binding at the *virB* promoter (73). However, an *in vitro* transcription study demonstrated that VirF does not function to counteract H-NS silencing, due to the inability of VirF to activate *virB* unless in the absence of H-NS (73). Thus, it is likely that VirF is either involved in RNAP recruitment or promoting RNAP stability for transcription initiation (73).

VirF is essential for the virulence of *Shigella* due to the necessity of IcsA and VirB for pathogenicity (5, 76, 81-83). Additionally, VirF as the first-tier regulator, kicks off the regulatory cascade, and is therefore indirectly regulating VirB and MxiE-regulated genes.

Second-tier transcriptional regulator: VirB

Following alleviation of repression by H-NS upon a shift to 37°C and transcriptional activation by VirF, VirB (referred to as InvE in *S. sonnei*) functions as the second-tier transcriptional regulator to activate the expression of around 50 genes on the VP (67, 73, 84). The VirB regulon includes the genes in the entry

region of the VP (i.e. T3SS), molecular chaperones, the third-tier transcriptional regulator, MxiE, and its co-activator, IpgC, as well as the early effector genes and other virulence-related genes (e.g. OspD1 and IcsP) (Figure 1.3B) (67, 82, 85-89). The VirB-dependent effector genes are expressed and pre-stored until host cell contact, which triggers their translocation via the T3SS needle into the host cell cytosol (Figure 1.3C). These effector proteins are necessary for host cell invasion. Due to the dependence of VirB for the expression of virulence-related proteins, VirB is essential for *Shigella* virulence (82).

Unlike other transcriptional regulators, VirB shares homology with plasmid-partitioning proteins, such as ParB, SopB, and KorB (82, 90-93). The region with high homology to ParB is the HTH motif, however, there is less homology in the oligomerization domain (90, 94). VirB does not function as a classical transcriptional activator to recruit or stabilize RNAP, but instead binds DNA to counteract H-NS-mediated silencing (73, 88, 89, 93, 95). It is thought that VirB will de-repress the genes on the VP in which a temperature shift to 37°C is not sufficient to alleviate repression by H-NS (Figure 1.4B) (79).

Studies of the *icsP*, *icsB*, and *ospZ* promoters demonstrated that VirB-mediated counter-silencing of H-NS requires DNA binding by VirB at sequence-specific sites [5'-(A/G)(A/T)GAAAT -3'] that are inverted repeats (termed Box 1 and Box 2) separated by a single nucleotide (85, 88, 96-98). VirB can function as a

counter-silencer from distant regions from H-NS binding, as observed by the presence of VirB binding sites more than 1 kb upstream, as is observed at the *icsP* and *ospD1* promoters (85, 86). The distance of the VirB binding sites from the TSS does not affect the ability of VirB to de-repress H-NS (96). VirB binding sites have also been found upstream of *virF* as well as its own gene, *virB*, indicating the presence of a positive feedback loop (99).

Binding of VirB to DNA, and its subsequent oligomerization, is thought to result in changes in the curvature of the surrounding DNA, which affects the binding of downstream H-NS oligomers such that H-NS can no longer silence transcription (Figure 1.4B) (79, 97). This is the second mechanism, besides temperature-mediated, that is known in *S. flexneri* for counter-silencing H-NS (Figure 1.4) (79).

Importantly, VirB also activates transcription of *mxiE*, which encodes the third-tier transcriptional regulator, as well as, *ipgC*, its co-activator (67). VirB is also tied into MxiE-dependent regulation through its activation of *ospD1*, which encodes the anti-activator of MxiE (67, 86). Therefore, VirF, which activates *virB*, and VirB are indirectly required for the regulation of MxiE-dependent genes.

Third-tier transcriptional regulator: MxiE

The expression of *mxiE*, encoding the third-tier transcriptional regulator, along with the gene encoding the MxiE co-activator, *ipgC*, is activated by VirB and functions to activate the expression of the late effector genes (67, 68, 100). Prior to host cell contact, MxiE is bound by an anti-activator, OspD1, and its chaperone, Spa15 (Figure 1.3B) (101). Also, IpgC is functioning as a chaperone for the translocons, IpaB and IpaC (Figure 1.3B) (56). Upon host cell contact, IpaB and IpaC form the pore in the host cell membrane for the direct injection, via the T3SS, of effectors, including OspD1, into the host cell cytosol (56, 86, 102-104). Activation of the T3SS frees MxiE and IpgC to interact and activate the expression of the late effector genes (Figure 1.3C) (68, 105). Numerous late effectors modulate the host cell immune signaling response to *Shigella* infection (31, 106). Therefore, MxiE is necessary for evading host immune responses but is not essential for *Shigella* virulence (68).

Studies on MxiE-dependent regulation can be conducted *in vitro* through the use of *mxiE* mutants, T3SS inducers, such as bile salts and Congo red dye, and by deletion of the T3SS needle tip proteins (IpaB or IpaD) to generate a constitutively active T3SS strain (61-63, 107, 108). The MxiE-dependent regulon was defined using: luciferase reporters for VP genes in WT compared to an *ipaB*-constitutively active T3SS, mutant strain, the use of GFP reporters in the presence and absence of MxiE, and by a microarray of VP genes (67, 68, 100). There are at

least 25 genes that are known to require MxiE for activation (67, 68, 100, 109). 16 of these genes are encoded on the VP and 9 genes are on the chromosome (Figure 1.5). Additionally, some of these genes, or operons (*ospB-phoN2*, *ospF-ospD2*, *ospC1* and *virA*), are co-regulated by VirB (Figure 1.5) (31).

MxiE, like VirF, is an AraC-type transcriptional regulator with a DBD comprised of 2 HTH motifs in its C-terminal region (69). Full-length MxiE is the product of transcriptional slippage and occurs approximately 30% of the time (110). The transcriptional slippage site is a stretch of 9 Ts, at which the RNAP stalls, adds an additional T and results in a frameshift (110). Without the frameshift, the smaller isoform of MxiE cannot activate the MxiE-dependent regulon (110). Additionally, the MxiE frameshift is necessary to express the downstream gene *mxiD,* a component of the T3SS. Due to this overlap in ORFs, a full deletion mxiE mutant is not feasible without disrupting the T3SS (111). This additional layer of MxiE regulation is thought to enhance the likelihood that activation of the late effector genes occurs at the right place and at the right time.

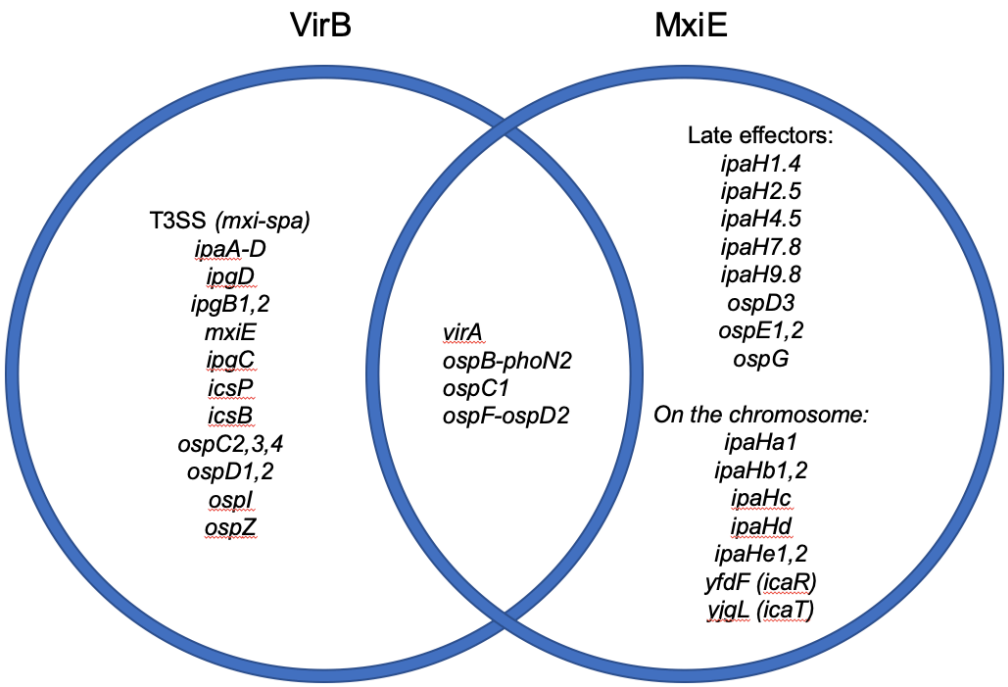

Figure 1.5. VirB- and MxiE-dependent regulons in *Shigella*.
Schematic adapted and updated from (Parsot, 2009) depicting the current genes known to be VirB and/or MxiE-dependent in *Shigella*.

The co-activator, IpgC, is required for MxiE-dependent gene regulation (100). Purified IpgC and MxiE proteins have been shown to co-immunoprecipitate, although this interaction has not been confirmed *in vivo* (105). Expression of MxiE or IpgC alone is not sufficient for MxiE-dependent gene activation, highlighting the importance of a MxiE/IpgC complex (100). This partner switching coupled to T3SS activation is also present in other bacteria, such as InvF/SicA in *Salmonella enterica* serovar Typimurium, ExsA and ExsC in *Pseudomonas aeruginosa*, and BsaN/BicA in *Burkholderia pseudomallei* (112).

MxiE-dependent activation relies on the presence of a 17 bp *cis*-acting regulatory sequence, termed the MxiE box (113, 114). The MxiE box is usually located in the vicinity of the -35 box in the promoter region of MxiE-dependent genes. Multiple alignment of MxiE boxes led to the establishment of the consensus sequence: GTATCGTTTTTTTAnAG. There are key positions within the MxiE box that are likely required for stabilizing the binding of the MxiE/IpgC complex (115). The box motif overlaps with a weak -35 region, and so it is thought that MxiE binds the box region and supports the recruitment of RNAP (113). Therefore, MxiE, in complex with IpgC, is considered to function as a classical transcriptional activator, similar to other AraC-like proteins, however, there is no experimental data to support this notion.

However, it has been recently shown that MxiE/IpgC can act outside of its normal transcriptional activator role to work in a negative feedback loop on the T3SS genes by negatively regulating the *virB* promoter, although it should be noted that the observed fold change was slight (116). This is unlikely mediated through VirF, because expression of *icsA*, the other VirF-dependent gene, is unchanged by MxiE/IpgC overexpression (116). Whether MxiE/IpgC is binding upstream of *virB*, and at what site, remains to be determined. Clearly there is still much to be discovered when it comes to MxiE-dependent gene regulation, as well as for homologous proteins in other bacterial pathogens.

Project Rationale

MxiE-dependent gene regulation is required for the secretion of late T3SS effector proteins. Many of these virulence effectors modulate the host innate immune response to *S. flexneri* infection. However, the complete MxiE-dependent regulon remains to be elucidated using a global approach. Here, we used RNA-seq to determine the entire MxiE-dependent regulon in *S. flexneri* by comparing gene expression levels in WT vs *mxiE* mutant strains following T3SS activation, via Congo red induction.

H-NS is known to be involved in the transcriptional repression of AT-rich genes in *S. flexneri,* including the genes encoding the T3SS. Although MxiE-regulated genes are AT-rich, it is unclear whether they may also be regulated by H-NS. Here, we investigate the interplay between MxiE-dependent and H-NS dependent gene regulation. This study provides novel contributions to our understanding of the regulation of *S. flexneri* virulence gene expression. Our findings could also provide insight for other pathogens with homologues to MxiE/IpgC, such as BsaN/BicA in *Burkholderia pseudomallei*.

2. Chapter 2: Investigation of MxiE- and H-NS-dependent gene regulation in *Shigella flexneri*

This chapter is a modified version of the published article: Hall CP, Jadeja NB, Sebeck N, and Agaisse H. "Characterization of MxiE- and H-NS-dependent expression of *ipaH7.8*, *ospC1*, *yccE,* and *yfdF* in *Shigella flexneri*." mSphere. 2022 November. doi: 10.1128/msphere.00485-22

Experimental Contributions: Hall CP designed and performed all experiments, wrote the manuscript, and created all figures, under the guidance and supervision of Agaisse H. Jadeja NB performed bioinformatic analysis and provided some graphics for the related figures. Sebeck N generated the pMMB CFP reporter vector backbone used for cloning.

2.1 Summary

Shigella flexneri uses a type 3 secretion system (T3SS) apparatus to inject virulence effector proteins into the host cell cytosol. Upon host cell contact, MxiE, a *S. flexneri* AraC-like transcriptional regulator, is required for the expression of a subset of T3SS effector genes encoded on the large virulence plasmid. Here, we defined the MxiE regulon using RNA-seq. We identified virulence plasmid- and chromosome-encoded genes that are activated in response to type 3 secretion in a MxiE-dependent manner. Bioinformatic analysis revealed that, similar to previously known MxiE-dependent genes, chromosome-encoded genes *yccE* and *yfdF* contain a regulatory element known as the MxiE box that was required for their MxiE-dependent expression. The significant A/T enrichment of MxiE-dependent genes suggested the involvement of H-NS. Using a dominant negative H-NS system, we demonstrated that H-NS silences the expression of MxiE-dependent genes located on the virulence plasmid (*ipaH7*.8 and *ospC1*) and on the chromosome (*yccE* and *yfdF*). Furthermore, we showed that MxiE was no longer required for the expression of *ipaH7.8*, *ospC1, yccE,* and *yfdF* when H-NS silencing was relieved. Finally, we showed that the H-NS anti-silencer VirB is not required for *ipaH7.8* and *yccE* expression upon MxiE/IpgC overexpression. Based on these genetic studies, we propose a model of MxiE-dependent gene regulation in which MxiE counteracts H-NS-mediated silencing.

2.2 Importance

The expression of horizontally acquired genes, including virulence genes, is subject to complex regulation involving the xenogeneic silencing protein, H-NS, and counter-silencing mechanisms. The pathogenic properties of *Shigella flexneri* mainly relies on the acquisition of the type 3 secretion system (T3SS) and cognate effector proteins, whose expression is repressed by H-NS. Based on previous studies, releasing H-NS-mediated silencing mainly relies on two mechanisms involving (i) a temperature shift leading to the release of H-NS at the *virF* promoter, and (ii) the virulence factor VirB, which dislodges H-NS upon binding to specific motifs upstream of virulence genes, including those encoding the T3SS. In this study, we provide genetic evidence supporting the notion that, in addition to VirB, the AraC family member MxiE also contributes to releasing H-NS-mediated silencing in *S. flexneri*.

2.3 Introduction

Shigella spp. are human-specific bacterial pathogens which are the causative agents of bacillary dysentery, also known as bloody diarrhea (1). Transmission occurs via the fecal-oral route and requires a very low infectious dose to cause disease (6). Disease is caused by invasion of the colonic epithelium and bacterial cell-to-cell spread, leading to destruction of the mucosa, vascular lesions and massive inflammation (5, 117). *Shigella* spp., as well as other Gram-negative bacteria, utilizes a type 3 secretion system (T3SS) needle-like apparatus to directly inject bacterial virulence effector proteins into the host cell cytosol (55). The translocated effector proteins are necessary for virulence through their roles in host cell invasion, cell-to-cell spread, and modulation of host cell signaling to promote immune evasion (64).

Descended from commensal *E. coli*, *S. flexneri* horizontally acquired its A/T-rich virulence plasmid, which encodes the proteins necessary for virulence (15, 18, 26). The presence of a global repressor known as histone-like nucleoid structuring protein (H-NS, previously referred to as VirR), that preferentially binds A/T-rich DNA, is thought to have allowed for the acquisition and maintenance of the energetically costly virulence genes (118, 119). Expression of the *S. flexneri* virulence genes follows a three-tiered regulatory cascade involving the transcriptional regulators VirF, VirB, and MxiE (67).

At 30°C, A/T-rich genes, including those on the virulence plasmid, are silenced by H-NS (73, 76, 85, 96, 120, 121). A shift in temperature to 37°C results in a change in DNA topology, which leads to the de-repression of the H-NS-bound *virF* promoter (77, 78, 119). Following *virF* expression at 37°C, VirF, the first-tier regulator, activates the expression of *icsA,* the gene required for actin-based motility and cell-to-cell spread, and *virB*, which encodes the second-tier regulator (73, 80, 122). VirB acts as an intermediate regulator of transcription, overcoming H-NS-mediated transcriptional silencing at a subset of promoters (85, 86, 89-91, 93, 96, 97, 119, 120). Genes whose expression relies on VirB include the genes encoding the T3SS, genes encoding virulence factors (*icsP*, *ospZ*, *ospD1*), and genes coding for the third-tier transcriptional regulator, MxiE, and its co-activator, IpgC (67, 82, 86, 87, 89, 96).

MxiE, as well as VirF, are members of the family of AraC-like transcriptional regulators, which are characterized by their DNA-binding domain (DBD) comprised of two helix-turn-helix (HTH) motifs that are thought to bind to the major groove of DNA (69). When the T3SS is not active, MxiE is bound by OspD1, which functions as an anti-activator, and the chaperone of OspD1, Spa15 (101). Meanwhile, IpgC is functioning as the chaperone for the translocon proteins, IpaB and IpaC (123). Upon host cell contact, IpaB and IpaC form the T3SS pore into the host cell membrane and OspD1 is secreted along with the

other first wave of effector proteins (56, 86, 102-104). This frees MxiE, which then interacts with its co-activator IpgC, leading to the expression of MxiE-dependent genes (67, 68, 100, 105). MxiE-dependent gene expression relies on the presence of a 17-bp *cis*-regulatory element, termed the MxiE box, located in the promoter region of MxiE-dependent genes (113, 115). Although MxiE and IpgC copurify as a complex, evidence that MxiE binds the MxiE box and functions as a transcriptional activator *in vitro* is lacking (105).

In this study, we use RNA-seq to determine the MxiE regulon. In addition to known MxiE-dependent genes located on the large virulence plasmid, we find MxiE-dependent genes located on the chromosome, including *yccE* and *yfdF*, and we demonstrate the functionality of bioinformatically identified MxiE box sequences in their promoter regions (109). Additionally, we demonstrate that H-NS silences the expression of MxiE-dependent genes located on the large virulence plasmid (*ipaH7.8* and *ospC1*) and on the chromosome (*yccE* and *yfdF*). Importantly, our genetic studies show that MxiE is no longer required for the expression of *ipaH7.8*, *ospC1, yccE,* or *yfdF* when H-NS silencing is relieved. Finally, we show that the anti-silencer VirB is not required for *ipaH7.8* and *yccE* expression upon MxiE/IpgC overexpression. Based on these genetic studies, we propose a model of MxiE-dependent gene regulation in which MxiE counteracts H-NS-mediated silencing.

2.4 Materials and Methods

Invasion assay

Human cancer-derived colonic epithelial cells, HT-29 (ATCC HTB-38), stably expressing plasma membrane-targeted YFP (mbYFP) were used for *Shigella* invasion assays (124). HT-29 mbYFP cells were cultured at 37°C and 5% CO_2 in McCoy's 5A medium (Gibco) that was supplemented with 10% heat-inactivated fetal bovine serum (FBS) (Invitrogen). Invasion assays were performed in 96-well assay plates (Corning, Cat# 3904) with confluent HT-29 mbYFP monolayers. Briefly, McCoy's media containing exponential phase *Shigella* containing a pMMB207 plasmid expressing CFP (pCFP) under an IPTG-inducible promoter was added to each well. The 96-well plate was then centrifuged at 1,000 rpm for 5 min to bring the bacteria into contact with the cell monolayer. The infection plate was then incubated at 37°C for 1 hr before adding gentamicin (50 μg/mL) to kill extracellular bacteria and IPTG (10 mM) to induce expression of pCFP in the bacteria. At 8 hours post-infection, the media in each well was aspirated and replaced with 4% paraformaldehyde/PBS to fix for 20 min at room temperature. After fixation, wells were washed 3x with 1X PBS prior to imaging. Each well was imaged using an ImageXpress Micro imaging system (Molecular Devices). The average number of infection foci per well was calculated using the CFP

channel and normalized to the bacterial Congo Red-positive CFU input. Three independent biological replicates were performed.

Bacterial strains and growth conditions

The *Shigella* wild-type strain used in this study is strain 2457T (3). Mutant strains (*mxiE*ΔDBD, Δ*virB*, *yccE* mutated MxiE box) were generated using a suicide vector, pSB890, for allelic exchange and homologous recombination (125). *E. coli* strains SM10λpir and Δ*nic*35 were used during the generation of mutant *Shigella* strains for maintenance of pSB890 constructs and conjugation, respectively. *E. coli* strain DH5α was used for cloning purposes. *E. coli* K-12 MC4100, both the WT strain and the *hns* mutant, were kindly provided by Marcia Goldberg (126, 127).

Prior to liquid culture, *Shigella* and *E. coli* strains were streaked to isolation from frozen glycerol stocks on LB (lysogeny broth, Fisher) agar plates containing the appropriate antibiotic for selection and incubated at 37°C overnight. Using a single isolated colony, overnight cultures in LB media were grown rotating on a wheel at 30°C or 37°C, for *Shigella* and *E. coli* strains, respectively.

For gene expression experiments, *Shigella* and *E. coli* cultures were grown at 30°C or 37°C (as indicated) on a rotating wheel for either 3hr or 6hr (dominant negative H-NS experiments) after back dilution (1:100) of an overnight culture in 5 mL LB media. Congo red dye (Fisher) was added (100 μg/mL) to LB agar to select red, i.e. virulence plasmid-containing, colonies and at the time of back

dilution of liquid *Shigella* cultures to activate secretion, i.e. MxiE-dependent gene activation. L-arabinose (0.2%, p*hns*ΔDBD and p*ipgC*; 1%, p*mxiE*) (Sigma) and isopropyl-β-D-thiogalactopyranoside (IPTG) (1 mM, p*mxiE*) (Fisher) were added at time of back dilution to induce expression of pBAD and pMMB constructs, respectively. 2,6-diaminopimelic acid (DAP) (Sigma Life Sciences) was supplemented (100 μg/mL) to LB media for the growth of *E. coli* strain Δ*nic*35. Depending on the strain and/or plasmid antibiotic-resistance, the following antibiotics were supplemented in LB media and agar: ampicillin (100 μg/mL), chloramphenicol (10 μg/mL), tetracycline (10 μg/mL), spectinomycin (100 μg/mL), kanamycin (30 μg/mL).

Plasmids and Cloning

All primers (with restriction sites for cloning indicated) used in this study are listed in Table A3. Overexpression constructs were made using either an arabinose-inducible pBAD promoter in vector pBAD18 (ATCC 87393) or an IPTG-inducible promoter in vector pMMB207 (ATCC 37809). The CFP-reporter constructs were made by cloning the promoter of interest upstream of CFP in a pMMB207 vector backbone. Briefly, we introduced mCherry, under the IPTG-inducible promoter, into pMMB207 with a linker and subsequently cloned in CFP with upstream KpnI/BglII cut sites for introducting promoter regions of interest (this study, Table S3). The promoter-less control is the pMMB CFP

reporter without a promoter introduced upstream. All plasmid constructs were verified using Sanger sequencing.

Plasmid DNA was isolated using a Miniprep kit (Qiagen). Ligations were performed using digested plasmid and PCR product DNA with T4 DNA ligase (New England Biolabs). Ligations were transformed into chemically competent DH5α or SM10λpir cells by heat shock at 42°C for 1 min, followed by the addition of SOC medium, recovery at 37°C for 1 hr, and subsequent plating onto LB agar with the appropriate antibiotic. pSB890 constructs were transformed into electrocompetent Δ*nic*35 cells by electroporation using a MicroPulser (BioRad) with the Ec2 setting, followed by recovery in SOC medium for 1 hr at 37°C on a rotating wheel and subsequent plating on LB agar supplemented with DAP and the appropriate antibiotic. pBAD and pMMB constructs were transformed into *Shigella* strains following multiple sterile water washes of a 10 mL exponential phase bacterial pellet followed by resuspension in 100 µL of sterile water with 10% glycerol added to generate competent bacteria. Plasmid DNA (~100-400 ng) was added to the tube of the competent *Shigella* and incubated on ice for 15 min. Following incubation with the DNA, the *Shigella* was electroporated and subsequently recovered and plated as detailed above.

RNA extraction, cDNA synthesis, and qPCR

The pelleted bacteria were resuspended in 1 mL of TRIzol reagent (Fisher). RNA was separated via chloroform extraction by adding 200 μL of chloroform to the TRIzol resuspension and vortexing to mix. The layers were separated by centrifugation at 12,000 rpm for 15 min at 4°C. The aqueous layer was transferred to a new tube and subsequently used in the Ribopure Bacterial RNA extraction kit (Invitrogen). Following RNA elution of the column, RNA was DNase I-treated using the kit reagents for 30 min at 37°C. DNase I-treated RNA was used to synthesize cDNA using SuperScript II reverse transcriptase and random primers (Invitrogen). Synthesized cDNA was diluted 1:5 with nuclease-free water prior to use.

qPCR was performed using a LightCycler 96 (Roche) with either the probe-based method (Roche Universal Probe Library) or SYBR Green (BioRad), depending on assay design availability. Primers used for qPCR are listed in Table S3. The $\Delta\Delta C_t$ method of analysis was performed to determine the relative fold change in gene expression compared to a control group. The housekeeping gene *rpoB* was used for normalization.

RNA-seq: Library construction and sequencing

RNA from WT and *mxiE*ΔDBD mutant *S. flexneri* cultures, with and without Congo red supplementation, was extracted as described above. Library preparation and RNA sequencing were outsourced to Novogene (California,

USA). Briefly, the library construction included steps of total RNA qualification, mRNA enrichment using Ribo-Zero rRNA removal kit specific for bacteria rRNA (Illumina, #MRZMB126), cDNA synthesis, end repair and adaptor ligation, size selection of fragments, and PCR followed by quality check. The quality checks before and after the library construction were performed using Nanodrop and agarose gel electrophoresis including an integrity check on a 2100 Bioanalyzer (Agilent Technologies) prior to sequencing. The NEB Next Ultra II RNA Library Prep Kit for Illumina (BioLabs, New England, MA, USA) was used for sequencing starting with the step of strand-specific library synthesis where the dTTPs were replaced by dUTPs during the synthesis of the second strand cDNA. The overhangs were converted to blunt ends, followed by adenylation of 3′ ends and adapter ligation using RNA 5' and RNA 3' adapters included in the kit. Library concentration of 1.5 ng/μl was used after ensuring the insert size in a quality assessment prior to sequencing. The resulting libraries were sequenced on Illumina where the libraries constructed were further subjected to cluster growth and sequencing, image acquisition, and base calling steps.

RNA-seq: Data analysis

The raw reads from the sequencing were subjected to analysis of adapter read identification and trimming of the same using Trimmomatic (128). Quality check pre and post-adapter trimming were performed using FastQC (129). Both

alignment-based and alignment-independent methods were used to align the clean paired-end reads generated for the four samples. The genome sequence available in NCBI (chromosome: AE014073.1 and plasmid pCP301: NC_004851.1) was used for alignment-based methods using Bowtie for Illumina (130). Fold change calculations were performed from the counts generated using featureCounts where annotations for gene regions were provided in the GTF format and transcripts per million (TPM) values using Kallisto (131, 132). The pseudo-alignments were performed using a reference transcriptome file for Kallisto and TPM values were generated. The counts were normalized considering the variation in size of datasets, varying gene lengths and gene assignments for estimated counts less than 100 in either one of the samples being compared were eliminated. Resulting values were used to calculate fold change and log2 fold-change values. The upregulated genes were tabulated based on these calculations (Table A1). RNA-seq results were validated via qPCR with three biological replicates for the genes of interest, such as *yccE* and *yfdF*.

MxiE motif search

The chromosome and plasmid sequence used for reference-based alignment (chromosome: AE014073.1 and plasmid pCP301: NC_004851.1) was subjected to motif search using FIMO (133). An .xml file was prepared by tabulating scores for the four nucleotides encoding the known MxiE box sequence (113, 115, 134).

This xml file was used to scan the chromosomal and plasmid sequence individually and the motif sequence matches were retrieved. Based on the location homology with the genes enlisted in Table A2 (upregulated and downregulated) the motif matches were retrieved. All the motif matches falling within the 400bp flanking regions of the MxiE-dependent genes in chromosome and plasmid sequence were retrieved. In case of known motifs that exceeded the length from the genes >400bp the sequences were manually aligned. The identified genes displaying the motif sequence were tabulated (Table A2).

Bamcompare from deepTools2 was used to compare the reads from RNA-Seq MxiEwCR and WTwCR aligned to the reference chromosome: AE014073.1 and plasmid pCP301: NC_004851.1 sequence in Galaxy server (135) (https://galaxyproject.org/). Here the genome was divided into bins of 50 bp size and the overlapping reads were used to calculate differences by subtracting the input from counts measured in experimental (MxiEwCR) dataset. In case of partial overlaps the respective fraction was considered in the calculations. A binary BigWig file was generated for visualization in IGB in alignment with the plasmid sequence and its gtf annotation file (136). The peak regions were visualized and the virulence genes encoded within the peak regions were identified through alignments with the plasmid sequence (221618 bp). The advanced search option in IGB was used to view the motifs and were color coded

based on similarity in motif sequences and their location could be mapped based on sequence searches and annotation file.

GC Percent

The GC percent of regions of interest was calculated using the GC-Profile tool with suggested parameters halting parameter set to 10, minimum length to segment set to100 bp and gap less than 10% in the input sequences were filtered (137).

***yccE* phylogeny analysis**

The 1257 bp sequence *yccE* gene sequence was analysed for phylogenetic relationships using the Neighbor-Joining and JTT matrix-based method for a bootstrap consensus tree with distances in MEGA11 and edited in iTOL (138, 139). Representatives of previously defined phylogroups were selected.

Data Availability: The RNA-Seq datasets generated in this study will be available under the Bioproject number: PRJNA868769

2.5 Results

Characterization of the *mxiE*ΔDBD strain

Previous *mxiE* mutants were generated by insertion of antibiotic resistance cassettes (68, 100). Generation of a full *mxiE* deletion mutant was not feasible due

to an overlap in reading frames with the downstream gene, *mxiD,* which requires the transcriptional slippage for the generation of full-length MxiE to occur (111). To generate a *mxiE* mutant that lacks regulatory function in the 2457T background, we deleted the DNA-binding domain (DBD), which is comprised of 2 helix-turn-helix (HTH) motifs (Figure 2.1A, *mxiE*ΔDBD). The Congo red dye is commonly used to activate *S. flexneri* type 3 secretion, which leads to the expression of MxiE-dependent genes (61, 62). We used qPCR to assay regulation of MxiE-dependent genes in the *mxiE*ΔDBD mutant compared to wild type (WT) and found significantly decreased expression of representative MxiE-dependent genes, *ipaH7.8* and *ospC1* (Figure 2.1D-E). Importantly, complementation with *mxiE* expressed in *trans* from a pBAD arabinose-inducible promoter fully restored gene expression (Figure 2.1D-E). Deletion of the DBD in *mxiE* did not affect T3SS expression, as determined by *ipgD* expression (Figure 2.1B). Accordingly, infection of a human colorectal cell line (HT-29) cells led to a similar number of infection foci, showing that the *mxiE*ΔDBD mutant strain was as invasive as wild type bacteria (Figure 2.1C). These data demonstrate that the *mxiE*ΔDBD strain has a regulatory defect for MxiE-dependent genes and that the deletion of the DBD does not affect the expression of the T3SS or virulence.

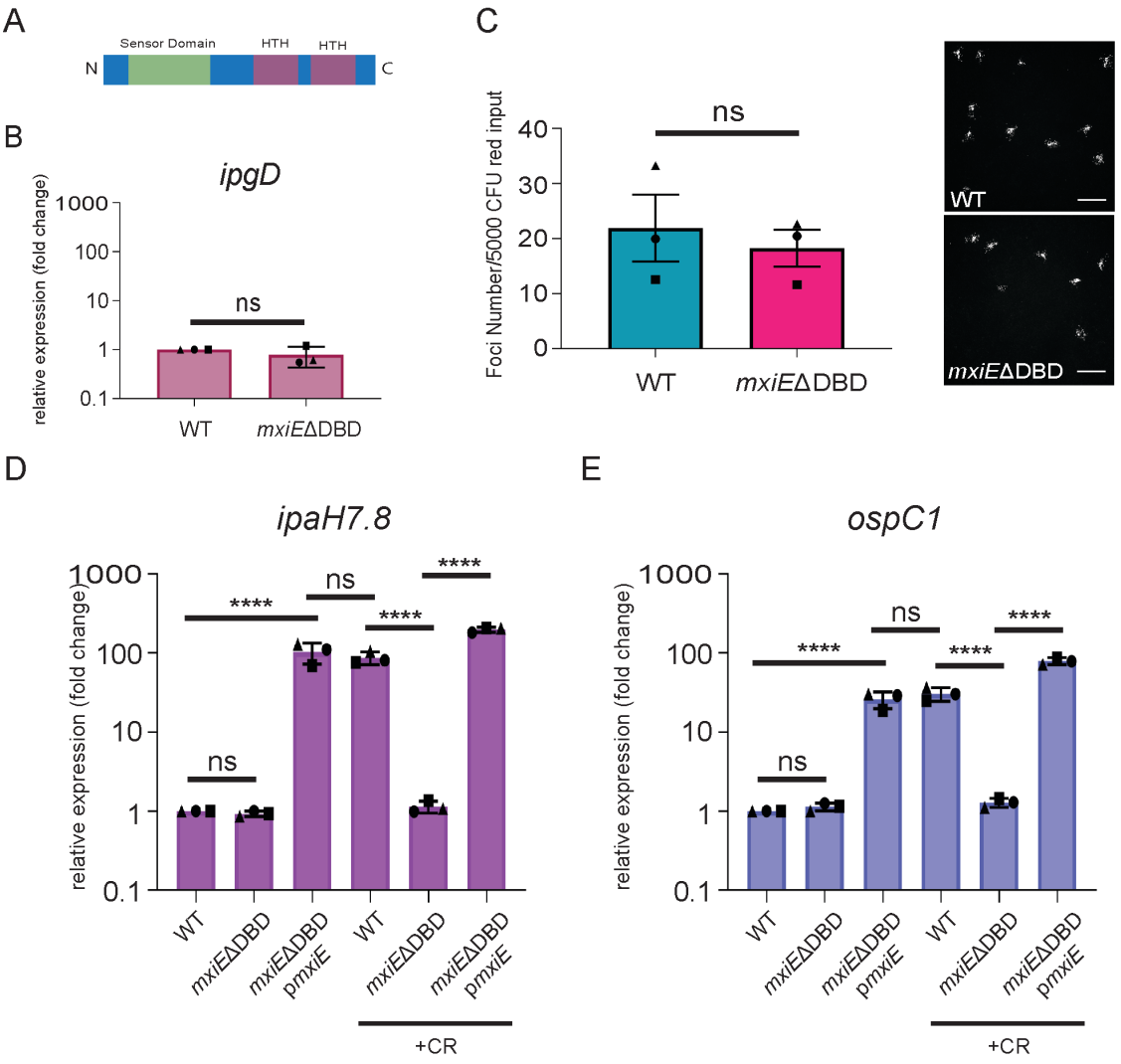

Figure 2.1: Design and validation of the *mxiE*ΔDBD strain. (A) Schematic of the MxiE protein domains, including the DNA-binding domain (DBD) which is comprised of two helix-turn-helix (HTH) motifs. **(B)** qPCR of *ipgD* in *mxiE*ΔDBD relative to WT. **(C)** Invasion assay where number of foci formed in HT-29 cells was quantified and compared relative to WT. Representative images of infection foci for WT and *mxiE*ΔDBD at 8 hr post-infection. The scale bar is 100 μm. WT, *mxiE*ΔDBD, and *mxiE*ΔDBD complemented with pBAD *mxiE* (p*mxiE*) strains were grown at 37°C without and with Congo Red dye (CR) and qPCR was performed for **(D)** *ipaH7.8* and **(E)** *ospC1* mRNA expression relative to WT. Data shown are the averages of three independent biological experiments and the error bars represent standard deviation. Student's T-test (B-C) or One-way ANOVA (D-E) with Tukey's multiple comparison test was performed; ns, not significant; ****, $p<0.0001$.

Defining the MxiE-dependent regulon

Utilizing comparative analysis of RNA-seq data, we identified 41 genes whose expression was increased at least two-fold upon growth of WT bacteria in presence of the Congo red dye (Table A1). With the exception of *zraP* and *spy*, all of these differentially expressed genes (DEGs) relied on MxiE for full expression in response to the Congo red dye (Table A1). As expected, we identified known MxiE-dependent T3SS genes located on the large virulence plasmid, such as *ipaH7.8* and *ospC1* (Table A1 and Figure 2.2C). We also identified T3SS effector genes of the IpaH family located on the chromosome, including *ipaH*_1 (pseudogene in 2457T), *ipaH_2*, *ipaH_4*, *ipaH_5*, and *ipaH_7* (Table A1). Interestingly, we identified additional DEGs located on the chromosome, including *yccE* (gene ID 1077473), *yfdF* (gene ID 1026565), and *yjgL* (gene ID 1027047) (pseudogene in 2457T), whose expression relied on MxiE (Figure 2.3A-B and Table A1).

To identify putative MxiE box sequences for the RNA-seq DEGs, we conducted a bioinformatic analysis using the MEME suite (Figure 2.2A). The MxiE motif (GTATCGTTTTTTTAnAG) search resulted in 47 matches in the virulence plasmid (Accession no. NC_004851.1) and 496 matches (with up to 4 potential substitutions) in the chromosome sequence (Accession no. AE014073.1)

(113, 115). We identified potential MxiE box motifs for 18 of the DEGs relying on MxiE for activation (Table A2). These DEGs included virulence plasmid-encoded effector genes (Figure 2.2B) as well as chromosome-encoded IpaH family members (Table A2). Interestingly, we found MxiE box motifs upstream of *yccE*, *yfdF, and yjgL* (Figure 2.3A-B and Table A2). Altogether, these data identify chromosomal genes whose expression is dependent on the activity of the T3SS and MxiE.

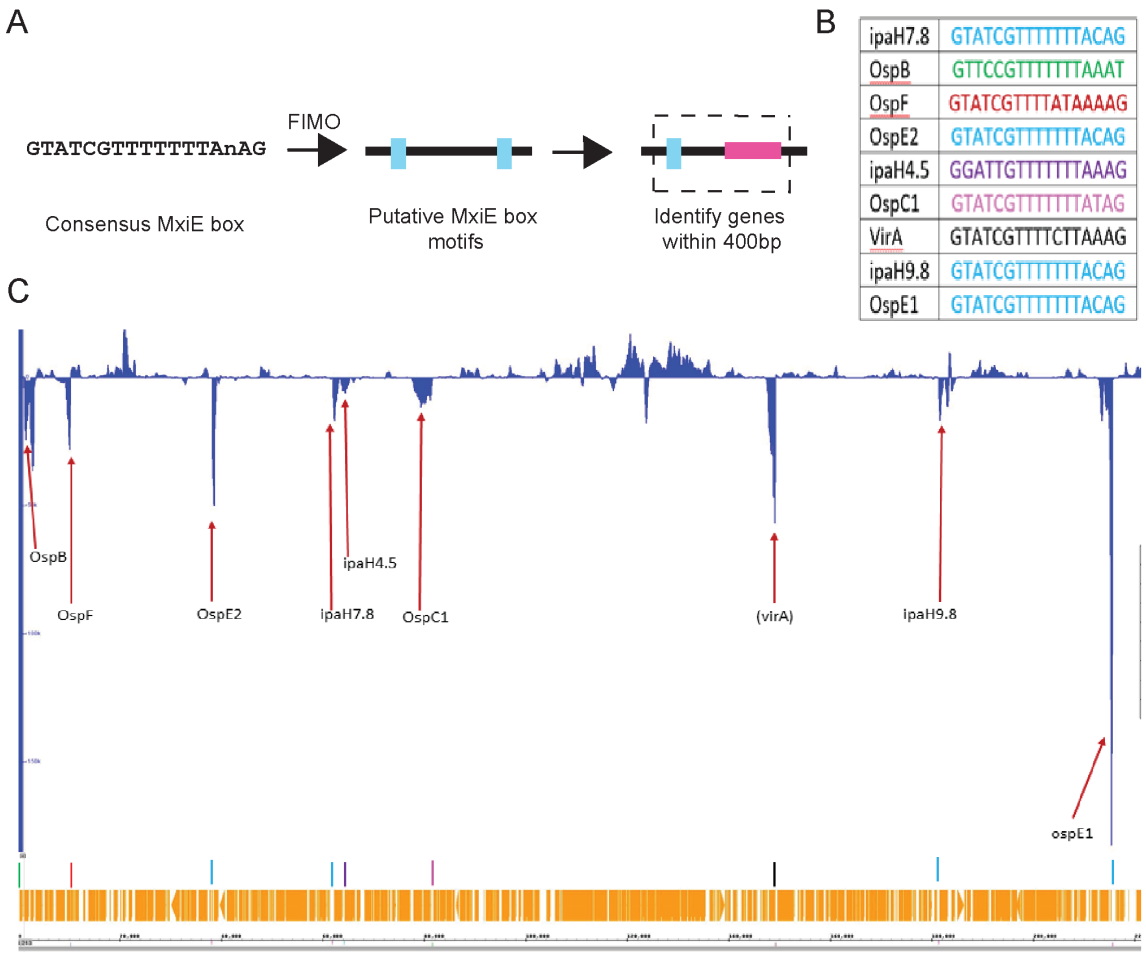

Figure 2.2: Validation of MxiE box motif search in RNA-seq identified DEGs. (A) Schematic of bioinformatics analysis to identify putative MxiE box motifs and genes downstream. **(B)** Resulting MxiE box motifs from FIMO analysis in the virulence plasmid. MxiE box sequences with same color have identical sequences. **(C)** Gene expression peaks in the virulence plasmid from RNA-seq comparison of WT without vs with addition of Congo red dye. MxiE box sequences were identified as described in **(A)** and marked with corresponding color in **(B)**.

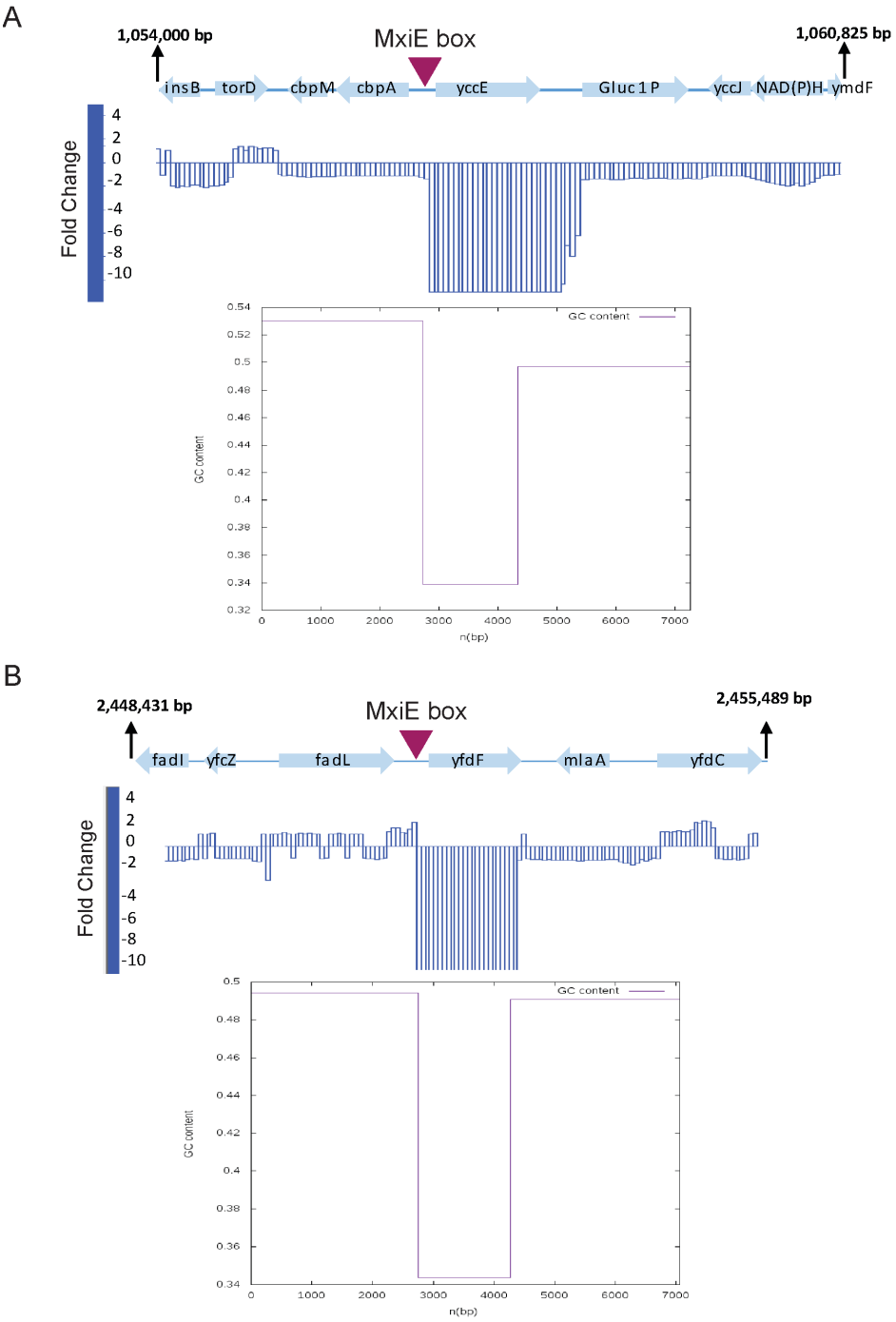

Figure 2.3: RNA-seq identified MxiE-dependent chromosomal genes. Gene expression peaks from the RNA-seq data comparison of *mxiE*ΔDBD vs wild type *S. flexneri*, both with the addition of Congo red dye, which revealed chromosome-encoded genes **(A)** *yccE* and **(B)** *yfdF* that are down-regulated in the *mxiE*ΔDBD mutant compared to wild type. MxiE box motifs found using FIMO bioinformatic analysis are indicated with the arrowheads. GC content for **(A)** *yccE* and **(B)** *yfdF* and the flanking regions is depicted below the gene expression peaks.

Validation of *yccE* and *yfdF* as MxiE-dependent genes

To validate our RNA-seq results, we sought to confirm the necessity of MxiE for the expression of the representative chromosomal genes of interest, *yccE* and *yfdF* (Figure 2.4, WT and *mxiE*ΔDBD -/+CR). We did not pursue *yjgL* as it is a pseudogene in *S. flexneri* 2457T. We performed qPCR using RNA isolated from bacterial cultures of the *mxiE*ΔDBD mutant and WT *Shigella* with overexpression of *mxiE* from an arabinose-inducible pBAD promoter. As expected, we saw a regulatory defect in the *mxiE*ΔDBD mutant, however, when *mxiE* was overexpressed upon addition of arabinose, we observed a rescue of expression to WT levels (Figure 2.4A-B). These data therefore confirm our RNA-seq results and demonstrate that MxiE is required for the expression of *yccE* and *yfdF*.

Our bioinformatic analysis supported the notion that *yccE* and *yfdF* harbor a putative MxiE box in the vicinity of their coding region (Figure 2.3 and Table A2). To test the functionality of these putative MxiE box sequences we used a CFP reporter construct with or without mutations (G6>C and T10>A) into the 17-bp MxiE box of *yccE* and *yfdF* and assayed CFP expression as a readout of promoter activation (nucleotides mutated are underlined in Figure 2.5A). We found that the WT promoter resulted in significant CFP expression compared to promoter-less control, and the introduction of the mutations in the MxiE box

abolished activation in response to the Congo red dye (Figure 2.5B-C). As a control, we assayed promoter activation in the *mxiE*ΔDBD mutant and as expected, we observed no significant activation of the WT *yccE* and *yfdF* promoters. However, activation was rescued by overexpressing *mxiE* using a pBAD arabinose-inducible construct (Figure 2.5B-C). These results provide evidence that the chromosomal genes *yccE* and *yfdF* have a functional MxiE box in their promoter region.

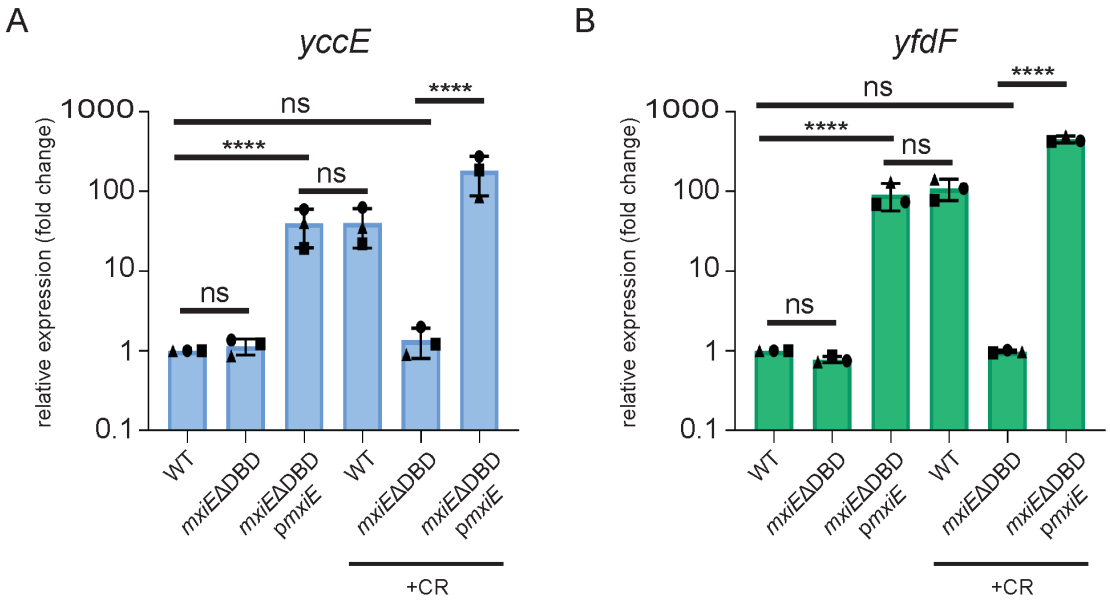

Figure 2.4: MxiE is necessary for *yccE* and *yfdF* expression. WT, *mxiE*ΔDBD, and *mxiE*ΔDBD complemented with pBAD *mxiE* (p*mxiE*) strains were grown at 37°C without and with Congo Red dye (CR) and qPCR was performed for **(A)** *yccE* and **(B)** *yfdF* mRNA expression relative to WT. Data shown are the averages of three independent biological experiments and the error bars represent standard deviation. One-way ANOVA with Tukey's multiple comparison test was performed; ns, not significant; ****, $p<0.0001$.

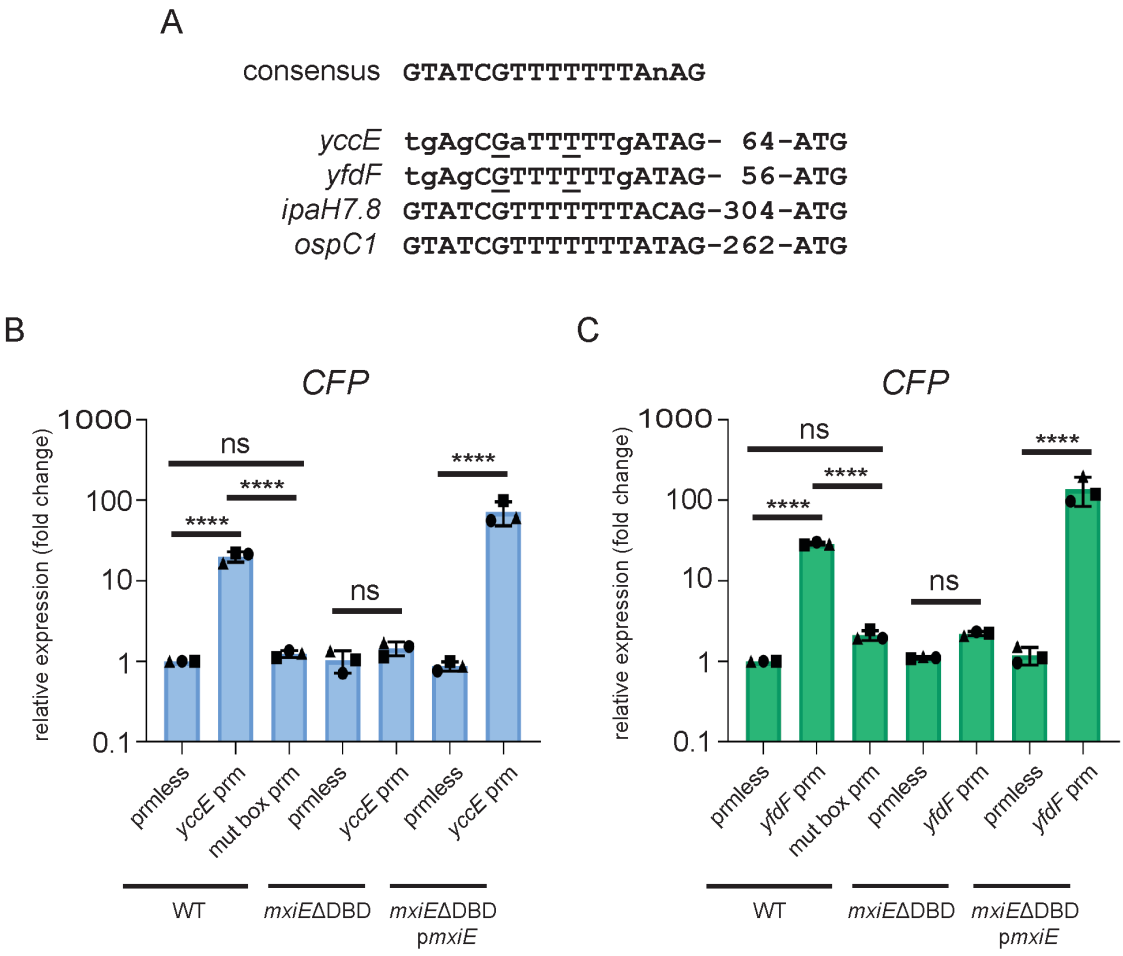

Figure 2.5: *yccE* and *yfdF* have functional MxiE box cis-regulatory elements. (A) Alignment of the MxiE box sequences of MxiE-regulated genes with mutation sites underlined. WT, *mxiE*ΔDBD, and *mxiE*ΔDBD complemented with pBAD *mxiE* (p*mxiE*) strains harboring the CFP reporter constructs, promoter-less control (prmless), *yccE*/*yfdF* promoter (*yccE*/*yfdF* prm), and *yccE*/*yfdF* mutated MxiE box promoter (mut box prm), were grown at 37°C with Congo Red dye (CR) to induce T3SS secretion and qPCR was performed for CFP mRNA expression as a proxy for **(B)** *yccE* and **(C)** *yfdF* promoter activation relative to WT promoter-less. Data shown are the averages of three independent biological experiments and the error bars represent standard deviation. One-way ANOVA with Tukey's multiple comparison test was performed; ns, not significant; ****, $p<0.0001$.

yccE phylogeny analysis

While virulence plasmid-encoded MxiE-dependent genes are uniquely found in *Shigella* spp., we found that, similar to *yfdF*, the chromosome-encoded gene *yccE* is conserved in *E. coli* (114) (Figure 2.6). The representatives of the phylogroups known to be closely related to *S. flexneri* strains revealed the homology of the gene with commensal *E. coli* strains that are usually classified under the phylogroups A and B1. The sequence homology was not conserved across these phylogroups indicating no significant correlation between phylogenicity and virulence (17, 140). The amino acid sequence alignments revealed more conserved sites in the second half of the gene, suggesting the presence of a conserved domain, although there were no domains predicted for YccE with high confidence. The *yccE* gene was absent in *S. boydii* and members of the B2 phylogroup and present but fragmented in *S. dysenteriae* and *S. sonnei*.

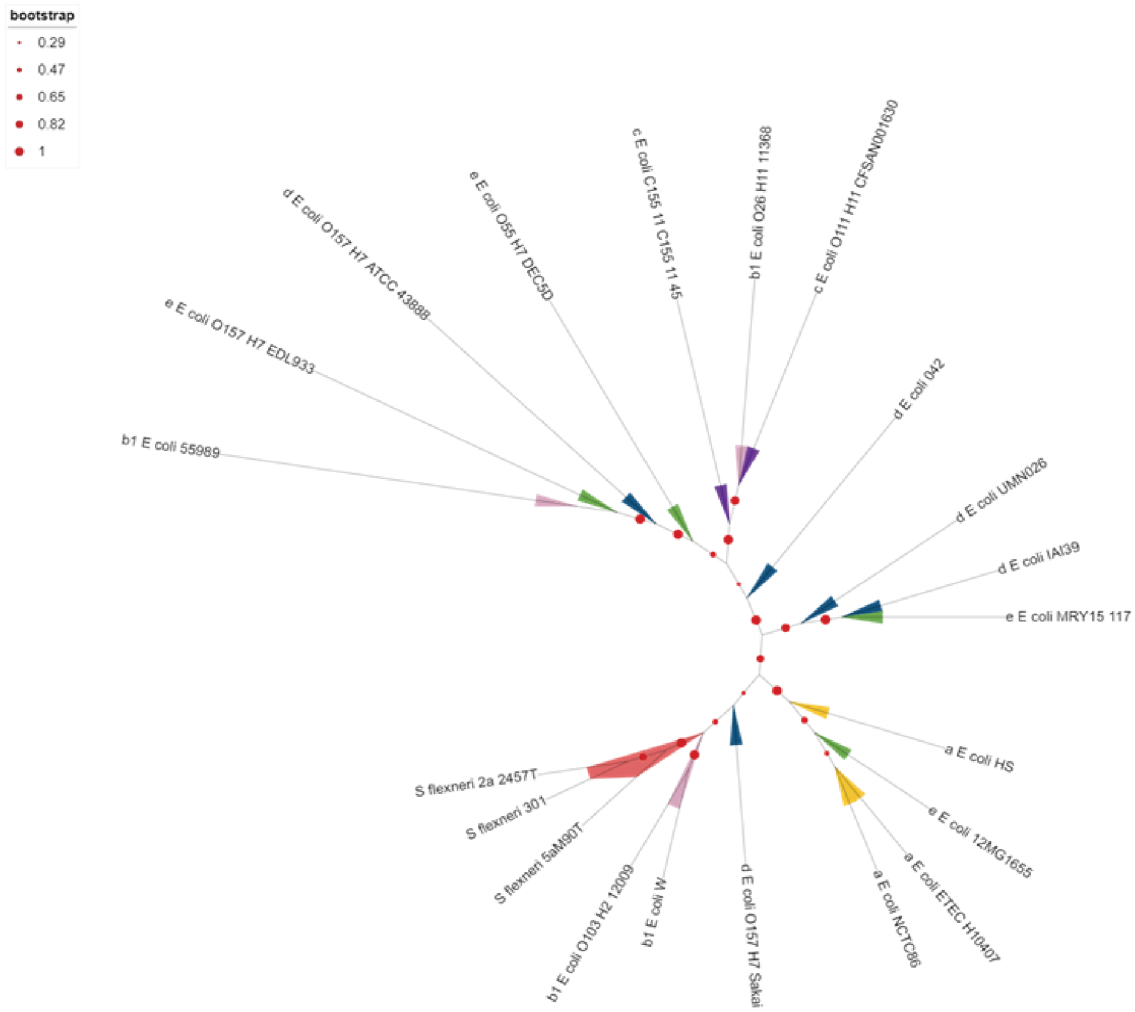

Figure 2.6: Phylogenetic tree of homologous proteins to YccE. An unrooted phylogenetic tree depicting evolutionary relationships of the identified homologous proteins to YccE using representatives of phylogroups of *Shigella* spp. and *E. coli*. The phylogroups are indicated in the tree as the first character before the bacterial name as well as with colors [i.e. *Shigella* (red), A (yellow), B1 (pink), C (purple), D (blue), or E (green)].

We further analyzed the gene arrangement surrounding the *yccE* locus using the PATRIC database. The *E. coli* strain MG1655 was the closest match to the gene arrangement at the *yccE* locus in *S. flexneri* strain 2a 301. By contrast, in addition to reductases, phosphatase and chaperone coding genes, IS elements (A-D) and genes encoding phage proteins were found interspersed in *S. flexneri* 2a 301 and *S. dysenteriae* Sd197 (Figure 2.7). Altogether, these data reveal the conservation of the *yccE* gene across many *E. coli* and *Shigella* strains, with a great variability of gene organization in the chromosome region surrounding the *yccE* locus.

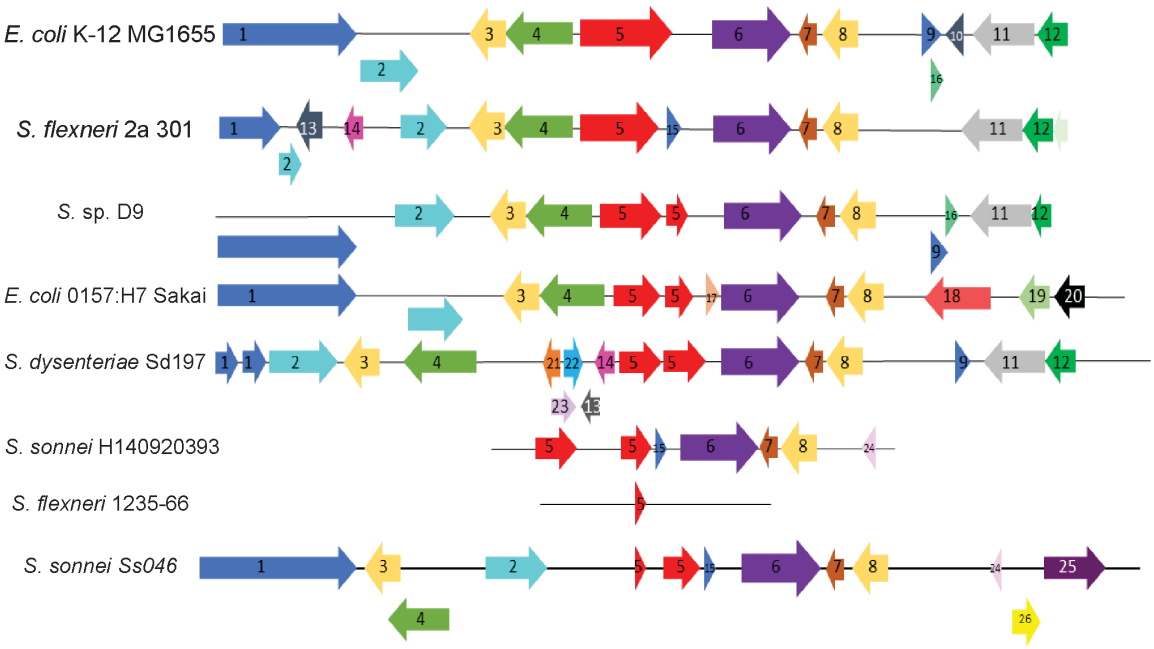

Figure 2.7: Gene arrangement for regions around *yccE*. Gene arrangement analysis for a 10,000 bp region including *yccE* for different *Shigella* spp. and non-pathogenic (K-12) and pathogenic (0157:H7) *E. coli* species. The length and direction of the arrows are indicative of gene length and orientation. The numbers on the arrows indicate the protein or insertion elements: 1) trimethylamine-N-oxide reductase (TorA), 2) TorA specific chaperone protein TorD, 3) Chaperone modulator protein CbpM, 4) DNA-J class molecular Chaperone CbpA, 5) YccE, 6) Glucose-1-phosphatase, 7) YccJ, 8) NAD(P)H dehydrogenase, 9) YmdF uncharacterized protein, 10) hypothetical protein, 11) pyrimidine permease RutG, 12) FMN reductase, 13) InsB, 14) InsA, 15) hypothetical protein,16) hypothetical protein, 17) hypothetical protein, 18) phage integrase, 19) phage protein, 20) phage protein, 21) transposase, 22) Ins C, 23) Ins D.

H-NS represses *ipaH7.8*, *ospC1*, *yccE*, *yfdF*, and the *E. coli* homologous genes of *yccE* and *yfdF*

Previous observations suggested that virulence genes encoding the T3SS as well as MxiE-dependent T3SS effector proteins, are A/T-rich compared to housekeeping genes in *S. flexneri* (26). We thus conducted a bioinformatic analysis of the GC content at the *yccE* and *yfdF* loci, including 3000 bp flanking their respective coding region (Fig.2). The analysis of the GC profile segmentation revealed a dramatic A/T enrichment (> 65%) at both loci compared to the surrounding chromosomal regions (Figure 2.3A-B).

H-NS, a protein involved in organization and regulation of the nucleoid, is known to preferentially bind A/T-rich regions of DNA (i.e. low GC content) (36, 141). Therefore, we hypothesized that H-NS may be involved in the transcriptional repression of MxiE-dependent genes, including *yccE* and *yfdF*. Failed attempts to generate a full deletion *hns* mutant in *S. flexneri* 2457T led us to suspect that a strain lacking *hns* may not be viable. We note that existing *hns* mutants were obtained by transposon mutagenesis which resulted in the production of a truncated polypeptide (73, 118). We thus turned to a dominant negative overexpression system, where a truncated form of H-NS is overexpressed using a pBAD arabinose-inducible promoter (p*hns*ΔDBD). Similar truncations of H-NS displaying dominant negative properties have been used in

enteropathogenic *E. coli* (EPEC) as well as in *Yersinia enterocolitica* (142, 143). By overexpressing the oligomerization domain of H-NS, the endogenous full-length H-NS that is capable of DNA binding is sequestered, allowing for activation of H-NS-repressed genes (Figure 2.8A). We validated the dominant negative system by showing that the H-NS-regulated gene, *virB,* was indeed de-repressed upon overexpression of dominant negative H-NS, while the expression of the housekeeping gene, *dnaA,* was unaffected (Figure 2.9) (73).

Using *ipaH7.8* and *ospC1* as representative virulence plasmid-encoded MxiE-dependent genes, we observed that sequestration of H-NS led to a significant increase in MxiE-dependent gene expression, similar to the activation observed in presence of the Congo red dye (Figure 2.8B-C). In addition, we found that the expression of the chromosomal genes *yccE* and *yfdF* was also significantly increased upon overexpression of the dominant negative H-NS (Figure 2.8D-E). We finally investigated whether H-NS repression of MxiE-dependent genes is conserved in non-pathogenic *E. coli*. Upon overexpression of the dominant negative H-NS in *E. coli* DH5α, we observed a significant increase in mRNA expression of the homologous *E. coli* genes *yccE* and *yfdF* (Figure 2.10A-B). We confirmed these results in strain MC1400 and its isogenic *hns* mutant (Figure 2.10C-D).

Altogether, these results indicate that H-NS silences the expression of representative MxiE-dependent genes, including *ipaH7.8* and *ospC1* on the virulence plasmid and *yccE* and *yfdF* on the chromosome.

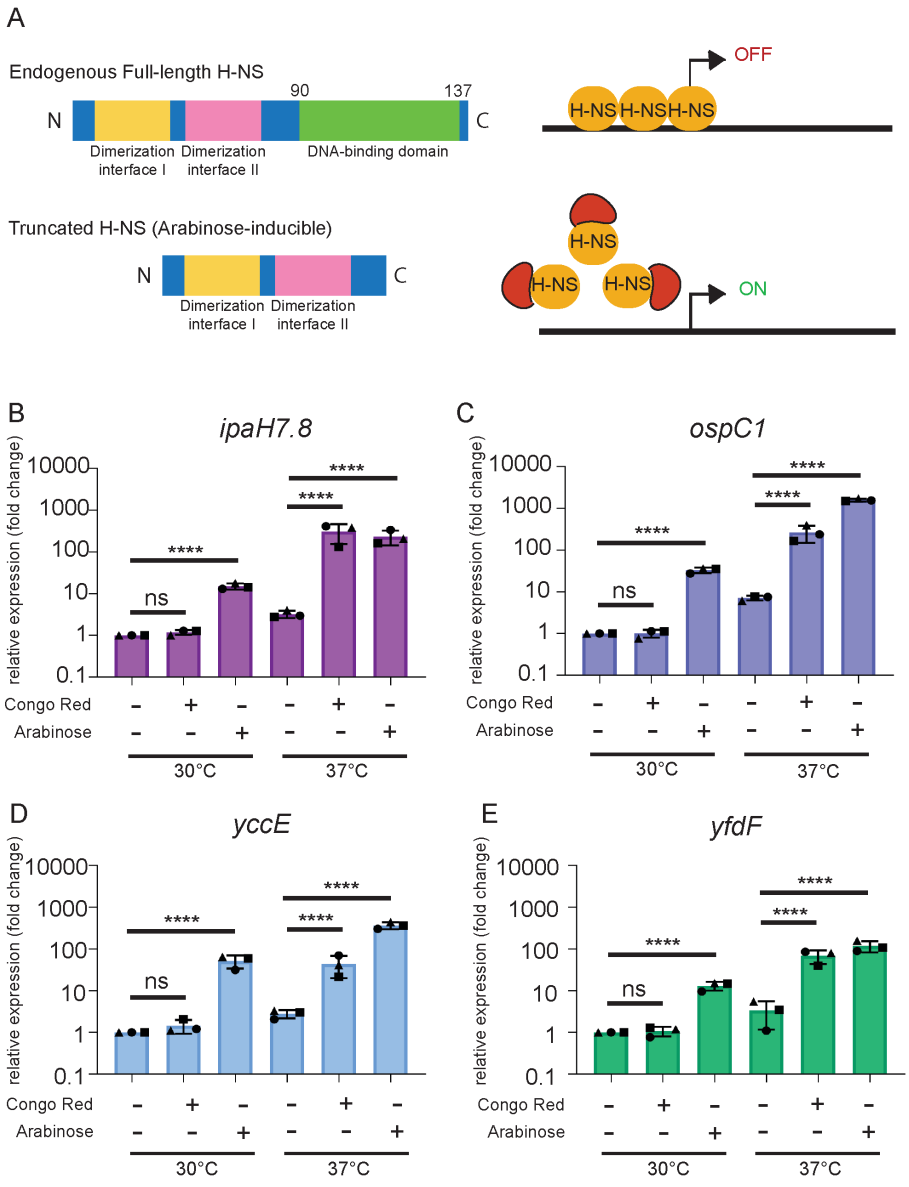

Figure 2.8: Sequestration of H-NS in *S. flexneri* leads to *ipaH7.8*, *ospC1*, *yccE*, and *yfdF* expression in non-permissive conditions. (A) Schematic of the H-NS dominant negative overexpression system where a truncated H-NS (ΔDBD) is induced by arabinose and oligomerizes with endogenous H-NS preventing DNA-binding and transcriptional repression. The *S. flexneri* WT strain with the dominant negative H-NS construct was grown at 30°C or 37°C with either no arabinose (-Ara), with arabinose (+Ara), or no arabinose but with Congo Red (-Ara +CR) and qPCR was performed for mRNA expression levels of **(B)** *ipaH7.8*, **(C)** *ospC1*, **(D)** *yccE*, and **(E)** *yfdF*. Data shown are the averages of three independent biological experiments and the error bars represent standard deviation. One-way ANOVA with Tukey's multiple comparison test was performed; ns, not significant; ***, p=0.0002; ****, p<0.0001.

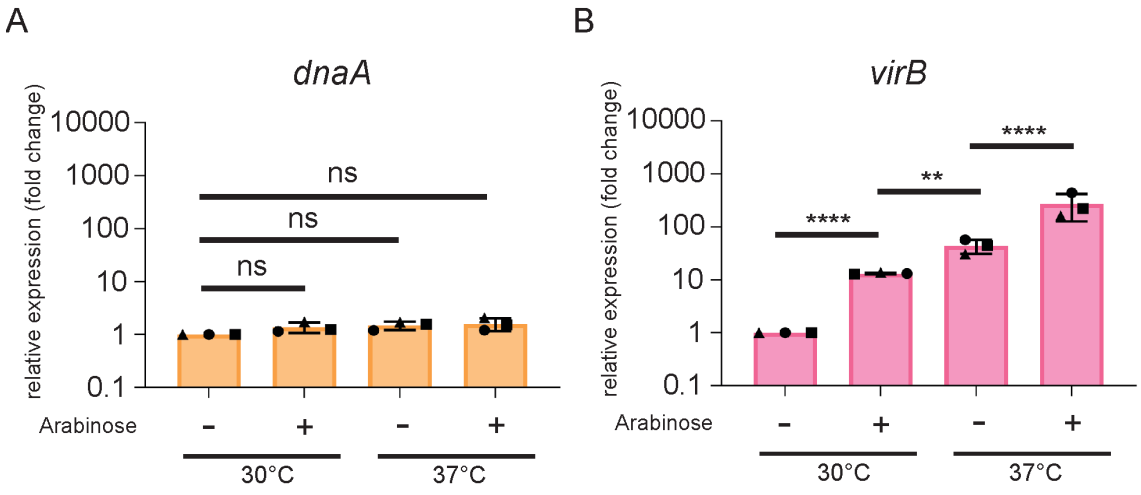

Figure 2.9: Validation of the dominant negative H-NS overexpression system. The *S. flexneri* WT strain with the dominant negative H-NS construct was grown at 30°C or 37°C with either no arabinose (-Ara) or with 0.2% arabinose (+Ara) and qPCR was performed for mRNA expression levels of a positive control for H-NS repression **(A)** *virB* and a negative control **(B)** *dnaA*. Data shown are the averages of three independent biological experiments and the error bars represent standard deviation. One-way ANOVA with Tukey's multiple comparison test was performed; ns, not significant; **, $p<0.01$; ****, $p<0.0001$.

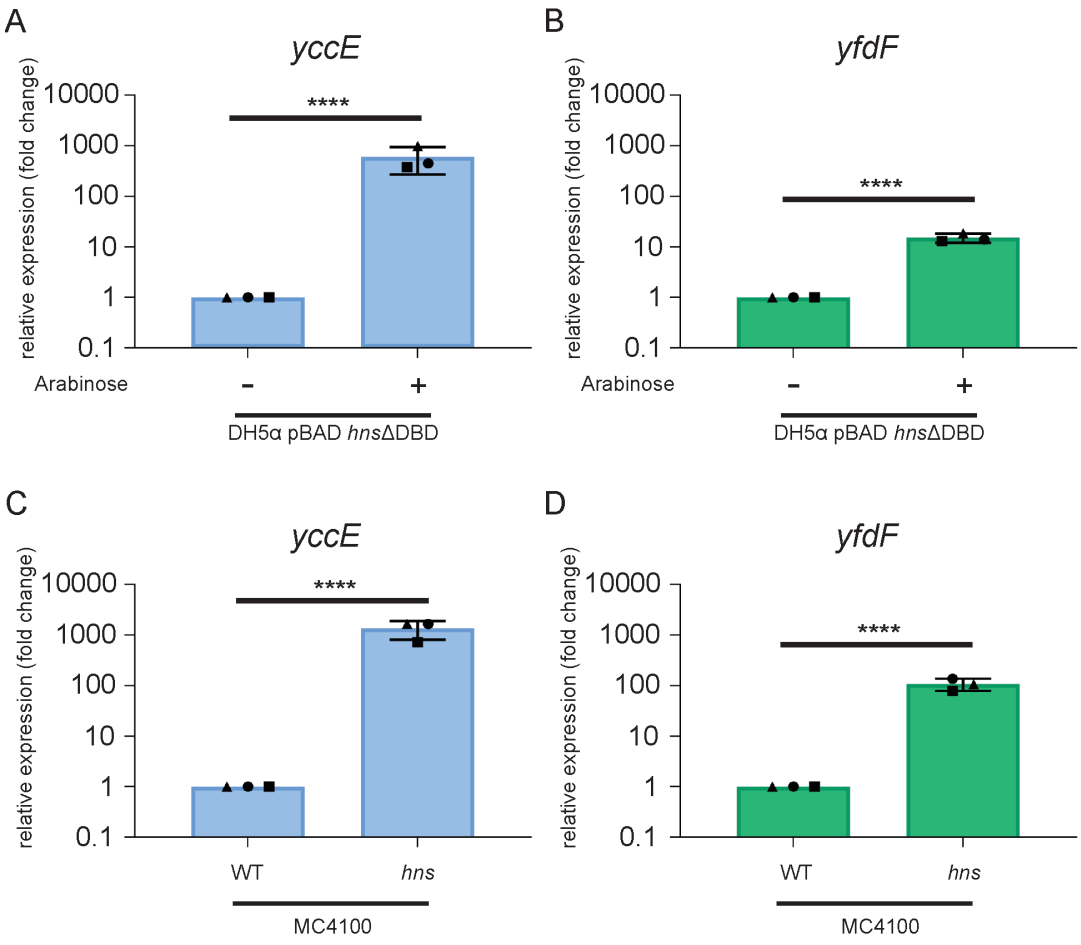

Figure 2.10: The *E. coli yccE* and *yfdF* homologous genes are repressed via H-NS. The *E. coli* K-12 DH5*α* strain with the dominant negative H-NS construct (p*hns*ΔDBD) was grown with and without Arabinose at 37°C **(A-B)** and the MC4100 WT and *hns* strains were grown at 37°C **(C-D)** and qPCR was performed to obtain mRNA expression levels of *E. coli* homologous genes to **(A,C)** *yccE* and **(B,D)** *yfdF* relative to WT without arabinose **(A,B)** or WT **(C,D)**. Data shown are the averages of three independent biological experiments and the error bars represent standard deviation. Student's T-test was performed; ****, $p<0.0001$.

MxiE is not necessary for the expression of *ipaH7.8*, *ospC1*, *yccE*, and *yfdF* when H-NS is depleted

Our results obtained in the *E. coli* MC1400 and isogenic *hns* mutant strains led us to hypothesize that MxiE-dependent genes can be fully expressed in the absence of MxiE, when H-NS is depleted (Figure 2.10C-D). To test this hypothesis in *S. flexneri*, we compared the expression levels of MxiE-dependent genes in wild type and *mxiE*ΔDBD mutant strains overexpressing the H-NS dominant negative construct. We found that both strains had similar expression levels of *ipaH7.8*, *ospC1*, *yccE*, and *yfdF* (Figure 2.11A-D), showing that MxiE is no longer required for their expression when H-NS is depleted.

In a complementary approach, we determined whether the expression of MxiE-dependent genes relies on the MxiE box when H-NS is depleted. To this end, we generated a *S. flexneri* strain harboring mutations in the MxiE box of *yccE* and introduced the dominant negative H-NS construct in the corresponding strain. As expected, *yccE* activation in response to the Congo red dye was abolished when the MxiE box was mutated (Figure 2.11E). However, overexpression of the dominant negative H-NS led to strong activation of *yccE* expression, regardless of the presence of a functional MxiE box (Figure 2.11E). Altogether, these results indicate that MxiE is not required for the expression of

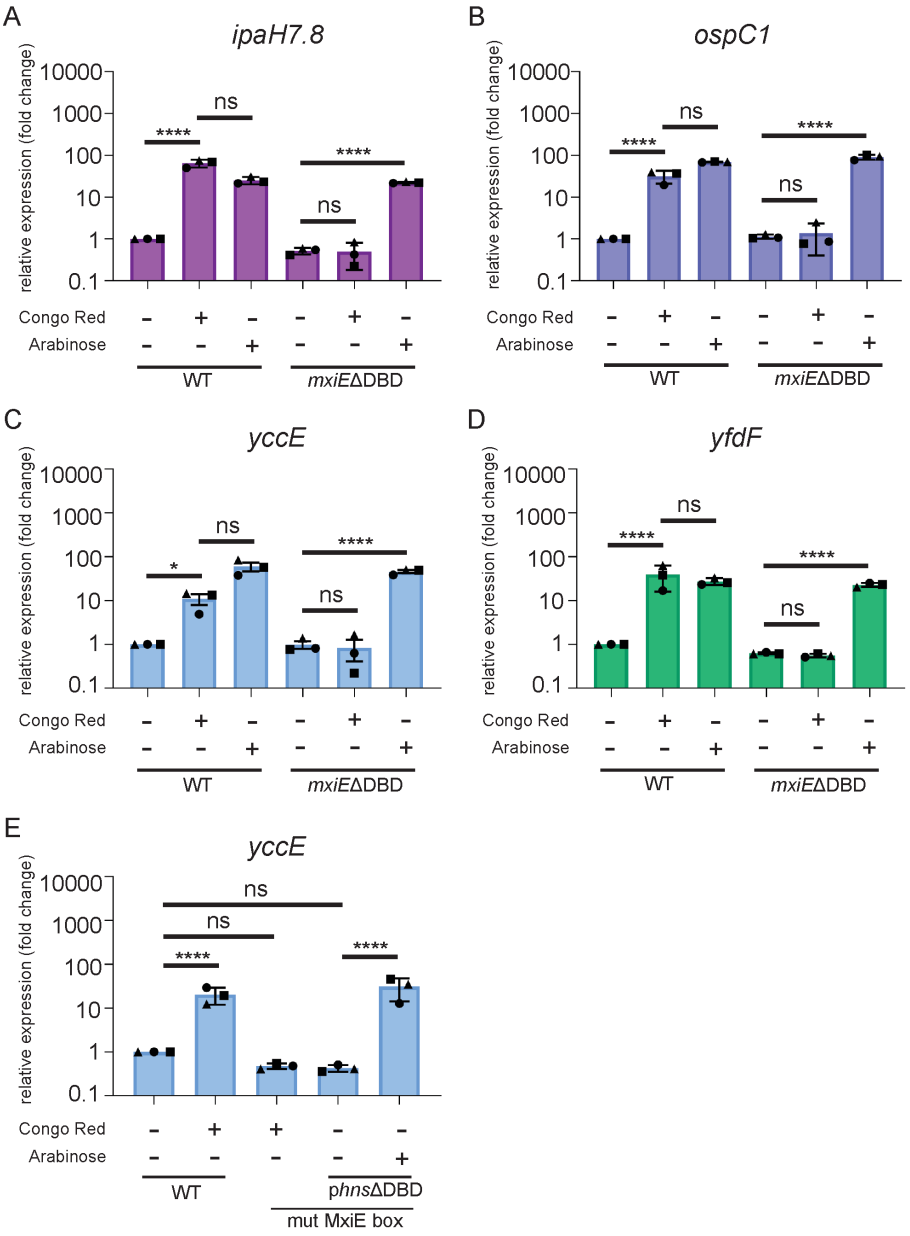

Figure 2.11: MxiE is not necessary for the expression of *ipaH7.8*, *ospC1*, *yccE*, or *yfdF* when H-NS is depleted. The *S. flexneri* WT and *mxiE*ΔDBD strains with the dominant negative H-NS construct (p*hns*ΔDBD) were grown at 37°C with or without Congo Red and/or Arabinose to induce expression of p*hns*ΔDBD and qPCR was performed for mRNA expression levels of **(A)** *ipaH7.8*, **(B)** *ospC1*, **(C)** *yccE*, and **(D)** *yfdF* relative to WT. A *S. flexneri* strain with a mutated MxiE box upstream of *yccE* without and with the dominant negative H-NS construct was grown at 37°C with or without Congo Red and/or Arabinose to induce expression of p*hns*ΔDBD and qPCR was performed for mRNA expression level of **(E)** *yccE* compared to WT. Data shown are the averages of three independent biological experiments and the error bars represent standard deviation. One-way ANOVA with Tukey's multiple comparison test was performed; ns, not significant; **, p=0.008 (ospC1), p=0.0013 (SF1005); ***, p=0.0003; ****, p<0.0001.

representative virulence plasmid-encoded genes, such as *ipaH7.8* and *ospC1*, and chromosome-encoded genes, such as *yccE* and *yfdF*, when H-NS is depleted.

VirB is not required for the expression of *ipaH7.8* and *yccE* upon MxiE/IpgC overexpression

To our knowledge, in *S. flexneri*, VirB is the main protein involved in counteracting H-NS-mediated silencing of virulence genes (85, 93). To investigate whether VirB may be involved in the expression of MxiE-dependent genes, we first designed a dual expression system in which *mxiE* and *ipgC* are expressed from an IPTG-inducible and arabinose-inducible promoter, respectively. This was necessary because the expression of *mxiE* and *ipgC* depends on VirB (82, 87). Using this system, we determined mRNA expression levels of representative virulence plasmid- and chromosome-encoded MxiE-dependent genes (*ipaH7.8*, *yccE*) in the *virB* mutant strain with and without overexpression of *mxiE* and *ipgC* (Figure 2.12A-B). As expected, we observed a significant decrease in *ipaH7.8* and *yccE* expression in the *virB* mutant, due to the dependency of *mxiE* and *ipgC* expression on *virB* expression. Overexpression of *mxiE* and *ipgC* was sufficient to restore mRNA expression of *ipaH7.8* and *yccE* to wild type levels in the presence

of the Congo red dye (Figure 2.12A-B). Importantly, overexpression of *mxiE* and *ipgC* did not restore expression of *ipgD*, a VirB-dependent gene (Figure 2.12C).

Altogether, these results indicate that VirB is not required for the expression of representative MxiE-dependent genes from the virulence plasmid (*ipaH7.8*) and chromosome (*yccE*), upon MxiE/IpgC overexpression.

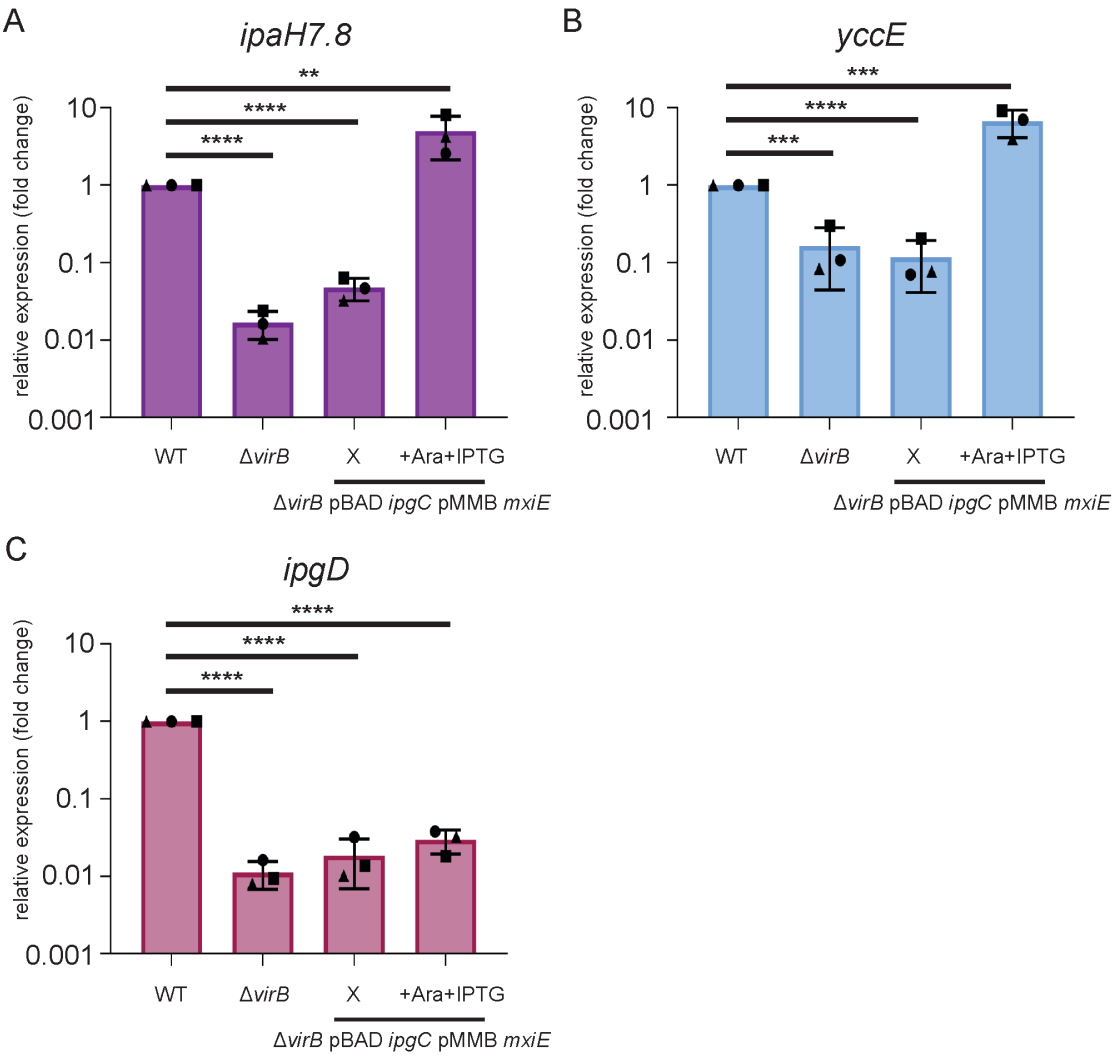

Figure 2.12: VirB is not required for the expression of *ipaH7.8* or *yccE* upon MxiE/IpgC overexpression. The *S. flexneri* WT, Δ*virB* deletion strain, and Δ*virB* with pMMB *mxiE* and pBAD *ipgC* were grown at 37°C with Congo Red and with either no induction (X) or induction of both *ipgC* and *mxiE* (+Ara +IPTG) and qPCR was performed for mRNA expression levels of **(A)** *ipaH7.8*, **(B)** *yccE*, and **(C)** *ipgD* relative to WT. Data shown are the averages of three independent biological experiments and the error bars represent standard deviation. One-way ANOVA with Tukey's multiple comparison test was performed; ns, not significant; **, p=0.0013; ***, p=0.0001 (Δ*virB*); ***, p=0.0002 (+Ara+IPTG); ****, p<0.0001.

2.6 Discussion

The MxiE-dependent genes have been determined previously by (i) comparing luciferase reporters for virulence plasmid-encoded genes in wild type *S. flexneri* and a *ipaB* constitutive secretion mutant strain, (ii) comparing GFP reporters in the presence or absence of MxiE, and (iii) comparing the transcriptional profiles of wild type *S. flexneri* and an *ipaB mxiE* mutant using a macroarray (67, 68, 100). Additionally, a recent study used RNA-seq in a constitutively secreting mutant (*ipaD*) to determine genes, located on the virulence plasmid or on the chromosome, that are differentially expressed based on the activity of the T3SS (109). Here, we used RNA-seq to identify genes that are differentially expressed in response to type 3 secretion induced by the Congo red dye, and we determined whether these genes rely on the integrity of MxiE for full expression (Figure 2.4).

Our RNA-seq analysis led to the identification of 41 genes differentially expressed by the Congo red dye (Table A1). Among those, 17 genes were previously shown to be MxiE-dependent, including *ipaH7.8* and *ospC1*. Two chromosome-encoded genes (*yfdF* and *yjgL*) were also discovered in a recent RNA-seq study and were first referred to as *gem*1 and *gem*3 and then renamed as *icaT* and *icaR*, respectively (109, 114) (Figure 2.3B and Table A1). In addition to these two genes, we found a third chromosome-encoded gene (*yccE*) that was not

previously identified (Figure 2.3A). Our bioinformatic analysis revealed the presence of putative MxiE box sequences in the vicinity of all previously identified genes (Table A2). Among the newly identified genes, 3 displayed a putative MxiE box, and we experimentally validated the importance of this regulatory motif in *yccE* and *yfdF* expression (Figure 2.5). The apparent absence of a MxiE box in the vicinity of 17 newly identified genes may suggest indirect effects of MxiE on global gene regulation (Table A1 and A2). We also identified two genes (*zraP* and *spy*) whose activation in presence of the Congo red dye did not rely on MxiE. Interestingly, these two genes may function in the envelop stress response, which may reflect a toxic effect of the Congo red dye on the cell wall, or the membrane.

Similar to a previous study conducted on *yfdF*, we found that the chromosome-encoded MxiE-dependent gene *yccE* is conserved in non-pathogenic *E. coli* strains, such as K-12 (Figure 2.6) (114). Additionally, we did not find *yccE* to be highly conserved in other *Shigella* spp. besides *S. flexneri*. It was absent in *S. boydii* and *S. dysenteriae* and fragmented in *S. sonnei*, and it was also absent from the B2 phylogroup of *E. coli* (Figure 2.6). This is in agreement with the notion that *S. flexneri* may have diverged from a different lineage of *E. coli* than *S. sonnei*, *S. boydii*, or *S. dysenteriae,* as previously suggested (140, 144).

Based on our bioinformatic analysis, we found that the DNA content of *yccE* and *yfdF* is A/T-rich compared to the surrounding chromosomal regions (Figure 2.3). Given that H-NS preferentially binds to A/T-rich regions of DNA, these data, together with the previous analysis of the GC content of the virulence plasmid sequence, led us to hypothesize that H-NS may silence the expression of MxiE-dependent genes (26, 36, 141). Our genetic study using a dominant negative version of H-NS revealed that representative virulence plasmid genes (*ipaH7.8* and *ospC1*) and chromosome-encoded genes (*yccE* and *yfdF*) are repressed by H-NS (Figure 2.8). H-NS has been proposed to silence extensive regions of A/T-rich loci by first binding to high affinity nucleation sites (tCGATAAATT) and then spreading along DNA (48). Due to the A/T-rich nature of the MxiE box and its similarity with the consensus H-NS binding site, it is possible that H-NS may use the MxiE box sequence as a portal of entry for nucleation. However, based on our results, where we mutated the MxiE box upstream of *yccE* and did not observe activation, unless we overexpressed the dominant negative H-NS (Figure 2.11E), it is unlikely that H-NS is using the MxiE box as a unique site for nucleation. Although further mutational analysis of the MxiE box will be required to confirm this assumption, we speculate that multiple high-affinity H-NS binding sites may be present in the A/T-rich coding regions of MxiE-dependent genes. In addition to high-affinity binding sites, other

factors such as DNA curvature may influence H-NS nucleation along DNA (48). Thus, further experiments are needed to determine how H-NS interacts with DNA at MxiE-dependent loci.

In addition to H-NS, *S. flexneri* possesses H-NS paralogues, including StpA and Sfh, which can be functionally redundant and form heterodimers with one another (44). The dominant negative H-NS system used in our study is a useful tool for bacterial species in which *hns* deletion is seemingly lethal, such as in enteropathogenic *E. coli* (EPEC) and *Yersinia enterocolitica* (142, 143). However, it is important to consider that oligomerization and sequestration can occur with the H-NS-like paralogues as well. While we provide genetic evidence that H-NS is specifically involved in the repression of *yccE* and *yfdF* based on the increased expression of *yccE* and *yfdF* in an *E. coli hns* mutant compared to wild type (Figure 2.10), the potential role of H-NS paralogues in MxiE-dependent gene silencing remains to be investigated.

How does MxiE regulate the expression of MxiE-dependent genes? MxiE is an AraC family member and is generally thought to function as a classical transcriptional activator that binds to the MxiE box overlapping with the -35 region of MxiE-dependent promoters (69, 115). Unlike the vast majority of AraC family members, MxiE-dependent activation relies on the presence of its co-activator, the IpgC chaperone (100, 105). This is similar to the situation in

Salmonella enterica serovar Typhimurium, where the AraC family member, InvF, homologous to MxiE, forms a complex with SicA, homologous to IpgC, and activates the expression of InvF-dependent genes, such as *sopB* (145, 146). *sopB* expression is also repressed by H-NS, but InvF is absolutely required for *sopB* expression, even in the absence of H-NS (147). This is in contrast with LuxR, a transcriptional regulator of quorum sensing genes in *Vibrio harveyi*, that is also thought to bind a specific motif and function as a transcriptional activator (148). However, a study by Chaparian *et al.* demonstrated that the expression of quorum sensing genes is repressed by H-NS in *V. harveyi* and that LuxR competes with H-NS for binding at promoter regions, leading to eviction of H-NS and activation of LuxR-dependent genes (149). Similarly, ToxR in *Vibrio cholerae* has also been shown to antagonize H-NS and is no longer required for ToxR-dependent gene expression when *hns* is absent (150). In this context, we found that MxiE is no longer required for *ipaH7.8*, *ospC1*, *yccE*, and *yfdF* expression when H-NS is depleted (Figure 2.11). These genetic data support the notion, that similar to LuxR and ToxR, MxiE may function to counter-silence H-NS. Additional biochemical studies will be required to further explore this notion.

Previous work established the existence of two mechanisms of H-NS anti-silencing in *S. flexneri*. One mechanism, occurring at the *virF* promoter, involves

changes in DNA topology upon a temperature shift to 37°C, resulting in H-NS release (77, 78, 119). The other mechanism is mediated by VirB, which binds to regulatory motifs located in the promoter regions of *icsB*, *icsP*, *ospD1*, and *ospZ* and is thought to subsequently dislodge H-NS via oligomerization along DNA (86, 88, 89, 93, 96, 97, 119). Importantly, our work demonstrates that MxiE/IpgC overexpression at 37°C was sufficient for the expression of *ipaH7.8* and *yccE* in a *virB* deletion strain, showing that VirB is not directly required for the anti-silencing of these MxiE-dependent genes under these experimental conditions (Figure 2.12A-B).

In summary, our genetic study provides support for a model in which MxiE mediates MxiE-dependent gene expression by counteracting H-NS-mediated silencing (depicted in Figure 2.13).

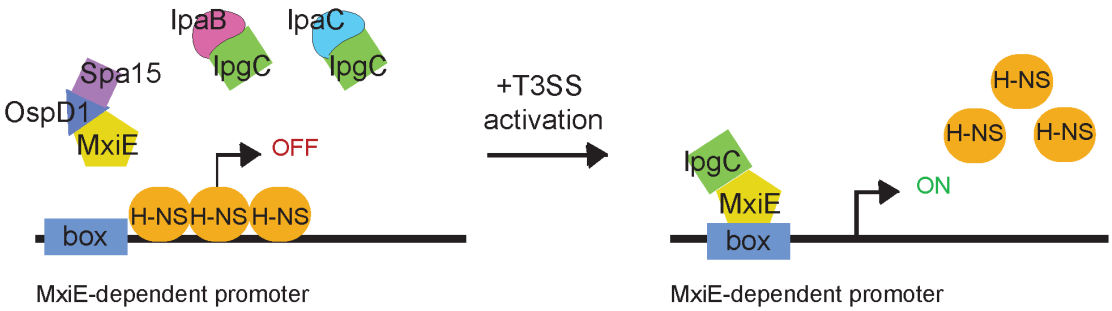

Figure 2.13: Proposed model of MxiE- and H-NS-dependent regulation in *S. flexneri*. Prior to T3SS activation at 37°C, MxiE is bound by anti-activator, OspD1, whose chaperone is Spa15, and IpgC is functioning as a chaperone for the translocon proteins, IpaB and IpaC. H-NS is repressing transcription of MxiE-dependent genes. Upon T3SS activation, IpaB and IpaC form the translocon pore and OspD1 is secreted. Transcription of MxiE-dependent genes is activated when MxiE and IpgC are both free to interact and MxiE binds the box sequence upstream, which results in counter-silencing of H-NS.

3. Chapter 3: Discussion

3.1 Summary of work

The culmination of my thesis work has provided insight into additional layers of gene regulation in *S. flexneri*. A *mxiE*ΔDBD mutant with a regulatory defect was generated and used to define the MxiE-dependent regulon. During this thesis work, another group published the identification of novel chromosomal MxiE-regulated genes (*yfdF* and *yjgL*), which we were able to confirm in our study. In addition, we uncovered a chromosomal gene (*yccE*) that was not previously identified. We validated that *yccE* and *yfdF* are MxiE-dependent for gene expression and that they require an intact MxiE box motif in their promoter region. Additionally, we discovered that H-NS represses MxiE-dependent genes on the virulence plasmid (*ipaH7.8* and *ospC1*) as well as the chromosome (*yccE* and *yfdF*). We found that VirB, a *S. flexneri* anti-silencing protein for H-NS, was not directly involved and presented genetic evidence that MxiE may function to counteract H-NS-mediated silencing for the investigated representative genes (*ipaH7.8*, *ospC1*, *yccE*, and *yfdF*). In this chapter, I will discuss what avenues of MxiE- and H-NS-dependent regulation in *S. flexneri* remain to be discovered as well as the implications of this work on the field.

3.2 Future Directions

3.2.1 A MxiE-mediated mechanism for counter-silencing H-NS

Prior to my thesis work, MxiE was thought to function as a classical transcriptional activator in *S. flexneri*. However, a recent study has shown that MxiE/IpgC can function outside of their normal roles by demonstrating that they also work as indirect transcriptional repressors on *virB* expression by interfering with VirF-dependent activation of *virB*, facilitating a negative feedback loop on virulence gene expression (116). Similarly, in my thesis work, genetic evidence suggests that MxiE, likely along with IpgC, is involved in the de-repression of H-NS-mediated silencing of MxiE-dependent genes, which is a novel role for MxiE (Figure 2.11). To my knowledge, this work is the first to implicate MxiE as an anti-silencer of H-NS. In support of my hypothesis, it is not uncommon for an AraC-type protein to antagonize H-NS (70, 151). However, these regulators are often also found to be required for RNAP recruitment, as is the case for ToxT in *Vibrio cholerae* and InvF in *Salmonella enterica* serotype Typhimurium (147, 152).

What remains to be discovered is whether or not MxiE is the chief protein responsible for this de-repression activity and by what mechanism this is being accomplished. A future experiment to address these questions could be an electromobility shift assay (EMSA) to demonstrate that MxiE can displace bound H-NS from the DNA of MxiE-regulated genes. Alternatively, if this proves to be

technically challenging, due to the difficult nature of purifying notoriously insoluble AraC-like regulators, including MxiE, chromatin immunoprecipitation sequencing (ChIP-seq) could be used to map where H-NS and MxiE bind in the *S. flexneri* genome. Comparison of H-NS and MxiE binding profiles would provide insight as to the overlap of their regulons.

If these experiments do not provide clear results, it is possible that the antagonism of H-NS by MxiE is indirect and is mediated by transcriptional elongation. Alternatively, it is possible that MxiE could not be the protein involved in anti-silencing H-NS-mediated repression. To address this, a pulldown of proteins bound to MxiE-regulated gene DNA could be performed, followed by mass spectrometry, to determine what additional bound proteins are present.

3.2.2 Does MxiE bind DNA?

To my knowledge, although MxiE is an AraC-like regulator with a conserved DBD, it has yet to be shown experimentally that MxiE binds to DNA (68, 69, 100). In addition, MxiE has been proposed to bind a 17-bp cis-regulatory element, known as the MxiE box. Although this motif has been shown to be necessary for MxiE-dependent activation, it has not been shown to be the sequence bound by MxiE (Figure 2.5) (113, 115). Thus, evidence and mapping of

the DNA binding sites of MxiE is important for future studies of the mechanisms underlying MxiE-dependent gene regulation. Perhaps this has not been previously accomplished due to the technical difficulty of purifying MxiE, which as an AraC-like regulator, is challenging to purify for solubility reasons. However, there has been one successful study by the Munson group to purify MxiE using a fusion with maltose binding protein (MBP) (105). Using an MBP-fused MxiE, a future experiment could be to perform DNase footprinting to determine where in the promoter or CDS of MxiE-regulated genes, MxiE is binding. An alternative technique could be to use an EMSA to provide direct evidence of MBP-MxiE binding to the DNA of MxiE-regulated genes via a gel shift upon MxiE-DNA binding. Additionally, the introduction of mutations in the MxiE box should lead to a loss of gel shift with MBP-MxiE, confirming that MxiE specifically binds to this sequence.

3.2.3 Importance of MxiE/IpgC interaction

When investigating MxiE-dependent gene regulation, it is important to consider the involvement of IpgC. It is known that MxiE and IpgC do interact from a study in which MxiE and IpgC were purified and used in a pulldown assay (105). However, because this was a pulldown experiment, which lacks the relevant context, the importance of this interaction remains to be investigated. It

has been previously shown, including in my thesis work, in which both *mxiE* and *ipgC* overexpression is required for MxiE-dependent gene expression in a *virB* mutant, that MxiE requires IpgC for its regulatory activity (Figure 2.12) (100). However, how and when MxiE interacts with IpgC is still unclear. Future experiments could include an EMSA of MxiE-dependent gene DNA with MxiE and -/+ IpgC to determine if the addition of IpgC is necessary for MxiE-DNA binding. This would demonstrate whether or not MxiE and IpgC are in complex at this regulatory step. Alternatively, a DNase footprinting assay could be performed with MxiE and with and without prior incubation of MxiE with IpgC to determine if the MxiE/IpgC complex is necessary to observe a region of protection, which is indicative of a binding site. IpgC does not have a DBD, so it is unlikely to bind DNA on its own (153).

If IpgC is found to not be important for MxiE-DNA binding, then perhaps IpgC is required for a different reason. This could be the case due to the recent study demonstrating that the MxiE/IpgC homologous proteins in *Salmonella* Typhimurium, InvF/SicA, are both required for the expression of their target genes, however, InvF does not require SicA for DNA binding (147). It could be that IpgC increases the stability of MxiE, however, this was shown to not be the case for InvF/SicA (145). However, experiments, such as western blots of cells

expressing MxiE -/+ IpgC and probing for an epitope-tagged MxiE, as no specific antibody is available, would need to be performed to rule out this possibility.

3.2.4 Where is H-NS binding?

The work detailed here demonstrates that H-NS is repressing MxiE-dependent genes, both on the VP and on the chromosome (Figure 2.8). However, it is still unknown where H-NS is binding on MxiE-regulated gene DNA. It is known that H-NS preferentially binds AT-rich DNA, so it is reasonable to start by investigating regions of DNA that are particularly AT-rich (154). By using a DNase footprinting assay, the regions of protection, or binding sites of H-NS can be determined for MxiE-dependent genes. Alternatively, ChIP-seq could be used to determine where H-NS binds across the whole *S. flexneri* genome. To my knowledge, ChIP-seq of H-NS bound regions has been conducted in other bacteria, such as *Vibrio harveyi*, but it has never been accomplished in *Shigella* (149).

H-NS nucleation sites are important to consider because although the future experiments listed above may demonstrate where H-NS is binding, these studies will not help determine a site for nucleation. In some cases, H-NS binds a region of high-affinity, i.e. the nucleation site, using this site for initial binding followed by oligomerization along the DNA at lower affinity regions (48, 155). To

determine a site used for nucleation in MxiE-regulated genes, mutational analysis of predicted regions which are particularly AT-rich could be used in either a DNase footprinting assay or EMSA.

3.2.5 How does H-NS prevent transcription at MxiE-dependent loci?

This thesis work demonstrates that H-NS represses MxiE-dependent genes on the VP (*ipaH7.8* and *ospC1*) and the chromosome (*yccE* and *yfdF*), however, it is still unknown how H-NS functions to repress their transcription (Figure 2.8). Mechanisms for H-NS-mediated transcriptional silencing has been investigated in numerous Gram-negative bacteria, but it is perhaps the most well studied in *E. coli* (156). There are three known mechanisms by which H-NS represses transcription involving: (i) blocking RNAP from binding, (ii) preventing transcriptional elongation, and (iii) forming a DNA loop, which could occlude the binding site from RNAP and/or trap bound RNAP (Figure 1.1) (50-54). To determine how H-NS is mediating the transcriptional repression of MxiE-dependent genes, it is important to elucidate the DNA structure when H-NS is bound as well as to localize RNAP. Computational approaches could be used to initially determine how H-NS binding affects local DNA topology at MxiE-regulated genes as well as what may occur when RNAP is added. Alternatively, atomic force microscopy could be utilized to visualize H-NS:DNA complexes

(157). Atomic force microscopy is useful tool for the study of individual protein:DNA complexes as it provides images with a topographical view to observe changes in DNA architecture upon the addition of the DNA-binding protein, which in this case is H-NS (158).

3.2.6 Potential redundancy of H-NS-like proteins, StpA and Sfh

In this thesis work, I determined that H-NS represses MxiE-dependent genes using a dominant negative H-NS in *S. flexneri* and an *hns* mutant in *E. coli* (Figure 2.8 and Figure 2.10). However, it is important to consider that the dominant negative H-NS, which is a truncated form of the protein, can also oligomerize with paralogues of H-NS, StpA and Sfh, in *S. flexneri (42)*. Although these data presented in this thesis with the *hns* mutant in *E. coli*, which also possesses StpA, is supportive of the conclusion that H-NS is the protein involved, we cannot rule out the possibility of StpA of Sfh involvement as they are sometimes functionally redundant (Figure 2.10C-D) (44). To elucidate the roles of each H-NS-like protein in the repression of MxiE-dependent genes, single mutants for each *stpA* and *sfh* should be generated using allelic exchange. Although we had technical issues making an *hns* mutant in *S. flexneri*, the *sfh*, *stpA*, and *sfh stpA* double mutants have been generated by other groups, so we do not anticipate problems (44, 45). However, in the event that making mutants

for *stpA* and *sfh* in *S. flexneri* is challenging, a *stpA* and *stpA hns* double mutant can be generated in *E. coli*, to use alongside the *hns* mutant, and each individual protein can be overexpressed in *trans* to determine their effect on gene expression.

3.2.7 Potential involvement of the Hha family of proteins

The work detailed in this thesis provides evidence for the involvement of H-NS in mediating transcriptional repression of MxiE-dependent genes, however, it does not address the potential involvement of other nucleoid-associated proteins (NAPs).

In particular, the Hha family of proteins, found in Gram-negative bacteria, are known to modulate the activity of H-NS and therefore H-NS regulated genes (159-161). The N-terminal oligomerization domain of Hha is similar to that of H-NS (162). Thus, it has been shown to oligomerize with H-NS in *Yersinia enterocolitica* and function to modulate H-NS-regulated genes (162). Similarly, YdgT, an Hha-like protein in *E. coli*, was shown to form heteromeric complexes with H-NS and an H-NS-like protein, StpA (163). Most studies on Hha/H-NS interactions have been conducted in *E. coli*, *Salmonella*, and *Yersinia*, therefore, it would be interesting to investigate any role that Hha may play in MxiE- and H-NS-dependent gene regulation in *S. flexneri*. It is important to consider the Hha-

like protein, YdgT, which is also present in *S. flexneri* (160). To accomplish this, individual and a double mutant of *hha* and *ydgT* could be generated to assay MxiE-dependent gene expression in the absence of Hha and Hha-like proteins that may have redundant activities.

3.2.8 Characterization of YccE and YfdF

One of the exciting discoveries of this work was the identification of novel MxiE-dependent chromosomal genes (*yccE*, *yfdF*, and *yjgL*). During the preparation of my manuscript, another group published an RNA-seq study that also found *yfdF* and *yjgL*, however, they did not identify *yccE* (109). Subsequently, they demonstrated that *yfdF* and *yjgL* are secreted by the T3SS, have functional MxiE box motifs, and their protein sequences are highly conserved in *E. coli* suggesting that they likely do not have roles in virulence (114). In addition to identifying *yfdF* and *yjgL*, I also identified *yccE* and demonstrated that it has a functional MxiE box in its promoter region (Figure 2.3).

Outstanding questions that remain are whether or not YccE is secreted by the T3SS and what role this protein may have in *S. flexneri* virulence. To determine if YccE is secreted, a secretion assay using Congo red dye induction of the T3SS in *S. flexneri* followed by a western blot probing for an epitope-tagged

YccE could be performed. Furthermore, to address the question of a role of YccE in *S. flexneri* virulence, a mutant strain could be generated and tested in *in vitro* infections in HT-29, human colonic epithelial cells, as well as in *in vivo* infections in the infant rabbit model.

3.2.9 Conservation across other bacteria

This work provides genetic evidence for the advancement of our molecular understanding of MxiE-dependent gene regulation in *S. flexneri*. However, these data could also provide insight for other conserved AraC-type transcriptional regulators, similar to MxiE (69). A database search identified 830 AraC family members, so there are many proteins that could be acting in a similar manner to MxiE (69).

VirF, the master regulator in *Shigella*, is also an AraC-type transcriptional regulator, however, there have been contradictory reports in the field on its mechanism of action (69, 81). In one study, it was reported that VirF functions as a counter-silencing protein of H-NS-mediated repression of *icsA* (74). However, in another study it was reported that VirF is absolutely required for *virB* expression in the absence of *hns*, and it was concluded that VirF is not a counter-silencing protein and rather a classical transcriptional activator (73). Importantly, these studies both used *E. coli hns* mutants for their experiments, and thus it is

necessary to consider what regulatory elements from *Shigella* may be missing. Thus, it is still unclear exactly how VirF is acting, whether as a counter-silencer of H-NS or a classical transcriptional activator, or perhaps it could also have dual roles, where both activities are required.

Outside of *Shigella*, there are additional AraC-type regulators in other bacterial pathogens that could be functioning in a similar manner. For instance, it was previously demonstrated that ToxT, the regulator of major virulence factors in *Vibrio cholerae*, acts to de-repress H-NS while also being required for RNAP activation (70, 164-166). Similar to ToxT and the role for MxiE defined in this work, there are many other AraC type regulators that have been reported to have H-NS anti-silencing roles (Figure 2.13) (Table 3.1) (74, 152, 167-173). Therefore, our contributions to the understanding of MxiE-dependent gene regulation in *S. flexneri*, could have broad impacts in the research of multiple other bacterial species.

Table 3.1. List of AraC-type regulators shown to de-repress H-NS. Adapted from (167).

Bacteria	AraC type regulator	Genes activated via H-NS de-repression
ETEC strain H10407	CfaD	CFA/I fimbriae genes (*cfaA*, *cfaB*, *cfaC*, *cfaE*)
E. coli	GadW and GadX	Glutamate decarboxylase (*gadA*)
EPEC	PerA	LEE virulence genes (*perABC* and *bfp*)
ETEC	Rns	CS1 pilus operon (*cooA*, *cooB*, *cooC*, *cooD*)
Shigella flexneri	VirF	Actin-based motility factor (*icsA*)
Shigella flexneri	MxiE	Later secreted effectors and chromosomal genes (*ipaH7.8*, *ospC1*, *yccE*, *yfdF*)
Salmonella enterica serovar Typhimurium	HilC, HilD, and RtsA	Virulence regulator (*rtsA*)
Vibrio cholerae	ToxT	Cholera toxin (*ctxAB*)
Citrobacter rodentium	RegA	Adhesion virulence factors (*adcA* and *kfc*)
Proteus mirabilis	UreR	Urease operon (*ureDABCEFG*)

3.2.10 **What significance does MxiE-dependent regulation have on pathogenesis in an infant rabbit model?**

Individual MxiE-regulated effectors (e.g. OspF, IpaH9.8, IpaH7.8, IpaH4.5, etc.) have been characterized to determine their effect on *S. flexneri* virulence (174-177). For instance, an *ospF* mutant was used in the rabbit ileal loop model of *S. flexneri* infection and was found to have more bacterial invasion and neutrophil infiltration, suggesting that OspF is involved in dampening these during infection (177). Additionally, an *ipaH9.8* mutant was characterized in a mouse model where *S. flexneri* had to be administered via an intravenous or intraperitoneal route and was found to have improved animal survival and bacterial burden compared to WT-infected mice (174). An *ipaH7.8* mutant was previously characterized in a mouse model in which *S. flexneri* was infected via the intranasal route and it was found that there was a decrease in bacterial load and inflammation in the *ipaH7.8* mutant-infected lungs compared to WT-infected or *ipaH7.8* complemented mice (175). Similarly, an *ipaH4.5* mutant was used in an intranasal *S. flexneri* infection of mice and was found to have improved animal survival and bacterial loads in the lungs compared to WT-infected mice (176).

However, due to the lack of previous studies in relevant animal models and the possible redundancy in effector function and/or coordinated activities of multiple effectors on *S. flexneri* pathogenesis, it is important to investigate the

overall significance of MxiE-dependent regulation during *S. flexneri* infection of infant rabbits. A future direction could be to determine the effect of the loss of MxiE-dependent gene activation, using the *mxiE*ΔDBD mutant generated in this work, on *S. flexneri* pathogenesis in the infant rabbit model (5). When infected with WT *S. flexneri*, the infant rabbits display bloody diarrhea, epithelial fenestration, and heterophil (i.e. neutrophil) influx by 24 hpi (5). A time course experiment of *mxiE*ΔDBD and WT *S. flexneri*-infected rabbits would help determine both when and at what stage of infection MxiE-dependent regulation is important *in vivo*. By using histology and immunofluorescence imaging of colonic sections from infected rabbits, the localization of the bacteria and impact of infection on host epithelial cell fenestration as well as immune cell recruitment could be determined across different time points. These data would provide evidence for the impact of MxiE-dependent regulation on pathogenesis in a relevant animal model.

3.2.11 Importance for the virulence regulatory cascade

Shigella virulence gene regulation consists of a sophisticated cascade involving three tiers of transcriptional regulators and multiple proteins involved in either anti- or co-activating gene expression (Figure 1.3). This thesis work demonstrates that there is an additional layer of complexity in that H-NS is not

only involved in the repression of VirF- and VirB-dependent genes, but also MxiE-dependent genes (Figure 2.8). The implication of this finding is important when considering its impact on the exquisitely fine-tuned coordination of the timing of the expression of the myriad of genes encoding virulence effector proteins so that they are present at the appropriate time and place to promote *S. flexneri* pathogenesis. To experimentally determine the role of MxiE- and H-NS-dependent regulation on timing and location of virulence gene expression in *S. flexneri*, a fluorescent reporter strain for a MxiE-dependent gene (i.e. *ipaH7.8*), in either the *mxiE*ΔDBD mutant strain or the WT strain with the dominant negative H-NS, could be used in infant rabbit infections across a time course and then fluorescence could be compared WT control levels. Not only could the timing and location of MxiE-dependent gene expression be determined, but the effects of the mis-regulation on *S. flexneri* pathogenesis (i.e. bloody diarrhea, immune cell recruitment, bacterial clearance, etc.) could be inferred as well.

3.2.12 Implications for therapeutic approaches

AraC-type virulence regulators, such as ToxT in *Vibrio cholerae*, RegA in *Citrobacter rodentium*, and VirF in *S. flexneri*, have been previously used as targets for drug development (72, 178, 179). Targeting AraC-type virulence regulators is favorable because their inhibition, and therefore inability to activate their

respective regulons, attenuates virulence without affecting bacterial growth (72). This is beneficial due to a potential reduction in the bacteria becoming drug resistant due to the absence of the selective pressure that a growth defect may exert (180-182). To my knowledge, MxiE, however, has not yet been the target for therapeutic approaches for *Shigella* infection.

Interestingly, an *S. flexneri* invasion study was conducted in mouse fibroblast cells (L-929) to evaluate VirF-dependent activation using the small molecule inhibitor SE-1, which is thought to bind the conserved DBD region of AraC-like regulators. However, the group did not test the effect of the drug on MxiE-dependent activation (72). It is possible that this drug could also target MxiE, which would then cover all of the major virulence regulators in *S. flexneri*, however, that remains to be investigated. The SE-1 study reported that the current effective dose was too high to be used in therapeutic approaches due to the potential for cell toxicity and off-target effects, so further drug development would be necessary (72).

Alternatively, a drug screen for small molecule inhibitors of MxiE could be performed. It should be noted, however, that the *mxiE*ΔDBD mutant in this work did not have an invasion defect in human colonic epithelial cells and so chemical inhibition will likely not prevent initial infection (Figure 2.1C). Rather, MxiE inhibition would probably affect the immune response to *S. flexneri*,

promoting faster clearance and recovery. However, we know from *S. flexneri* infections in the infant rabbit model with an *icsA* mutant that cell-to-cell spread is necessary for disease and likely contributes to epithelial cell fenestration and ultimately bloody diarrhea (5). Therefore, a therapeutic approach that would target VirF as well as MxiE would be preferred. Ideally, identification of a pan-AraC family inhibitor would be optimal because it could be applicable for many pathogenic bacteria, which would be useful in instances where a person may be infected with multiple pathogens simultaneously or in cases where the identity of the bacteria is unknown.

3.3 Conclusions and significance of work

The work detailed here provides additional knowledge regarding MxiE- and H-NS-dependent gene regulation in *S. flexneri*. We have shown that the MxiE-dependent regulon is larger than previously appreciated, with the addition of novel chromosomal genes (*yccE*, *yfdF*, and *yjgL*). Furthermore, we have demonstrated that both *yccE* and *yfdF* have functional MxiE box *cis*-regulatory elements in their promoter regions that are essential for gene expression. Using a dominant negative H-NS, we demonstrated that representative MxiE-dependent genes on the VP (*ipaH7.8* and *ospC1*) and chromosome (*yccE* and *yfdF*) are repressed by H-NS. Importantly, we demonstrate that the known H-NS anti-

silencing protein, VirB, is not required for MxiE-dependent gene expression, which rules out the possibility of its involvement in counter-silencing H-NS. An exciting finding was that sequestration of endogenous H-NS was sufficient for MxiE-dependent gene expression in a *mxiE*ΔDBD mutant.

In conclusion, we propose a model in which MxiE mediates the de-repression of H-NS, which presents a novel mechanism of both MxiE- and H-NS-dependent gene regulation in *S. flexneri* (Figure 2.13). Future studies will provide direct evidence for MxiE antagonism of H-NS-mediated repression to support our proposed model. Finally, the implications of this work will have broad impacts on the understanding of bacterial gene regulation, which could influence the development of novel therapeutics.

Appendix: Supplementary Tables in Chapter 2

Table A1. Differentially expressed genes from RNA-seq of *S. flexneri* WT and *mxiE*ΔDBD with and without addition of Congo red dye.

Locus tag in *S. flexneri* str. 2457T	Gene Id in *S. flexneri* str. 301	Gene Symbol	Gene Name/Protein name	WT CR	WT	MxiE CR	MxiE	Genes up-regulated in WT CR (fold change)	Genes up-regulated in MxiE CR (fold change)	MxiE motif	Location
	SF_p0078	ipaH7.8	invasion plasmid antigen	228.47625	2.193022222	1.61736	1.808970588	104.1832808	0.894077555	+	Plasmid
S_RS23500	SF4238	yjgL	hypothetical protein	87.60875	1.325788889	1.21072667	1.115505882	66.08046781	1.085361078	+	Chromosome
S_RS13440	SF2423	yfdF	hypothetical protein	150.8	2.43265	2.56001333	2.404376471	61.99001089	1.064730655	+	Chromosome
S_RS05600	SF1005	yccE	YccE family protein	21.337125	0.459496667	0.83904	0.712711765	46.43586461	1.177250105	+	Chromosome
	SF_p0265a	ospE1	OspE1	18844.5	623.0833333	403.666667	396.5894118	30.24394811	1.017845295	+	Plasmid
S_RS10285	SF1880	ipaH_4	invasion plasmid antigen	29.881125	1.002205556	0.76057333	0.860129412	29.81536555	0.884254535	+	Chromosome
	SF_p0226	ipaH9.8	invasion plasmid antigen, secreted by the Mxi-Spa secretion machinery	187.779375	7.080722222	6.19017333	5.820835294	26.51980534	1.063451038	+	Plasmid
	SF_p0094	ospC1	protein OspC1	465.231875	18.96805556	17.5386667	18.12423529	24.52712528	0.967691402	+	Plasmid
S_RS19090	SF4074	zraP	zinc resistance sensor/chaperone ZraP	163.73375	6.732277778	186.501333	9.90676471	24.32070622	18.82565488		Chromosome
S_RS11210	SF2022	ipaH_5	invasion plasmid antigen	93.65375	6.440833333	6.02144	5.642935294	14.54062621	1.067075854	+	Chromosome
	SF_p0265	ipaH1.4	invasion plasmid antigen, secreted by	186.054375	13.04938889	9.53906667	10.01682353	14.2577079	0.952304554	+	Plasmid

			the Mxi-Spa secretion machinery								
	SF_p0003	ospB	OspB protein	1099.98125	109.3566667	66.5581333	89.07117647	10.05865745	0.747246595	+	Plasmid
S_RS04880	SF0887	ipaH_2	IpaH family type III secretion system E3 ubiquitin--protein ligase	18.97775	1.997677778	2.26236667	1.873747059	9.499905446	1.207402384	+	Chromosome
	SF_p0048	ospE2	OspE2	23299.3125	2761.372222	1611.25333	1587.847059	8.437584876	1.014740887	+	Plasmid
S_RS23240	SF4195	yjiC	DUF2686 family protein	5.043106625	0.601688889	0.67294667	0.952782353	8.381584475	0.706296317		Chromosome
S_RS08415	SF1483	spy	ATP-independent periplasmic protein-refolding chaperone	230.361875	27.75838889	281.502667	29.75194118	8.298820076	9.46165714		Chromosome
S_RS03965	SF0722	ipaH_1	E3 ubiquitin-protein ligase	97.21625	11.78066667	9.25046667	9.016117647	8.252185785	1.025992232	+	Chromosome
	SF_p0004	phoN2/apy	PhoN2 (Apy), periplasmic phosphatase, apyrase, ATP diphosphohydrolase	1882.29375	247.9277778	120.688667	181.6035294	7.592105116	0.664572253		Plasmid
S_RS14580	SF2610	ipaH_7	IpaH family type III secretion system E3 ubiquitin--protein ligase	7.2675	0.981638889	1.10981333	1.098417647	7.403435298	1.010374639	+	Chromosome
	SF_p0093	*ospD3*	hypothetical protein	397.698125	57.90388889	79.3306667	80.16705882	6.868245512	0.989566885		Plasmid
S_RS18580	SF4157	yjbM	DUF2713 domain-containing protein	3.558543375	0.540313889	0.79809333	1.019435294	6.586067512	0.782877872		Chromosome
S_RS22045	SF3539	yhiS	hypothetical protein	2.4438125	0.372413889	0.363768	0.352543529	6.562087433	1.031838538		Chromosome
	SF_p0079	ipaH4.5	invasion plasmid antigen	101.424375	15.83433333	15.4320667	16.14217647	6.405345452	0.956009042	+	Plasmid
S_RS12430	SF2231	preT	NAD-dependent dihydropyrimidine dehydrogenase subunit	17.10506 25	3.136911111	3.04006	3.301458824	5.452836212	0.920823237		Chromosome

	SF_p0181	virA	VirA protein	1870.59375	352.4733333	271.901333	269.6229412	5.307050415	1.00845029	+	Plasmid
S_RS16690	SF2996	yeeS	RadC family protein	7.795375	2.089816667	2.28586667	2.155182353	3.730171706	1.060637242		Chromosome
S_RS15075	SF2699	ygaC	DUF2002 family protein	159.533125	45.05983333	58.6210667	40.31211765	3.540473038	1.454179787		Chromosome
S_RS01000	SF0191	yaeD/gmhB	D-glycero-beta-D-manno-heptose 1,7-bisphosphate 7-phosphatase	3.9467875	1.202816667	1.49708667	1.343852941	3.281287672	1.114025665		Chromosome
S_RS12435	SF2232	yeiA/preA	NAD-dependent dihydropyrimidine dehydrogenase subunit PreA	5.0673	1.671266667	1.66234667	1.906235294	3.032011648	0.872057438		Chromosome
	SF_p0010	ospF	OspF	1551.40625	520.925	358.030667	374.6988235	2.978175841	0.955515855	+	Plasmid
S_RS23735	SF4283	S4548	sugar phosphate isomerase/epimerase	2.54348125	0.874805556	0.8803	0.814917647	2.907481821	1.080231853		Chromosome
S_RS03235	NA	kdpC	K +-transporting ATPase subunit C	10.3220625	3.597172222	3.08246667	3.371388235	2.869493553	0.914301899		Chromosome
S_RS06620	SF1179	dadX	catabolic alanine racemase DadX	21.1985	8.258611111	4.32947333	2.502141176	2.566835962	1.730307376		Chromosome
	SF_p0009	ospD2	hypothetical protein	163.661875	66.81388889	67.8846667	68.84352941	2.449518771	0.986071854		Plasmid
S_RS12440	SF2233	mglC	galactose/methyl galactoside ABC transporter permease	3.9483	1.727938889	0.84620667	0.674047059	2.284976642	1.255411852		Chromosome
S_RS18700	SF4128	yjcH	DUF485 domain-containing protein	22.781875	10.03983333	7.50073333	4.582882353	2.269148724	1.636684679		Chromosome
S_RS21305	SF3681	pyrE	orotate phosphoribosyltransferase	40.849375	18.26016667	39.9332	23.71311765	2.237075693	1.684013068		Chromosome
S_RS06615	SF1178	dadA	D-amino acid dehydrogenase	11.74975	5.384888889	2.98645333	2.136417647	2.181985598	1.397878986		Chromosome
S_RS02380	SF0446	gcl	glyoxylate carboligase	5.15700625	2.374438889	1.74457333	1.317217647	2.171884176	1.324438173		Chromosome

S_RS19360	SF4031	yijO	AraC family transcriptional regulator	5.956275	2.778105556	3.10054667	3.016317647	2.144006007	1.027924453		Chromosome
S_RS03095	SF0574	sdhA	succinate dehydrogenase flavoprotein subunit	119.93625	59.83	35.3422667	21.00029412	2.004617249	1.682941509		Chromosome
					Normalized TPM values						Chromosome

Table A2. MxiE box motifs identified upstream of RNA-seq differentially expressed genes.

Gene Symbol	Locus tag	Gene/Protein Name	Gene-Start	Gene-Stop	Gene Length	Distance to motif start site	Motiff Start	matched_sequence
ipaH_1	S_RS03965	E3 ubiquitin--protein ligase	744072	745834	1763	59	745893	GGCGCGTTTTTTTAAAG
ipaH_2	S_RS04880	IpaH family type III secretion system E3 ubiquitin--protein ligase	913648	915474	1827	376	915850	GTACTGTTTTTTTAAAG
ipaH_4	S_RS10285	invasion plasmid antigen	1887119	1888870	1749	212	1886907	GTATCGTTTTTTTACAT
ipaH_5	S_RS11210	invasion plasmid antigen	2023205	2024848	1644	135	2023070	GTATCGTTTTTTTACAG
ipaH_7	S_RS14580	IpaH family type III secretion system E3 ubiquitin-protein ligase	2679457	2681283	1826	392	2679065	GTACTGTTTTTTTAAAG
ipaH1.4	SF_p0265	invasion plasmid antigen, secreted by the Mxi-Spa secretion machinery	214879	213152	267	71	215605	GTATCGTTTTTTTACAG
ipaH4.5	SF_p0079	invasion plasmid antigen	64339	66063	1725	74	64265	GGATTGTTTTTTTAAAG
ipaH7.8	SF_p0078	invasion plasmid antigen	62214	63911	1698	321	61893	GTATCGTTTTTTTACAG
ipaH9.8	SF_p0226	invasion plasmid antigen, secreted by the Mxi-Spa secretion machinery	181458	183095	1638	146	181312	GTATCGTTTTTTTACAG
ospB	SF_p0003	OspB protein	1176	2042	867	106	1070	GTTCCGTTTTTTTAAAT
ospC1	SF_p0094	protein OspC1	81351	79939	1413	263	81614	GTATCGTTTTTTTATAG
ospE1	SF_p0265a	OspE1	215534	215268	267	71	215605	GTATCGTTTTTTTACAG
ospE2	SF_p0048	OspE2	38249	38515	267	86	38163	GTATCGTTTTTTTACAG
ospF	SF_p0010	OspF	10295	9576	720	54	10349	GTATCGTTTTATAAAAG
yccE	S_RS05600	YccE family protein	1056569	1057825	1256	81	1056488	TGAGCGATTTTTGATAG
yfdF	S_RS13440	hypothetical protein	2451431	2452489	1059	73	2451358	TGAGCGTTTTTTGATAG
virA	SF_p0181	VirA protein	149115	147913	1203	91	149206	GTATCGTTTTCTTAaAG
yjgL	S_RS23500	hypothetical protein	4411715	4410958	758	58	4411773	AGAGCGTTTTTTGATAT

Table A3. List of primers used in Chapter 2.

Primers pairs (name and sequence) and corresponding templates used in this study			
Cloning of pSB890-mxiEΔDBD (to create mxiEΔDBD mutant)			
Constructed by overlapping PCR			
	Primers		**Template**
PCR A1	5mxiE_Not1	AATT GCGGCCGC CGATTCATTAATTAGTGTCTTTG	Wild type *S. flexneri* genomic DNA
	MxiE_DBD_R	ATTTTTTTCACTAAAAAAGTTGACTCAGTCATTCGTATCATAGC	
PCR A2	MxiE_DBD_F	GCTATGATACGAATGACTGAGTCAACTTTTTTAGTGAAAAAAAT	Wild type *S. flexneri* genomic DNA
	3mxiE_Blunt	CGTTCTACAACAGTAGCCACC	
PCR B	5mxiE_Not1	AATT GCGGCCGC CGATTCATTAATTAGTGTCTTTG	PCR A1+A2
	3mxiE_Blunt	CGTTCTACAACAGTAGCCACC	
Cloning of pSB890-YccE mut box (to create mutated MxiE box upstream of yccE strain)			
Constructed by overlapping PCR			
	Primers		**Template**
PCR A1	5YccEKan792_Not 1	AATT GCGGCCGC CGGGATAGTCAGCAAAATGCT	Wild type *S. flexneri* genomic DNA
	3YccEPRMmut	CAACTATCAATAATGGCTCACCCTTTTTCACCTG	

PCR A2	5YccEPRMmut	GGTGAGCCATTATTGATAGTTGAACCAGGCAC			Wild type *S. flexneri* genomic DNA
	3YccEKan792_Blunt	AGTAAACGCATCTACCAGCGA			
PCR B	5YccEKan792_Not1	AATT GCGGCCGC CGGGATAGTCAGCAAAATGCT			PCR A1+A2
	3YccEKan792_Blunt	AGTAAACGCATCTACCAGCGA			
Cloning of pSB890-upVirB-kan-downVirB (to create virB mutant)					
Constructed by overlapping PCR					
	Primers				**Template**
PCR A1	5virB_Not1	AATT GCGGCCGC CCACTTCCCTATCAAAAGTATTAAAG			Wild type *S. flexneri* genomic DNA
	3virB-KmR	CATTTTAGCCATTTATTATTTCCTTCCTCATCACACCCTGTTTATTCATATTG			
PCR A2	5virB-KmR	CAATATGAATAAACAGGGTGTGATGAGGAAGGAAATAATAAATGGCTAAAATG			pSB890-kan
	3KmR-virB	GGGCAGTTTACATCAGTGTTCGATGTCTAAAACAATTCATCCAGTAAAATATAATATT			
PCR A3	5KmR_virB	AATATTATATTTTACTGGATGAATTGTTTTAGACATCGAACACTGATGTAAACTGCCC			Wild type *S. flexneri* genomic DNA
	3virB_Blunt	GTCGGTCATTTTATGGGAAGATTAGG			
PCR B	5virB_Not1	AATT GCGGCCGC CCACTTCCCTATCAAAAGTATTAAAG			PCR A1+A2
	3KmR-virB	GGGCAGTTTACATCAGTGTTCGATGTCTAAAACAATTCATCCAGTAAAATATAATATT			

PCR C	5virB_Not1		AATT GCGGCCGC CCACTTCCCTATCAAAAGTATTAAAG	PCR B+A3
	3virB_Blunt		GTCGGTCATTTTATGGGAAGATTAGG	
Cloning of pBAD_MxiE				
	Primers			**Template**
	5MxiEab_EcoRI		AATT GAATTC TCGAGGGATATAATTGTATTGTG	Wild type *S. flexneri* genomic DNA
	3MxiEab_NotI		AATT GCGGCCGC TTAAATTTTTTCATTTATTTTTTTCACT	
Cloning of pBAD_IpgC				
	Primers			**Template**
	5IpgC_EcoRI		AATT GAATTC AAAGGAGACCTTATGTCTTT	Wild type *S. flexneri* genomic DNA
	3IpgC_NotI		AATT GCGGCCGC TTACTCCTTGATATCCTGAAT	
Cloning of pBAD_hnsΔDBD (dominant negative construct)				
	Primers			**Template**
	5HNS_EcoRI		AATT GAATTC TATAAGTTTGAGATTACTACAATG	Wild type *S. flexneri* genomic DNA
	3HNSdDBD_NotI		AATT GCGGCCGC TTATTTAGCTTTGGTGCCAGATT	
Cloning of pMMB_MxiE (not CFP reporter; mxiE is cloned into pMMB207 with ptac promoter)				
	Primers			**Template**
	5MxiEab_EcoRI		AATT GAATTC TCGAGGGATATAATTGTATTGTG	Wild type *S. flexneri* genomic DNA
	3MxiEab_BamHI		AATT GGATCC TTAAATTTTTTCATTTATTTTTTTCACT	

Cloning of pMMB207_mCherry				
	Primers			**Template**
	5Cherry_EcoRI		AATT GAATTC ACATAAGGAGGAACTACTATGGTGAGCAAGGGCGAGGAGG	Plasmid DNA with mCherry
	3Cherry_BamHI		AATT GGATCC CTACTTGTACAGCTCGTCCATGCC	
Cloning of pMMB207_mCherry_Link (KpnI-NotI linker)				
	Primers			**Template**
PCR A1	UP_link_insert		GCGGCCGCTTCTCGAGTTGGTACCAAATGAGCTGTTGACAATTAATCAT	pMMB207
	ChL1_REV (down EcoRI)		ATCCTCCTCGCCCTTGCTCACCAT	
PCR A2	UP_ApaI		CCAGACGCAGACGCGCCGAGACAG	pMMB207
	DWN_link_insert		GGTACCAACTCGAGAAGCGGCCGCAGAATATTTGCCAGAACCGTTAT	
PCR B	UP_ApaI		CCAGACGCAGACGCGCCGAGACAG	PCR A1 + A2
	ChL1_REV		ATCCTCCTCGCCCTTGCTCACCAT	
Clone product of PCR B into pMMB207_mCherry using ApaI and EcoRI sites to introduce a KpnI-NotI linker.				
Cloning of pMMB_CFP reporter				
	Primers			**Template**
	5KpnI_BglII_SwaI_STOP_CFP		ATATA GGTACC AGATCT ATTTAAA TGATTAATT GAAAGGAGGTTTATTAAAATGGCT	Plasmid DNA with CFP
	3CFP_NotI_PstI		AATTGCGGCCGCCTGCAGTTATTTGTAGAGCTCATCCATGCC	
Clone PCR product into pMMB207_mCherry_Link using KpnI and NotI sites. Use this construct to clone in promoters of interest upstream of CFP using KpnI/BglII.				

Cloning of pMMB_YccE prm-CFP (CFP reporter for yccE promoter)				
	Primers			**Template**
	5PRM200_KpnI		ATTA GGTACC AGCGTTATCTCGCGTAAATC	Wild type *S. flexneri* genomic DNA
	3YccEprm_BglII		AATT AGATCT ATATAGCGTCTATAAAATTTAATAAATAATG	
Cloning of pMMB_YccE prm mut box-CFP (CFP reporter for yccE promoter with mut MxiE box)				
Constructed by overlapping PCR				
	Primers			**Template**
PCR A1	5PRM200_KpnI		ATTA GGTACC AGCGTTATCTCGCGTAAATC	Wild type *S. flexneri* genomic DNA
	3mut_YccEPRMmut		CAACTATCAATAATGGCTCACCCTTTTTCACCTG	
PCR A2	5YccEPRMmut		GGTGAGCCATTATTGATAGTTGAACCAGGCAC	Wild type *S. flexneri* genomic DNA
	3YccEprm_BglII		AATT AGATCT ATATAGCGTCTATAAAATTTAATAAATAATG	
PCR B	5PRM200_KpnI		ATTA GGTACC AGCGTTATCTCGCGTAAATC	PCR A1+A2
	3YccEprm_BglII		AATT AGATCT ATATAGCGTCTATAAAATTTAATAAATAATG	
Cloning of pMMB_YfdF prm-CFP (CFP reporter for yfdF promoter)				
	Primers			**Template**
	5YfdFprm_KpnI		AATT GGTACC TAACGCGTTCGCCTGGATAA	Wild type *S. flexneri* genomic DNA

	3YfdF_BglII		AATT AGATCT TATAAGGATCGTCGTTTACTC	
Cloning of pMMB_YfdF prm mut box-CFP (CFP reporter for yfdF promoter with mut MxiE box)				
Constructed by overlapping PCR				
	Primers			**Template**
PCR A1	5YfdFprm_KpnI		AATT GGTACC TAACGCGTTCGCCTGGATAA	Wild type *S. flexneri* genomic DNA
	3YfdF_MutBox		CTATCAATAAAGGCTCATTTA	
PCR A2	5YfdF_MutBox		TGAGCCTTTATTGATAGTCTA	Wild type *S. flexneri* genomic DNA
	3YfdF_BglII		AATT AGATCT TATAAGGATCGTCGTTTACTC	
PCR B	5YfdFprm_KpnI		AATT GGTACC TAACGCGTTCGCCTGGATAA	PCR A1+A2
	3YfdF_BglII		AATT AGATCT TATAAGGATCGTCGTTTACTC	
qPCR primers for mRNA expression levels				
Gene	**Primers**			
rpoB	rpoB left probe 33		ATCAACGGTACTGAGCGTGTT	
	rpoB right probe 33		AAAGAAGACGCCCGGACTAC	
dnaA	dnaA left probe 11		AGTTTTTCCACACCTTCAACG	
	dnaA right probe 11		CGATCCGAGGTGAGAATGAT	

virB	virB left probe 158		AAGGGAGATTGATGGTAGAATTGA
	virB right probe 158		CATATATTGCAGATGCTCTTCTACG
ipgD	ipgD left probe 73		AGAGCTGTTGCTGCTCGTAAT
	ipgD right probe 73		TCTGCTATATAATGCTGCGCTTAC
ipaH7.8	ipaH7.8_left_7		TCTGAGAATCCTGACTGAATGG
	ipaH7.8_right_7		AAGCAATGCCTCGCTCTTC
ospC1	ospC1_left_106		CCCCTGTGGATCTGGATAGA
	ospC1_right_106		TTTGAAGTTTTCTGTACTTACCATCC
yccE	yccE_left_44		TTGTCTGTTAAGAGCCATACTGGT
	yccE_right_44		TCGTATACTTGCTTTTGCGTCT
E.coli yccE	EcYccE_left130		CATTAATGCGTGTGATGATGTTT
	EcYccE_right_130		CGGCGTATTTATCCGCTCT
CFP	CFP_left_probe3		TGACCACATGGTCCTTCTTG
	CFP_right_probe3		CTCATCCATGCCACGTGTA
yfdF (SYBR)	5yfdF_qPCR2		GAAAAGCGAACCAACGGACT
	3yfdF_qPCR2		TGAAGCACTCCTGGCGTTTT

References

1. Musher DM, Musher BL. 2004. Contagious acute gastrointestinal infections. N Engl J Med 351:2417-27.
2. Zumla A. 2010. Mandell, Douglas, and Bennett's principles and practice of infectious diseases., 7th ed, vol 10. Churchill Livingstone, The Lancet, Infectious Diseases.
3. Labrec EH, Schneider H, Magnani TJ, Formal SB. 1964. Epithelial Cell Penetration as an Essential Step in the Pathogenesis of Bacillary Dysentery. J Bacteriol 88:1503-18.
4. Takeuchi A, Sprinz H, LaBrec EH, Formal SB. 1965. Experimental bacillary dysentery. An electron microscopic study of the response of the intestinal mucosa to bacterial invasion. Am J Pathol 47:1011-44.
5. Yum LK, Byndloss MX, Feldman SH, Agaisse H. 2019. Critical role of bacterial dissemination in an infant rabbit model of bacillary dysentery. Nat Commun 10:1826.
6. DuPont HL, Levine MM, Hornick RB, Formal SB. 1989. Inoculum size in shigellosis and implications for expected mode of transmission. J Infect Dis 159:1126-8.
7. Lampel KA, Formal SB, Maurelli AT. 2018. A Brief History of Shigella. EcoSal Plus 8.
8. Khalil IA, Troeger C, Blacker BF, Rao PC, Brown A, Atherly DE, Brewer TG, Engmann CM, Houpt ER, Kang G, Kotloff KL, Levine MM, Luby SP, MacLennan CA, Pan WK, Pavlinac PB, Platts-Mills JA, Qadri F, Riddle MS, Ryan ET, Shoultz DA, Steele AD, Walson JL, Sanders JW, Mokdad AH, Murray CJL, Hay SI, Reiner RC, Jr. 2018. Morbidity and mortality due to shigella and enterotoxigenic Escherichia coli diarrhoea: the Global Burden of Disease Study 1990-2016. Lancet Infect Dis 18:1229-1240.
9. Kotloff KL, Riddle MS, Platts-Mills JA, Pavlinac P, Zaidi AKM. 2018. Shigellosis. Lancet 391:801-812.
10. Williams PCM, Berkley JA. 2018. Guidelines for the treatment of dysentery (shigellosis): a systematic review of the evidence. Paediatr Int Child Health 38:S50-S65.
11. Ranjbar R, Farahani A. 2019. Shigella: Antibiotic-Resistance Mechanisms And New Horizons For Treatment. Infect Drug Resist 12:3137-3167.
12. Lennox ES. 1955. Transduction of linked genetic characters of the host by bacteriophage P1. Virology 1:190-206.
13. Luria SE, Burrous JW. 1957. Hybridization between Escherichia coli and Shigella. J Bacteriol 74:461-76.
14. Pupo GM, Karaolis DK, Lan R, Reeves PR. 1997. Evolutionary relationships among pathogenic and nonpathogenic Escherichia coli strains inferred from multilocus enzyme electrophoresis and mdh sequence studies. Infect Immun 65:2685-92.

15. Pupo GM, Lan R, Reeves PR. 2000. Multiple independent origins of Shigella clones of Escherichia coli and convergent evolution of many of their characteristics. Proc Natl Acad Sci U S A 97:10567-72.
16. Wei J, Goldberg MB, Burland V, Venkatesan MM, Deng W, Fournier G, Mayhew GF, Plunkett G, 3rd, Rose DJ, Darling A, Mau B, Perna NT, Payne SM, Runyen-Janecky LJ, Zhou S, Schwartz DC, Blattner FR. 2003. Complete genome sequence and comparative genomics of Shigella flexneri serotype 2a strain 2457T. Infect Immun 71:2775-86.
17. Lan R, Lumb B, Ryan D, Reeves PR. 2001. Molecular evolution of large virulence plasmid in Shigella clones and enteroinvasive Escherichia coli. Infect Immun 69:6303-9.
18. Sansonetti PJ, Kopecko DJ, Formal SB. 1982. Involvement of a plasmid in the invasive ability of Shigella flexneri. Infect Immun 35:852-60.
19. Hale TL, Sansonetti PJ, Schad PA, Austin S, Formal SB. 1983. Characterization of virulence plasmids and plasmid-associated outer membrane proteins in Shigella flexneri, Shigella sonnei, and Escherichia coli. Infect Immun 40:340-50.
20. Harris JR, Wachsmuth IK, Davis BR, Cohen ML. 1982. High-molecular-weight plasmid correlates with Escherichia coli enteroinvasiveness. Infect Immun 37:1295-8.
21. Groisman EA, Ochman H. 1997. How Salmonella became a pathogen. Trends Microbiol 5:343-9.
22. Maurelli AT. 2007. Black holes, antivirulence genes, and gene inactivation in the evolution of bacterial pathogens. FEMS Microbiol Lett 267:1-8.
23. Siguier P, Gourbeyre E, Chandler M. 2014. Bacterial insertion sequences: their genomic impact and diversity. FEMS Microbiol Rev 38:865-91.
24. Yang F, Yang J, Zhang X, Chen L, Jiang Y, Yan Y, Tang X, Wang J, Xiong Z, Dong J, Xue Y, Zhu Y, Xu X, Sun L, Chen S, Nie H, Peng J, Xu J, Wang Y, Yuan Z, Wen Y, Yao Z, Shen Y, Qiang B, Hou Y, Yu J, Jin Q. 2005. Genome dynamics and diversity of Shigella species, the etiologic agents of bacillary dysentery. Nucleic Acids Res 33:6445-58.
25. Hale TL. 1991. Genetic basis of virulence in Shigella species. Microbiol Rev 55:206-24.
26. Buchrieser C, Glaser P, Rusniok C, Nedjari H, D'Hauteville H, Kunst F, Sansonetti P, Parsot C. 2000. The virulence plasmid pWR100 and the repertoire of proteins secreted by the type III secretion apparatus of Shigella flexneri. Mol Microbiol 38:760-71.
27. Sansonetti PJ, d'Hauteville H, Ecobichon C, Pourcel C. 1983. Molecular comparison of virulence plasmids in Shigella and enteroinvasive Escherichia coli. Ann Microbiol (Paris) 134A:295-318.
28. Maurelli AT, Baudry B, d'Hauteville H, Hale TL, Sansonetti PJ. 1985. Cloning of plasmid DNA sequences involved in invasion of HeLa cells by Shigella flexneri. Infect Immun 49:164-71.
29. Sasakawa C, Kamata K, Sakai T, Makino S, Yamada M, Okada N, Yoshikawa M. 1988. Virulence-associated genetic regions comprising 31 kilobases of the 230-kilobase plasmid in Shigella flexneri 2a. J Bacteriol 170:2480-4.

30. Sasakawa C, Komatsu K, Tobe T, Suzuki T, Yoshikawa M. 1993. Eight genes in region 5 that form an operon are essential for invasion of epithelial cells by Shigella flexneri 2a. J Bacteriol 175:2334-46.
31. Parsot C. 2009. Shigella type III secretion effectors: how, where, when, for what purposes? Curr Opin Microbiol 12:110-6.
32. Jin Q, Yuan Z, Xu J, Wang Y, Shen Y, Lu W, Wang J, Liu H, Yang J, Yang F, Zhang X, Zhang J, Yang G, Wu H, Qu D, Dong J, Sun L, Xue Y, Zhao A, Gao Y, Zhu J, Kan B, Ding K, Chen S, Cheng H, Yao Z, He B, Chen R, Ma D, Qiang B, Wen Y, Hou Y, Yu J. 2002. Genome sequence of Shigella flexneri 2a: insights into pathogenicity through comparison with genomes of Escherichia coli K12 and O157. Nucleic Acids Res 30:4432-41.
33. Sansonetti PJ, Hale TL, Dammin GJ, Kapfer C, Collins HH, Jr., Formal SB. 1983. Alterations in the pathogenicity of Escherichia coli K-12 after transfer of plasmid and chromosomal genes from Shigella flexneri. Infect Immun 39:1392-402.
34. Will WR, Navarre WW, Fang FC. 2015. Integrated circuits: how transcriptional silencing and counter-silencing facilitate bacterial evolution. Curr Opin Microbiol 23:8-13.
35. Dorman CJ. 2014. H-NS-like nucleoid-associated proteins, mobile genetic elements and horizontal gene transfer in bacteria. Plasmid 75:1-11.
36. Navarre WW, Porwollik S, Wang Y, McClelland M, Rosen H, Libby SJ, Fang FC. 2006. Selective silencing of foreign DNA with low GC content by the H-NS protein in Salmonella. Science 313:236-8.
37. Arold ST, Leonard PG, Parkinson GN, Ladbury JE. 2010. H-NS forms a superhelical protein scaffold for DNA condensation. Proc Natl Acad Sci U S A 107:15728-32.
38. Hommais F, Krin E, Laurent-Winter C, Soutourina O, Malpertuy A, Le Caer JP, Danchin A, Bertin P. 2001. Large-scale monitoring of pleiotropic regulation of gene expression by the prokaryotic nucleoid-associated protein, H-NS. Mol Microbiol 40:20-36.
39. Bouffartigues E, Buckle M, Badaut C, Travers A, Rimsky S. 2007. H-NS cooperative binding to high-affinity sites in a regulatory element results in transcriptional silencing. Nat Struct Mol Biol 14:441-8.
40. Navarre WW, McClelland M, Libby SJ, Fang FC. 2007. Silencing of xenogeneic DNA by H-NS-facilitation of lateral gene transfer in bacteria by a defense system that recognizes foreign DNA. Genes Dev 21:1456-71.
41. Renault M, Garcia J, Cordeiro TN, Baldus M, Pons M. 2013. Protein oligomers studied by solid-state NMR--the case of the full-length nucleoid-associated protein histone-like nucleoid structuring protein. FEBS J 280:2916-28.
42. Williams RM, Rimsky S, Buc H. 1996. Probing the structure, function, and interactions of the Escherichia coli H-NS and StpA proteins by using dominant negative derivatives. J Bacteriol 178:4335-43.
43. Ceschini S, Lupidi G, Coletta M, Pon CL, Fioretti E, Angeletti M. 2000. Multimeric self-assembly equilibria involving the histone-like protein H-NS. A thermodynamic study. J Biol Chem 275:729-34.

44. Deighan P, Beloin C, Dorman CJ. 2003. Three-way interactions among the Sfh, StpA and H-NS nucleoid-structuring proteins of Shigella flexneri 2a strain 2457T. Mol Microbiol 48:1401-16.
45. Beloin C, Deighan P, Doyle M, Dorman CJ. 2003. Shigella flexneri 2a strain 2457T expresses three members of the H-NS-like protein family: characterization of the Sfh protein. Mol Genet Genomics 270:66-77.
46. Tendeng C, Bertin PN. 2003. H-NS in Gram-negative bacteria: a family of multifaceted proteins. Trends Microbiol 11:511-8.
47. Doyle M, Dorman CJ. 2006. Reciprocal transcriptional and posttranscriptional growth-phase-dependent expression of sfh, a gene that encodes a paralogue of the nucleoid-associated protein H-NS. J Bacteriol 188:7581-91.
48. Lang B, Blot N, Bouffartigues E, Buckle M, Geertz M, Gualerzi CO, Mavathur R, Muskhelishvili G, Pon CL, Rimsky S, Stella S, Babu MM, Travers A. 2007. High-affinity DNA binding sites for H-NS provide a molecular basis for selective silencing within proteobacterial genomes. Nucleic Acids Res 35:6330-7.
49. Gordon BR, Li Y, Cote A, Weirauch MT, Ding P, Hughes TR, Navarre WW, Xia B, Liu J. 2011. Structural basis for recognition of AT-rich DNA by unrelated xenogeneic silencing proteins. Proc Natl Acad Sci U S A 108:10690-5.
50. Winardhi RS, Yan J, Kenney LJ. 2015. H-NS Regulates Gene Expression and Compacts the Nucleoid: Insights from Single-Molecule Experiments. Biophys J 109:1321-9.
51. Dorman CJ, Deighan P. 2003. Regulation of gene expression by histone-like proteins in bacteria. Curr Opin Genet Dev 13:179-84.
52. Rangarajan AA, Schnetz K. 2018. Interference of transcription across H-NS binding sites and repression by H-NS. Mol Microbiol 108:226-239.
53. Schroder O, Wagner R. 2000. The bacterial DNA-binding protein H-NS represses ribosomal RNA transcription by trapping RNA polymerase in the initiation complex. J Mol Biol 298:737-48.
54. Ueguchi C, Mizuno T. 1993. The Escherichia coli nucleoid protein H-NS functions directly as a transcriptional repressor. EMBO J 12:1039-46.
55. Galan JE, Lara-Tejero M, Marlovits TC, Wagner S. 2014. Bacterial type III secretion systems: specialized nanomachines for protein delivery into target cells. Annu Rev Microbiol 68:415-38.
56. Menard R, Sansonetti P, Parsot C. 1994. The secretion of the Shigella flexneri Ipa invasins is activated by epithelial cells and controlled by IpaB and IpaD. EMBO J 13:5293-302.
57. Blocker A, Gounon P, Larquet E, Niebuhr K, Cabiaux V, Parsot C, Sansonetti P. 1999. The tripartite type III secreton of Shigella flexneri inserts IpaB and IpaC into host membranes. J Cell Biol 147:683-93.
58. Hu B, Morado DR, Margolin W, Rohde JR, Arizmendi O, Picking WL, Picking WD, Liu J. 2015. Visualization of the type III secretion sorting platform of Shigella flexneri. Proc Natl Acad Sci U S A 112:1047-52.
59. Muthuramalingam M, Whittier SK, Picking WL, Picking WD. 2021. The Shigella Type III Secretion System: An Overview from Top to Bottom. Microorganisms 9.

60. Tamano K, Aizawa S, Katayama E, Nonaka T, Imajoh-Ohmi S, Kuwae A, Nagai S, Sasakawa C. 2000. Supramolecular structure of the Shigella type III secretion machinery: the needle part is changeable in length and essential for delivery of effectors. EMBO J 19:3876-87.
61. Bahrani FK, Sansonetti PJ, Parsot C. 1997. Secretion of Ipa proteins by Shigella flexneri: inducer molecules and kinetics of activation. Infect Immun 65:4005-10.
62. Parsot C, Menard R, Gounon P, Sansonetti PJ. 1995. Enhanced secretion through the Shigella flexneri Mxi-Spa translocon leads to assembly of extracellular proteins into macromolecular structures. Mol Microbiol 16:291-300.
63. Pope LM, Reed KE, Payne SM. 1995. Increased protein secretion and adherence to HeLa cells by Shigella spp. following growth in the presence of bile salts. Infect Immun 63:3642-8.
64. Schroeder GN, Hilbi H. 2008. Molecular pathogenesis of Shigella spp.: controlling host cell signaling, invasion, and death by type III secretion. Clin Microbiol Rev 21:134-56.
65. Ashida H, Toyotome T, Nagai T, Sasakawa C. 2007. Shigella chromosomal IpaH proteins are secreted via the type III secretion system and act as effectors. Mol Microbiol 63:680-93.
66. Mattock E, Blocker AJ. 2017. How Do the Virulence Factors of Shigella Work Together to Cause Disease? Front Cell Infect Microbiol 7:64.
67. Gall TL, Mavris M, Martino MC, Bernardini ML, Denamur E, Parsot C. 2005. Analysis of virulence plasmid gene expression defines three classes of effectors in the type III secretion system of Shigella flexneri. Microbiology (Reading) 151:951-962.
68. Kane CD, Schuch R, Day WA, Jr., Maurelli AT. 2002. MxiE regulates intracellular expression of factors secreted by the Shigella flexneri 2a type III secretion system. J Bacteriol 184:4409-19.
69. Gallegos MT, Schleif R, Bairoch A, Hofmann K, Ramos JL. 1997. Arac/XylS family of transcriptional regulators. Microbiol Mol Biol Rev 61:393-410.
70. Egan SM. 2002. Growing repertoire of AraC/XylS activators. J Bacteriol 184:5529-32.
71. Emanuele AA, Garcia GA. 2015. Mechanism of Action and Initial, In Vitro SAR of an Inhibitor of the Shigella flexneri Virulence Regulator VirF. PLoS One 10:e0137410.
72. Koppolu V, Osaka I, Skredenske JM, Kettle B, Hefty PS, Li J, Egan SM. 2013. Small-molecule inhibitor of the Shigella flexneri master virulence regulator VirF. Infect Immun 81:4220-31.
73. Tobe T, Yoshikawa M, Mizuno T, Sasakawa C. 1993. Transcriptional control of the invasion regulatory gene virB of Shigella flexneri: activation by virF and repression by H-NS. J Bacteriol 175:6142-9.
74. Tran CN, Giangrossi M, Prosseda G, Brandi A, Di Martino ML, Colonna B, Falconi M. 2011. A multifactor regulatory circuit involving H-NS, VirF and an antisense RNA modulates transcription of the virulence gene icsA of Shigella flexneri. Nucleic Acids Res 39:8122-34.

75. Schleif R. 2010. AraC protein, regulation of the l-arabinose operon in Escherichia coli, and the light switch mechanism of AraC action. FEMS Microbiol Rev 34:779-96.
76. Falconi M, Colonna B, Prosseda G, Micheli G, Gualerzi CO. 1998. Thermoregulation of Shigella and Escherichia coli EIEC pathogenicity. A temperature-dependent structural transition of DNA modulates accessibility of virF promoter to transcriptional repressor H-NS. EMBO J 17:7033-43.
77. Prosseda G, Falconi M, Giangrossi M, Gualerzi CO, Micheli G, Colonna B. 2004. The virF promoter in Shigella: more than just a curved DNA stretch. Mol Microbiol 51:523-37.
78. Prosseda G, Fradiani PA, Di Lorenzo M, Falconi M, Micheli G, Casalino M, Nicoletti M, Colonna B. 1998. A role for H-NS in the regulation of the virF gene of Shigella and enteroinvasive Escherichia coli. Res Microbiol 149:15-25.
79. Picker MA, Wing HJ. 2016. H-NS, Its Family Members and Their Regulation of Virulence Genes in Shigella Species. Genes 7:112.
80. Bernardini ML, Mounier J, d'Hauteville H, Coquis-Rondon M, Sansonetti PJ. 1989. Identification of icsA, a plasmid locus of Shigella flexneri that governs bacterial intra- and intercellular spread through interaction with F-actin. Proc Natl Acad Sci U S A 86:3867-71.
81. Sakai T, Sasakawa C, Yoshikawa M. 1988. Expression of four virulence antigens of Shigella flexneri is positively regulated at the transcriptional level by the 30 kiloDalton virF protein. Mol Microbiol 2:589-97.
82. Adler B, Sasakawa C, Tobe T, Makino S, Komatsu K, Yoshikawa M. 1989. A dual transcriptional activation system for the 230 kb plasmid genes coding for virulence-associated antigens of Shigella flexneri. Mol Microbiol 3:627-35.
83. Durand JM, Dagberg B, Uhlin BE, Bjork GR. 2000. Transfer RNA modification, temperature and DNA superhelicity have a common target in the regulatory network of the virulence of Shigella flexneri: the expression of the virF gene. Mol Microbiol 35:924-35.
84. Watanabe H, Arakawa E, Ito K, Kato J, Nakamura A. 1990. Genetic analysis of an invasion region by use of a Tn3-lac transposon and identification of a second positive regulator gene, invE, for cell invasion of Shigella sonnei: significant homology of invE with ParB of plasmid P1. J Bacteriol 172:619-29.
85. Castellanos MI, Harrison DJ, Smith JM, Labahn SK, Levy KM, Wing HJ. 2009. VirB alleviates H-NS repression of the icsP promoter in Shigella flexneri from sites more than one kilobase upstream of the transcription start site. J Bacteriol 191:4047-50.
86. McKenna JA, Wing HJ. 2020. The Antiactivator of Type III Secretion, OspD1, Is Transcriptionally Regulated by VirB and H-NS from Remote Sequences in Shigella flexneri. J Bacteriol 202.
87. Tobe T, Nagai S, Okada N, Adler B, Yoshikawa M, Sasakawa C. 1991. Temperature-regulated expression of invasion genes in Shigella flexneri is controlled through the transcriptional activation of the virB gene on the large plasmid. Mol Microbiol 5:887-93.

88. Weatherspoon-Griffin N, Picker MA, Pew KL, Park HS, Ginete DR, Karney MM, Usufzy P, Castellanos MI, Duhart JC, Harrison DJ, Socea JN, Karabachev AD, Hensley CT, Howerton AJ, Ojeda-Daulo R, Immak JA, Wing HJ. 2018. Insights into transcriptional silencing and anti-silencing in Shigella flexneri: a detailed molecular analysis of the icsP virulence locus. Mol Microbiol 108:505-518.
89. Wing HJ, Yan AW, Goldman SR, Goldberg MB. 2004. Regulation of IcsP, the outer membrane protease of the Shigella actin tail assembly protein IcsA, by virulence plasmid regulators VirF and VirB. J Bacteriol 186:699-705.
90. Beloin C, McKenna S, Dorman CJ. 2002. Molecular dissection of VirB, a key regulator of the virulence cascade of Shigella flexneri. J Biol Chem 277:15333-44.
91. McKenna S, Beloin C, Dorman CJ. 2003. In vitro DNA-binding properties of VirB, the Shigella flexneri virulence regulatory protein. FEBS Lett 545:183-7.
92. Taniya T, Mitobe J, Nakayama S, Mingshan Q, Okuda K, Watanabe H. 2003. Determination of the InvE binding site required for expression of IpaB of the Shigella sonnei virulence plasmid: involvement of a ParB boxA-like sequence. J Bacteriol 185:5158-65.
93. Turner EC, Dorman CJ. 2007. H-NS antagonism in Shigella flexneri by VirB, a virulence gene transcription regulator that is closely related to plasmid partition factors. J Bacteriol 189:3403-13.
94. Surtees JA, Funnell BE. 2001. The DNA binding domains of P1 ParB and the architecture of the P1 plasmid partition complex. J Biol Chem 276:12385-94.
95. Porter ME, Dorman CJ. 1997. Differential regulation of the plasmid-encoded genes in the Shigella flexneri virulence regulon. Mol Gen Genet 256:93-103.
96. Basta DW, Pew KL, Immak JA, Park HS, Picker MA, Wigley AF, Hensley CT, Pearson JS, Hartland EL, Wing HJ. 2013. Characterization of the ospZ promoter in Shigella flexneri and its regulation by VirB and H-NS. J Bacteriol 195:2562-72.
97. Gao X, Zou T, Mu Z, Qin B, Yang J, Waltersperger S, Wang M, Cui S, Jin Q. 2013. Structural insights into VirB-DNA complexes reveal mechanism of transcriptional activation of virulence genes. Nucleic Acids Res 41:10529-41.
98. Karney MM, McKenna JA, Weatherspoon-Griffin N, Karabachev AD, Millar ME, Potocek EA, Wing HJ. 2019. Investigating the DNA-Binding Site for VirB, a Key Transcriptional Regulator of Shigella Virulence Genes, Using an In Vivo Binding Tool. Genes (Basel) 10.
99. Kane KA, Dorman CJ. 2012. VirB-mediated positive feedback control of the virulence gene regulatory cascade of Shigella flexneri. J Bacteriol 194:5264-73.
100. Mavris M, Page AL, Tournebize R, Demers B, Sansonetti P, Parsot C. 2002. Regulation of transcription by the activity of the Shigella flexneri type III secretion apparatus. Mol Microbiol 43:1543-53.
101. Parsot C, Ageron E, Penno C, Mavris M, Jamoussi K, d'Hauteville H, Sansonetti P, Demers B. 2005. A secreted anti-activator, OspD1, and its chaperone, Spa15, are involved in the control of transcription by the type III secretion apparatus activity in Shigella flexneri. Mol Microbiol 56:1627-35.

102. Enninga J, Mounier J, Sansonetti P, Tran Van Nhieu G. 2005. Secretion of type III effectors into host cells in real time. Nat Methods 2:959-65.
103. Veenendaal AK, Hodgkinson JL, Schwarzer L, Stabat D, Zenk SF, Blocker AJ. 2007. The type III secretion system needle tip complex mediates host cell sensing and translocon insertion. Mol Microbiol 63:1719-30.
104. Watarai M, Tobe T, Yoshikawa M, Sasakawa C. 1995. Contact of Shigella with host cells triggers release of Ipa invasins and is an essential function of invasiveness. EMBO J 14:2461-70.
105. Pilonieta MC, Munson GP. 2008. The chaperone IpgC copurifies with the virulence regulator MxiE. J Bacteriol 190:2249-51.
106. Ashida H, Sasakawa C. 2015. Shigella IpaH Family Effectors as a Versatile Model for Studying Pathogenic Bacteria. Front Cell Infect Microbiol 5:100.
107. Demers B, Sansonetti PJ, Parsot C. 1998. Induction of type III secretion in Shigella flexneri is associated with differential control of transcription of genes encoding secreted proteins. EMBO J 17:2894-903.
108. Sankaran K, Ramachandran V, Subrahmanyam YV, Rajarathnam S, Elango S, Roy RK. 1989. Congo red-mediated regulation of levels of Shigella flexneri 2a membrane proteins. Infect Immun 57:2364-71.
109. Silue N, Marcantonio E, Campbell-Valois FX. 2020. RNA-Seq analysis of the T3SA regulon in Shigella flexneri reveals two new chromosomal genes upregulated in the on-state. Methods 176:71-81.
110. Penno C, Sansonetti P, Parsot C. 2005. Frameshifting by transcriptional slippage is involved in production of MxiE, the transcription activator regulated by the activity of the type III secretion apparatus in Shigella flexneri. Mol Microbiol 56:204-14.
111. Penno C, Parsot C. 2006. Transcriptional slippage in mxiE controls transcription and translation of the downstream mxiD gene, which encodes a component of the Shigella flexneri type III secretion apparatus. J Bacteriol 188:1196-8.
112. Brutinel ED, Yahr TL. 2008. Control of gene expression by type III secretory activity. Curr Opin Microbiol 11:128-33.
113. Mavris M, Sansonetti PJ, Parsot C. 2002. Identification of the cis-acting site involved in activation of promoters regulated by activity of the type III secretion apparatus in Shigella flexneri. J Bacteriol 184:6751-9.
114. Silue N, Campbell-Valois FX. 2022. icaR and icaT are Ancient Chromosome Genes Encoding Substrates of the Type III Secretion Apparatus in Shigella flexneri. mSphere 7:e0011522.
115. Bongrand C, Sansonetti PJ, Parsot C. 2012. Characterization of the promoter, MxiE box and 5' UTR of genes controlled by the activity of the type III secretion apparatus in Shigella flexneri. PLoS One 7:e32862.
116. McKenna JA, Karney MMA, Chan DK, Weatherspoon-Griffin N, Becerra Larios B, Pilonieta MC, Munson GP, Wing HJ. 2022. The AraC/XylS Protein MxiE and Its Coregulator IpgC Control a Negative Feedback Loop in the Transcriptional Cascade That Regulates Type III Secretion in Shigella flexneri. J Bacteriol 204:e0013722.

117. Sansonetti PJ. 1998. Molecular and cellular mechanisms of invasion of the intestinal barrier by enteric pathogens. The paradigm of Shigella. Folia Microbiol (Praha) 43:239-46.
118. Maurelli AT, Sansonetti PJ. 1988. Identification of a chromosomal gene controlling temperature-regulated expression of Shigella virulence. Proc Natl Acad Sci U S A 85:2820-4.
119. Picker MA, Wing HJ. 2016. H-NS, Its Family Members and Their Regulation of Virulence Genes in Shigella Species. Genes (Basel) 7:112.
120. Beloin C, Dorman CJ. 2003. An extended role for the nucleoid structuring protein H-NS in the virulence gene regulatory cascade of Shigella flexneri. Mol Microbiol 47:825-38.
121. Maurelli AT, Blackmon B, Curtiss R, 3rd. 1984. Temperature-dependent expression of virulence genes in Shigella species. Infect Immun 43:195-201.
122. Jost BH, Adler B. 1993. Site of transcriptional activation of virB on the large plasmid of Shigella flexneri 2a by VirF, a member of the AraC family of transcriptional activators. Microb Pathog 14:481-8.
123. Menard R, Sansonetti P, Parsot C, Vasselon T. 1994. Extracellular association and cytoplasmic partitioning of the IpaB and IpaC invasins of S. flexneri. Cell 79:515-25.
124. Dragoi AM, Agaisse H. 2015. The class II phosphatidylinositol 3-phosphate kinase PIK3C2A promotes Shigella flexneri dissemination through formation of vacuole-like protrusions. Infect Immun 83:1695-704.
125. Koseoglu VK, Hall CP, Rodriguez-Lopez EM, Agaisse H. 2019. The Autotransporter IcsA Promotes Shigella flexneri Biofilm Formation in the Presence of Bile Salts. Infect Immun 87.
126. Casadaban MJ. 1976. Transposition and fusion of the lac genes to selected promoters in Escherichia coli using bacteriophage lambda and Mu. J Mol Biol 104:541-55.
127. Yamada H, Yoshida T, Tanaka K, Sasakawa C, Mizuno T. 1991. Molecular analysis of the Escherichia coli hns gene encoding a DNA-binding protein, which preferentially recognizes curved DNA sequences. Mol Gen Genet 230:332-6.
128. Bolger AM, Lohse M, Usadel B. 2014. Trimmomatic: a flexible trimmer for Illumina sequence data. Bioinformatics 30:2114-20.
129. Andrews. 2010. FastQC,
130. Langmead B, Trapnell C, Pop M, Salzberg SL. 2009. Ultrafast and memory-efficient alignment of short DNA sequences to the human genome. Genome Biol 10:R25.
131. Bray NL, Pimentel H, Melsted P, Pachter L. 2016. Near-optimal probabilistic RNA-seq quantification. Nat Biotechnol 34:525-7.
132. Liao Y, Smyth GK, Shi W. 2014. featureCounts: an efficient general purpose program for assigning sequence reads to genomic features. Bioinformatics 30:923-30.
133. Grant CE, Bailey TL, Noble WS. 2011. FIMO: scanning for occurrences of a given motif. Bioinformatics 27:1017-8.

134. Bailey TL, Boden M, Buske FA, Frith M, Grant CE, Clementi L, Ren J, Li WW, Noble WS. 2009. MEME SUITE: tools for motif discovery and searching. Nucleic Acids Res 37:W202-8.
135. Ramirez F, Ryan DP, Gruning B, Bhardwaj V, Kilpert F, Richter AS, Heyne S, Dundar F, Manke T. 2016. deepTools2: a next generation web server for deep-sequencing data analysis. Nucleic Acids Res 44:W160-5.
136. Freese NH, Norris DC, Loraine AE. 2016. Integrated genome browser: visual analytics platform for genomics. Bioinformatics 32:2089-95.
137. Gao F, Zhang CT. 2006. GC-Profile: a web-based tool for visualizing and analyzing the variation of GC content in genomic sequences. Nucleic Acids Res 34:W686-91.
138. Letunic I, Bork P. 2019. Interactive Tree Of Life (iTOL) v4: recent updates and new developments. Nucleic Acids Res 47:W256-W259.
139. Tamura K. SG, and Kumar S. . 2021. MEGA 11: Molecular Evolutionary Genetics Analysis Version 11. Mol Biol Evol doi:https://doi.org/10.1093/molbev/msab120.
140. The HC, Thanh DP, Holt KE, Thomson NR, Baker S. 2016. The genomic signatures of Shigella evolution, adaptation and geographical spread. Nat Rev Microbiol 14:235-50.
141. Lucchini S, Rowley G, Goldberg MD, Hurd D, Harrison M, Hinton JC. 2006. H-NS mediates the silencing of laterally acquired genes in bacteria. PLoS Pathog 2:e81.
142. Banos RC, Pons JI, Madrid C, Juarez A. 2008. A global modulatory role for the Yersinia enterocolitica H-NS protein. Microbiology (Reading) 154:1281-1289.
143. Williamson HS, Free A. 2005. A truncated H-NS-like protein from enteropathogenic Escherichia coli acts as an H-NS antagonist. Mol Microbiol 55:808-27.
144. Holt KE, Baker S, Weill FX, Holmes EC, Kitchen A, Yu J, Sangal V, Brown DJ, Coia JE, Kim DW, Choi SY, Kim SH, da Silveira WD, Pickard DJ, Farrar JJ, Parkhill J, Dougan G, Thomson NR. 2012. Shigella sonnei genome sequencing and phylogenetic analysis indicate recent global dissemination from Europe. Nat Genet 44:1056-9.
145. Darwin KH, Miller VL. 2001. Type III secretion chaperone-dependent regulation: activation of virulence genes by SicA and InvF in Salmonella typhimurium. EMBO J 20:1850-62.
146. Darwin KH, Miller VL. 2000. The putative invasion protein chaperone SicA acts together with InvF to activate the expression of Salmonella typhimurium virulence genes. Mol Microbiol 35:949-60.
147. Romero-Gonzalez LE, Perez-Morales D, Cortes-Avalos D, Vazquez-Guerrero E, Paredes-Hernandez DA, Estrada-de Los Santos P, Villa-Tanaca L, De la Cruz MA, Bustamante VH, Ibarra JA. 2020. The Salmonella Typhimurium InvF-SicA complex is necessary for the transcription of sopB in the absence of the repressor H-NS. PLoS One 15:e0240617.

148. van Kessel JC, Ulrich LE, Zhulin IB, Bassler BL. 2013. Analysis of activator and repressor functions reveals the requirements for transcriptional control by LuxR, the master regulator of quorum sensing in Vibrio harveyi. mBio 4.
149. Chaparian RR, Tran MLN, Miller Conrad LC, Rusch DB, van Kessel JC. 2020. Global H-NS counter-silencing by LuxR activates quorum sensing gene expression. Nucleic Acids Res 48:171-183.
150. Kazi MI, Conrado AR, Mey AR, Payne SM, Davies BW. 2016. ToxR Antagonizes H-NS Regulation of Horizontally Acquired Genes to Drive Host Colonization. PLoS Pathog 12:e1005570.
151. Dorman CJ. 2004. Virulence Gene Regulation in Shigella. EcoSal Plus 1.
152. Stone JB, Withey JH. 2021. H-NS and ToxT Inversely Control Cholera Toxin Production by Binding to Overlapping DNA Sequences. J Bacteriol 203:e0018721.
153. Lunelli M, Lokareddy RK, Zychlinsky A, Kolbe M. 2009. IpaB-IpgC interaction defines binding motif for type III secretion translocator. Proc Natl Acad Sci U S A 106:9661-6.
154. Owen-Hughes TA, Pavitt GD, Santos DS, Sidebotham JM, Hulton CS, Hinton JC, Higgins CF. 1992. The chromatin-associated protein H-NS interacts with curved DNA to influence DNA topology and gene expression. Cell 71:255-65.
155. Fang FC, Rimsky S. 2008. New insights into transcriptional regulation by H-NS. Curr Opin Microbiol 11:113-20.
156. Dorman CJ. 2004. H-NS: a universal regulator for a dynamic genome. Nat Rev Microbiol 2:391-400.
157. Dame RT, Wyman C, Goosen N. 2000. H-NS mediated compaction of DNA visualised by atomic force microscopy. Nucleic Acids Res 28:3504-10.
158. Beckwitt EC, Kong M, Van Houten B. 2018. Studying protein-DNA interactions using atomic force microscopy. Semin Cell Dev Biol 73:220-230.
159. Banos RC, Vivero A, Aznar S, Garcia J, Pons M, Madrid C, Juarez A. 2009. Differential regulation of horizontally acquired and core genome genes by the bacterial modulator H-NS. PLoS Genet 5:e1000513.
160. Madrid C, Balsalobre C, Garcia J, Juarez A. 2007. The novel Hha/YmoA family of nucleoid-associated proteins: use of structural mimicry to modulate the activity of the H-NS family of proteins. Mol Microbiol 63:7-14.
161. Vivero A, Banos RC, Mariscotti JF, Oliveros JC, Garcia-del Portillo F, Juarez A, Madrid C. 2008. Modulation of horizontally acquired genes by the Hha-YdgT proteins in Salmonella enterica serovar Typhimurium. J Bacteriol 190:1152-6.
162. Nieto JM, Madrid C, Miquelay E, Parra JL, Rodriguez S, Juarez A. 2002. Evidence for direct protein-protein interaction between members of the enterobacterial Hha/YmoA and H-NS families of proteins. J Bacteriol 184:629-35.
163. Paytubi S, Madrid C, Forns N, Nieto JM, Balsalobre C, Uhlin BE, Juarez A. 2004. YdgT, the Hha paralogue in Escherichia coli, forms heteromeric complexes with H-NS and StpA. Mol Microbiol 54:251-63.
164. DiRita VJ, Parsot C, Jander G, Mekalanos JJ. 1991. Regulatory cascade controls virulence in Vibrio cholerae. Proc Natl Acad Sci U S A 88:5403-7.

165. Higgins DE, Nazareno E, DiRita VJ. 1992. The virulence gene activator ToxT from Vibrio cholerae is a member of the AraC family of transcriptional activators. J Bacteriol 174:6974-80.
166. Yu RR, DiRita VJ. 2002. Regulation of gene expression in Vibrio cholerae by ToxT involves both antirepression and RNA polymerase stimulation. Mol Microbiol 43:119-34.
167. Stoebel DM, Free A, Dorman CJ. 2008. Anti-silencing: overcoming H-NS-mediated repression of transcription in Gram-negative enteric bacteria. Microbiology (Reading) 154:2533-2545.
168. Jordi BJ, Dagberg B, de Haan LA, Hamers AM, van der Zeijst BA, Gaastra W, Uhlin BE. 1992. The positive regulator CfaD overcomes the repression mediated by histone-like protein H-NS (H1) in the CFA/I fimbrial operon of Escherichia coli. EMBO J 11:2627-32.
169. Murphree D, Froehlich B, Scott JR. 1997. Transcriptional control of genes encoding CS1 pili: negative regulation by a silencer and positive regulation by Rns. J Bacteriol 179:5736-43.
170. Olekhnovich IN, Kadner RJ. 2007. Role of nucleoid-associated proteins Hha and H-NS in expression of Salmonella enterica activators HilD, HilC, and RtsA required for cell invasion. J Bacteriol 189:6882-90.
171. Porter ME, Mitchell P, Roe AJ, Free A, Smith DG, Gally DL. 2004. Direct and indirect transcriptional activation of virulence genes by an AraC-like protein, PerA from enteropathogenic Escherichia coli. Mol Microbiol 54:1117-33.
172. Tramonti A, De Canio M, Delany I, Scarlato V, De Biase D. 2006. Mechanisms of transcription activation exerted by GadX and GadW at the gadA and gadBC gene promoters of the glutamate-based acid resistance system in Escherichia coli. J Bacteriol 188:8118-27.
173. Yang J, Hart E, Tauschek M, Price GD, Hartland EL, Strugnell RA, Robins-Browne RM. 2008. Bicarbonate-mediated transcriptional activation of divergent operons by the virulence regulatory protein, RegA, from Citrobacter rodentium. Mol Microbiol 68:314-27.
174. Li P, Jiang W, Yu Q, Liu W, Zhou P, Li J, Xu J, Xu B, Wang F, Shao F. 2017. Ubiquitination and degradation of GBPs by a Shigella effector to suppress host defence. Nature 551:378-383.
175. Suzuki S, Mimuro H, Kim M, Ogawa M, Ashida H, Toyotome T, Franchi L, Suzuki M, Sanada T, Suzuki T, Tsutsui H, Nunez G, Sasakawa C. 2014. Shigella IpaH7.8 E3 ubiquitin ligase targets glomulin and activates inflammasomes to demolish macrophages. Proc Natl Acad Sci U S A 111:E4254-63.
176. Zheng Z, Wei C, Guan K, Yuan Y, Zhang Y, Ma S, Cao Y, Wang F, Zhong H, He X. 2016. Bacterial E3 Ubiquitin Ligase IpaH4.5 of Shigella flexneri Targets TBK1 To Dampen the Host Antibacterial Response. J Immunol 196:1199-208.
177. Arbibe L, Kim DW, Batsche E, Pedron T, Mateescu B, Muchardt C, Parsot C, Sansonetti PJ. 2007. An injected bacterial effector targets chromatin access for transcription factor NF-kappaB to alter transcription of host genes involved in immune responses. Nat Immunol 8:47-56.

178. Hung DT, Shakhnovich EA, Pierson E, Mekalanos JJ. 2005. Small-molecule inhibitor of Vibrio cholerae virulence and intestinal colonization. Science 310:670-4.
179. Yang J, Hocking DM, Cheng C, Dogovski C, Perugini MA, Holien JK, Parker MW, Hartland EL, Tauschek M, Robins-Browne RM. 2013. Disarming bacterial virulence through chemical inhibition of the DNA binding domain of an AraC-like transcriptional activator protein. J Biol Chem 288:31115-26.
180. Hughes D. 2003. Exploiting genomics, genetics and chemistry to combat antibiotic resistance. Nat Rev Genet 4:432-41.
181. Schmidt FR. 2004. The challenge of multidrug resistance: actual strategies in the development of novel antibacterials. Appl Microbiol Biotechnol 63:335-43.
182. Silver LL. 2016. Appropriate Targets for Antibacterial Drugs. Cold Spring Harb Perspect Med 6.